

ANTICANCER ACTIVITY OF 20(S) PROTOPANAXADIOL
ON CANCER CELLS

By

YAN ZHAO

M.D., China Medical University, 1987

A THESIS SUBMITTED IN PARTIAL FULFILLMENT OF
THE REQUIRMENTS FOR THE DEGREE OF
MASTER OF SCIENCE

in

THE FACULTY OF GRADUATE STUDIES

(SURGERY)

THE UNIVERSITY OF BRITISH COLUMBIA

October 2005

© Yan Zhao, 2005

ABSTRACT

Current anticancer therapy is often ineffective resulting in tumor relapse due to factors including multiple drug resistance and minimal residual diseases. In this study, 20(S)-protopanaxadiol (aPPD), one of the aglycone metabolic products of ginsenosides in human gastrointestinal tract, has been characterized and shows strong anticancer activities. It can induce apoptosis in glioma and other cancer cells through multiple apoptotic pathways, and synergistically enhances the efficacy of chemotherapeutic drugs in multi-drug resistant cancer cells. The ability of aPPD to reverse p-glycoprotein (p-gp) mediated multidrug resistance was determined, aPPD-resistant glioma cell lines were established and the difference of the gene expression profiles of both aPPD resistant and sensitive cell lines was exhibited. The results showed that aPPD inhibits the activity of P-gp in multiple drug resistant cell lines MCF-7adr and P388adr through a mechanism that is different from that of verapamil, a typical P-gp blocker. The aPPD-resistant glioma SF188C2R2 cells displayed cross-resistance to several chemotherapeutics and lost the ability of G2-arrest caused by aPPD in the parental cells. Gene expression profiles of resting SF188 and SF188C2R2 are very different than in cells treated with aPPD. Fifty-eight percent of genes were differentially expressed in these two cell lines at resting status. In the presence of aPPD, SF188 had 10-fold more genes changed in their expression than in SF188C2R2. These results demonstrated that this compound has the potential to be developed as an anti-cancer drug for clinical application. Further analysis of validated gene expression profiles of the SF188 and its aPPD-resistant cell line SF188C2R2 may reveal the mechanisms of anticancer effects by aPPD.

TABLE OF CONTENTS

ABSTRACT	ii
TABLE OF CONTENTS	iii
LIST OF TABLES	v
LIST OF FIGURES	vi
ABBREVIATIONS	viii
ACKNOWLEDGEMENT	ix
CHAPTER 1. INTRODUCTION AND BACKGROUND	1
1.1 Current cancer therapies	1
1.2 Chemotherapy	2
1.2.1 Mechanisms of anticancer drug inhibiting cancer	2
1.2.2 Cell death pathways as targets for chemotherapy	4
1.3 Defects of cancer therapy.....	9
1.4 Multiple drug resistance.....	9
1.5 Current management of drug resistance and limitation	17
1.6 Ginsenosides and 20(S)-protopanaxadiol (aPPD)	19
1.7 Objective	23
1.8 Hypothesis.....	23
REFERENCES	25
CHAPTER 2. EFFECT OF APPD ON P-GLYCOPROTEIN IN MULTIDRUG RESISTANT CELLS	36
2.1 Introduction.....	36
2.2 Materials and methods	43
2.2.1 Drugs and chemicals	43
2.2.2 Cell lines	44
2.2.3 In vitro cell viability assay	44
2.2.4 Fluorescent calcein formation assay	45
2.2.5 Calcein AM efflux inhibition assay	45
2.2.6 ATPase activity of P-gp assay	46
2.2.7 Additive effect of aPPD with verapamil in P-gp inhibition.....	47
2.2.8 Endurable effect of P-gp inhibition assay	48
2.2.9 Statistical analysis.....	48
2.3 Results.....	49
2.3.1 Equal cytotoxicity on P-gp positive and negative cells by aPPD	49
2.3.2 Inhibited P-gp by aPPD	49
2.3.3 Reversibly blocked P-gp activity by aPPD	53
2.3.4 Ineffective ATPase activity of P-gp by aPPD.....	56
2.3.5 An additive effect on P-gp inhibition between verapamil and aPPD.....	56
2.4 Discussion	60
REFERENCES	63

CHAPTER 3. CHARACTERIZATION OF APPD SELECTED DRUG-RESISTANCE CELL LINE SF188C2R2.....	69
3.1 Introduction.....	69
3.2 Materials and methods.....	70
3.2.1 drugs and chemicals.....	70
3.2.2 Cell viability assay.....	71
3.2.3 Generation of aPPD-resistant cell lines.....	71
3.2.4 Flow cytometry analysis.....	72
3.2.5 Colony formation assay.....	72
3.2.6 Growth curve and doubling time.....	73
3.2.7 Transfection with PHR'-CMV-EGFP plasmid DNA.....	73
3.3 Results.....	74
3.3.1 aPPD- resistant cell line SF188C2R2.....	74
3.3.2 Growth characteristics of SF188C2R2.....	78
3.3.3 Cell cycle distribution of SF188C2R2.....	78
3.3.4 Drug resistance profile of SF188C2R2.....	84
3.3.5 Resistance to DNA transfection of SF188C2R2.....	84
3.4 Discussion.....	96
REFERENCES.....	103
CHAPTER 4. PRELIMINARY RESULTS OF GENE EXPRESSION PROFILES OF SF188 AND SF188C2R2 CELLS TREATED WITH OR WITHOUT APPD.....	107
4.1 Introduction.....	107
4.2 Methods and materials.....	111
4.2.1 Drugs and chemicals.....	111
4.2.2 Cell lines.....	111
4.2.3 Cell culture and RNA isolation.....	112
4.2.4 Reverse transcription analysis.....	112
4.2.5 Gene expression using bioarrays.....	113
4.2.6 Array data analysis.....	113
4.2.7 Quantitative real-time PCR.....	115
4.2.8 Polymerase chain reaction (PCR) analysis.....	116
4.3 Results.....	116
4.3.1 SF188C2R2 gene expression profile differed to that of SF188.....	116
4.3.2 Gene expression changes in both SF188C2R2 and SF188 treated by aPPD.....	122
4.3.2.1 Apoptotic gene expression in SF188 and SF188C2R2 treated by aPPD.....	122
4.3.2.2 Anti-apoptotic gene expression in SF188 and SF188C2R2 treated by aPPD.....	126
4.4 Discussion.....	140
REFERENCES.....	144
CHAPTER 5. GENERAL CONCLUSION.....	148

LIST OF TABLES

Table 2-1 IC ₅₀ of ginsenosides with P-gp inhibitory effect on multiple drug resistant P388 cells	42
Table 2-2 P-gp inhibitory effect of verapamil and ginsenosides	59
Table 3-1 The characteristics of SF188C2R2 and SF188 cell lines	79
Table 3-2 Colony formation assay of SF188 and SF188C2R2 cell lines	81
Table 3-3 Effect of aPPD on cell cycle distribution in SF188C2R2 and SF188	83
Table 3-4 Cytotoxicity of aPPD and other anticancer drugs in SF188C2R2 and SF188	92
Table 3-5 Biological features of SF188C2R2 versus SF188	97
Table 3-6 Characteristics of SF188C2R2 and SF188TR	99
Table 3-7 Comparison of drug resistant profiles of SF188C2R2 and SF188 TR	101
Table 4-1 CodeLink UniSet Human 20K I gene classification	114
Table 4-2 Gene expression in SF188C2R2 and SF188 in the presence or absence of aPPD	120
Table 4-3 Gene expression relating to cell proliferation	121
Table 4-4 Significantly changed apoptotic genes in aPPD treated SF188 cells	127
Table 4-5 Significantly changed apoptotic genes in aPPD treated SF188C2R2 cells	130
Table 4-6 Anti-apoptosis gene expression	137

LIST OF FIGURES

Fig. 1-1. Two main target chemotherapy pathways.....	5
Fig. 1-2. Cell cycle model.....	11
Fig. 1-3. Chemical structure of protopanaxadiol family.....	22
Fig. 2-1. P-gp model	37
Fig. 2-2. Viability of P388 adr and P388wt cells in the presence of aPPD and DOX.	51
Fig. 2-3. Fluorescent calcein formation in MCF-7adr cells.....	52
Fig. 2-4. P-gp efflux of P388adr (A) and P388wt (B) in the presence of aPPD.....	54
Fig. 2-5. Endurable effect of P-gp inhibition of aPPD	55
Fig. 2-6. Effect of crude aPPD on ATPase activity of P-gp	57
Fig. 2-7. The additive effect of aPPD and verapamil on P-gp efflux ability	58
Fig. 3-1. Viability of SF188 and C2R cell lines in the presence of aPPD	76
Fig. 3-2. Viability of SF188C2R2 and SF188 in the presence of aPPD.....	77
Fig. 3-3. Growth curve of SF188C2R2 and SF188	80
Fig. 3-4. Flow cytometric profiles of SF188C2R2 and SF188 treated with aPPD.....	82
Fig. 3-5. Cross-resistance of SF188C2R2 to various chemotherapeutics.....	88
Fig. 3-6. SF188C2R2 and parental SF188 incubated with DOX and BCNU.....	91
Fig. 3-7. Fluorescent Calcein formation assay in SF188 C2R2 and SF188	93
Fig. 3-8. SF188C2R2 transfection with PHR'-CMV-EGFP	94
Fig. 3-9. Transfection efficiency of SF188 and SF188C2R2 with lentiviral vector PHR' – CMV – EGFP.....	95
Fig. 4-1. Gene clustering.....	119

Fig. 4-2. Gene expression pattern in SF188C2R2 (C2R2) and SF188 (Wt) in the presence or absence of aPPD	123
Fig. 4-3. Apoptotic gene cluster.....	124
Fig. 4-4. Apoptotic gene expression pattern	125
Fig. 4-5. TNF- α and NF- κ B pathway network	133
Fig. 4-6. SKIP3 pathway.....	134
Fig. 4-7. Real-time quantitative RT-PCR for SKIP3	135
Fig. 4-8. Real-time quantitative RT-PCR for ATF4.....	136
Fig. 4-9. Anti-apoptotic gene expression patterns	139

ABBREVIATIONS

- aPPD: aglycone 20(S)-protopanaxadiol
- ATF4: activating transcription factor 4
- BDNF: brain-derived neurotrophic factor
- BND: ATP-binding sites of P-gp
- DAP3: death associated protein 3
- DISC: death-initiating signaling complex
- DOX: doxorubicin
- FADD: Fas associated death domain protein
- Fas: APO-1 or CD95
- IC₅₀: inhibitory concentration 50%
- MAPK: mitogen activated protein kinase
- MDR: multiple drug resistance
- NF- κ B: nuclear factor - κ B
- P-gp: P-glycoprotein
- PPT: aglycone 20(S)-protopanaxatriol
- SKIP3: tribbles homolog 3 (Drosophila)
- TMZ: temozolomide
- TM: transmembrane regions of P-gp
- TNF: tumor necrosis factor
- TRAIL: TNF-related apoptosis inducing ligand

ACKNOWLEDGEMENT

I am greatly indebted to Dr. William Jia, my supervisor for his advice, enthusiasm, consideration and constant support throughout the course of my research. His extensive knowledge has been a major asset to my graduate studies and the completion of thesis. I would like to thank the members of my supervisory committee: Dr. Gang Li, Dr. Emma Guns and Dr. Thomas K. H. Chang for their support and advice. I am grateful to Luke Bu for advice on the study strategies and technique through my study, to Hang Yan for cell line preparation and animal experiment assistant, to Dr Lawrence Mayer in BC Cancer Agency for providing MCF-7adr and parental cell lines, to Weijia Nie, Wendey Wen for DNA Microarray sample preparation, to Dr. Shive Pasta for helping cDNA microarray analysis, to Andy Jonathan in Biomedical Research Center for technical support on Flow cytometry, Dr. Zhongjun Ma, Yan Yu and Joe Zhou for cell culture, and to Dr. Wentao Yue for Western blot image skill instruction.

CHAPTER 1. INTRODUCTION AND BACKGROUND

1.1 Current cancer therapies

Cancer is a fatal disease characterized by local abnormal proliferation and it spreads directly through invasion and metastasis to other sites of body. It is estimated that one in four people will develop cancer in their life time and one in five dies [1, 2]. Surgery, radiotherapy and chemotherapy remain the mainstay of treatment in clinical practice. Radical surgery and radiotherapy are potentially curative treatments for localized non-metastatic tumors and the only chance to cure the majority of patients with cancer. On the other hand, chemotherapy can destroy cancer cells that have broken off from solid tumors and spread through the blood and lymph systems to various parts of the body [3]. Because each therapy has its own weakness, a combination of these treatment strategies is usually adopted and has shown substantial improvement of the prognosis in cancer patients [4]. Meanwhile, many new strategies are emerging, such as immunotherapy and gene therapy [5-9]. However, cancer therapies often fail in that tumors remain unresponsive to the treatment and resulting in relapse. Chemotherapy is the only major modality of cancer with the treatment potential to eradicate disseminated diseases; therefore, the hopes of eradicating cancer rests on explorations into chemotherapy. Efforts for overcoming the limitations of anticancer agents have been stimulated by understanding the mechanisms of anticancer activity and the deficiencies of chemotherapy.

1.2 Chemotherapy

Chemotherapy, using chemicals to inhibit cancer, remains curative for a proportion of patients with cancers, such as Hodgkin's disease, High-grade non-Hodgkin's lymphoma and ovarian cancer [10-12]. As a common treatment modality used in oncology, chemotherapy is used alone or as an adjuvant to surgery or radiation. Adjuvant chemotherapy after surgery and radiotherapy has been shown to improve the survival rate in a number of carcinomas, such as, rectal, breast, head and neck [12, 13]. Animal and clinical studies have shown that adjuvant regimens produce the most dramatic responses in metastatic or recurrent disease and also have the greatest likelihood of being curative in adjuvant chemotherapy [4]. Accordingly, new drugs and combinations of drugs are constantly being explored as strategies to improve the effects of chemotherapy [12].

1.2.1 Mechanisms of anticancer drug inhibiting cancer

There are approximately 60 different chemical compounds currently approved for clinical treatment of cancer (not including hormones or biological response modifiers). These compounds are of diverse structure and from a variety of sources. Anticancer drugs are designed to kill particular tumor cells developing upon the biological characteristics of the cancer cells; for instance, rapid rates of cell proliferation are a characteristic. The biological characteristics of tumor cells make them more susceptible to anticancer drugs than normal cells [12]. Many of the drugs in chemotherapy appear to exert their therapeutic effect by interfering with the processes involved in cell division. This interference results in the cells being physically disrupted or death [14]. Generally, anticancer drugs can be classified into seven

categories. Each class of drugs kills cells at different stages of the cell cycle using different mechanisms [1, 15].

Antimetabolites are drugs, which attack tumor cells during the process of cell division, when they are most vulnerable. Antimetabolites imitate normal cell nutrients and are mistaken by the cells for normal metabolites. They either inhibit critical enzymes involved in nucleic acid synthesis or become incorporated into the nucleic acid and produce incorrect codes. Both mechanisms result in inhibition of DNA synthesis and cause cell death. For example, Methotrexate, known as "antivitamin", resembles normal vitamin B and folic acid. It inhibits the dihydrofolate reductase and results in the depletion of reduced intracellular folates necessary for thymidylate and purine biosynthesis. Consequently, methotrexate blocks the synthesis of thymidylic acid, resulting in a deficiency of DNA synthesis.

Alkylating agents are anticancer drugs, such as Carmustine (BCNU) and cisplatin, which attacks all tumor cells regardless of their cell cycle status. These drugs bind to the DNA of the cells in various ways, thus prevent reproduction.

Antitumor antibiotics are drugs such as doxorubicin and antinomycin D. They insert themselves into strands of DNA, and cause double strand breaks. They either break up the chromosomes or inhibit the DNA-directed synthesis of RNA, which the cell needs to grow.

Alkaloids are drugs, such as vincristine, vinblastine and paclitaxel, which act to prevent the formation of chromosome spindles necessary for cell division.

Hormones are drugs such as estrogen and progesterone, they inhibit the growth of some cancers, such as prostate cancer and breast cancer [16], but the mechanism is unclear.

Molecularly targeted agents are the drugs targeting to signal transduction pathways. Tyrosine kinase inhibitors, such as imatinib mesylate, gefitinib and iressa, are signal transduction inhibitors. Monoclonal antibodies, such as Alemtuzumab and gemtuzumab are derived from murine antibodies. They can induce cytotoxicity through complement-mediated lysis, antibody-dependent cellular cytotoxicity and induction of apoptosis; while gene expression modulators, such as retinoids and rexinoides, affect the expression of genes and act to inhibit cell growth and differentiation [15, 17].

Biological response modifier, such as, interleukin-2, is one of the drugs involved in tumor inhibition. It enhances mitogenesis of T cells, natural killer cells and lymphokine-activated killer cells and induces production of interferon- γ [1, 15].

1.2.2 Cell death pathways as targets for chemotherapy

Biochemical and molecular investigation have indicated that current anticancer drugs may induce apoptosis by activating several pathways simultaneously in cancer cells [14, 18]. Two of these pathways are believed to be the main targets of anticancer drugs (Fig.1-1). In first signaling pathway, drugs induce damage to cell death, which involves the mitochondrial release of proapoptotic molecules to activate the caspase cascade under the control of the Bcl-2 family of proteins. The second pathway

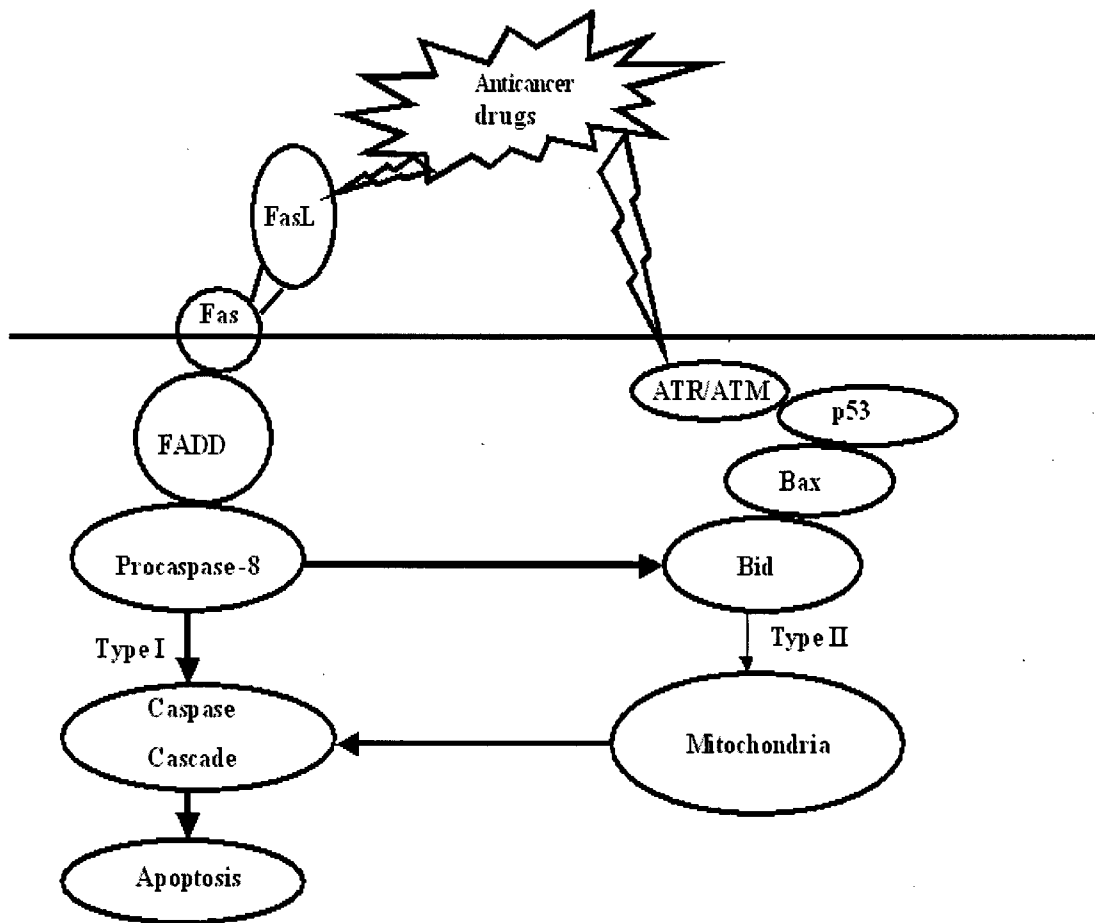


Fig. 1-1. Two main target chemotherapy pathways

including death receptors of the tumor necrosis factor (TNF) receptor superfamily, mainly Fas (APO-1/CD95), is induced by some drugs, and may play a role in linking drug-induced damage to the apoptotic machinery [14, 19].

The mitochondrial pathway

The drug induced mitochondrial apoptosis pathway is triggered by mitochondrial dysfunction, which is regulated by Bcl-2 family proteins. The Bcl-2 family proteins consist of three subfamilies including proapoptotic Bax, BH-3 and the antiapoptotic Bcl-2 subfamily. The proapoptotic Bax subfamily includes Bax, Bak and Bok proteins, and the BH-3 subfamily includes Bik, Bim, Bad, and Bid proteins. When anticancer drugs induce apoptosis, the proapoptotic proteins, including Bax, Bak and Bad, is induced in accordance with their sensitivity to the anticancer drugs. In turn, the activation of the Bax gene leads to an increase in the number of proteins that form Bax homodimers or heterodimers with Bak. The dimerized Bax is translocated from the cytoplasm to the mitochondria, and result in the release of cytochrome c, which activates the caspase cascade. The release of cytochrome c, which can also be activated by PUMA (p53-upregulated modulator of apoptosis) and Noxa (PMA-induced protein) [20], has been shown to promote apoptosome formation via the oligomerization of a cytochrome c/Apaf-1/procaspase-9 complex. Consequently, apoptosome activates caspase-9 resulting in the cleavage of downstream effector caspase-3 and -7 leading to apoptosis [14, 21].

The death-receptor dependent pathway

In some cell types, cytotoxic-drug-induced apoptosis involves the death receptor Fas, known as APO-1 or CD95, a 45-kDa type I membrane death receptor protein belonging to the TNF receptor superfamily. Fas ligand (FasL, APO-1L, CD95L) exists mainly as a 40-kDa membrane-bound protein [22]. The apoptotic cell death pathway triggered by FasL is believed to precede a series of events. FasL binds to Fas and induces clustering of the death domain (DD), which is the intracellular portion of Fas containing a characteristic 85-amino-acid region. A complex known as the death-initiating signaling complex (DISC) is formed and involves an adaptor protein named FADD (for Fas -associated death domain) [23] and procaspase-8. FADD binds to Fas through the interaction of DD on both FADD and Fas. Through a second interacting region called the death effector domain (DED), FADD binds to procaspase-8 and releases fully active caspase-8. Basing on the level of DISC formed in each cell type, procaspase-8 can either directly activate the effector caspases (type I cells) or cleave Bid in the BH3 subfamily (type II cells) [24, 25]. In turn, translocation to the mitochondria of the truncated Bid acts in combination with Bax, the previously described mitochondrial pathway to cell death (Fig.1-1). The Fas-FasL system regulates the normal development of T lymphocytes. The Fas/FasL system is down-regulating immune reactions because of the self-destruction of the activated T cells. Fas-FasL interaction is also one of the pathways by which cytotoxic immune cells can kill Fas-expressing target cells [22]. Up-regulation of Fas has been detected following the treatment of chemotherapeutic agents in cell lines [26]. This suggests that the Fas-

FasL pathway may be important as a mechanism for drug-induced apoptosis in some tumors [14].

Unfortunately, the clinical applicability of this approach has been limited because the attempts to kill neoplastic cells *in vivo*, by stimulating TNFR1 or Fas/Apo1 have produced excessive toxicity with severe systemic inflammatory syndrome. The benefit of combining cytokines of the TNF superfamily to systemic anticancer therapy appeared limited until the identification of TRAIL [14, 27]. TRAIL (TNF-related apoptosis inducing ligand) also known as Apo-2 ligand, is a transmembrane protein that also exists as a soluble molecule. Recently, TRAIL/APO-2L has become more and more attractive for specifically killing transformed cancer cells without damaging the majority of normal cells. Interestingly, a wide range of normal tissues expressing TRAIL mRNA are resistant to TRAIL- induced cell death. This differential sensitivity of normal cells and tumor cells to TRAIL remain unknown. The preferential expression of “decoy” receptors, such as DcR1 and DcR2, in normal versus neoplastic cells, is proposed as one mechanism for TRAIL/APO-2L selective kills [28]. TRAIL/APO-2L interacts with the cell surface “death receptors” (DR4 and DR5) to initiate programmed cell death. TRAIL/APO-2L also binds to “decoy” receptors to antagonize its interaction with “death receptors” [28]. The selective response of tumor cells to TRAIL, its safety when administered to animals, its MDR independent tumor cell line inhibition [29], and its efficacy in suppressing tumor growth, suggest that TRAIL-based tumor therapy hold great promise [14, 27, 30].

1.3 Defects of cancer therapy

Anticancer therapy often fails to cure cancer. Even though surgery, radiotherapy in combination with chemotherapy acquired a high positive response to cancers, most patients, who attain chemotherapy-induced remission, relapse and eventually die [31]. Intrinsic or acquired drug resistance of tumors after exposure to anticancer agents or radiotherapy is mainly responsible for the failure of anticancer treatments. Even though there are various anticancer drugs to inhibit cancer cells via different mechanisms, one thing that they appear to have in common is that cancer cells have the capacity to display resistance to every one of them [32]. In addition, the presence of the blood-brain barrier (BBB) restricts the entry of many chemotherapeutic agents into the brain, and contributes to low efficacy of chemotherapy for intracranial tumors. Gliomas, one of the most malignant tumors, often characterize relapse after treatment. This failure to achieve even local control over primary brain tumors has stimulated efforts to improve the treatment response of gliomas. However, the results have been uniformly poor over the past two decades because the potential intrinsic drug resistance and the action of the BBB to block the penetration of anticancer drugs. Effective chemotherapy for gliomas is particularly lacking and since the recurrence of gliomas is uncontrolled, they hold the most dismal prognosis [33].

1.4 Multiple drug resistance

Multiple drug resistance (MDR) is the ability of tumors to exhibit simultaneous resistant to a number of structurally and functionally unrelated chemotherapeutic

agents [34]. Cancer cells with multiple drug resistance are associated with proliferation, relapse, and metastasis, as well as unresponsiveness to the chemotherapy; therefore, drug resistance remains one of the most important causes of failure in cancer treatment. Tumor cells become resistant to chemotherapeutic agents in a variety of ways. Generally, they can be divided into two categories: kinetic resistance and genetic resistance.

1.4.1 Kinetic resistance

Kinetic resistance of tumors takes place during the cell cycle. A full cell cycle is composed of four phases, including M, G1, S and G2 (Fig.1-2). The cells in G0 phase, out of the cell cycle are nonproliferating or “resting”. At the end of M phase, two daughter cells are formed. The daughter cells consist of three subpopulations: (1) cells that are nondividing and terminally differentiated, termed the nonproliferating population, (2) cells that are continually proliferating, are termed proliferating population or growth fraction, (3) cells that are resting but may be recruited into the cell cycle termed stem cell population. All three populations exist simultaneously in tumors [35, 36]. Kinetic resistance is based on the cell population kinetics relating to cell cycle and phase specificity, growth fractions and the implications of these factors for responsiveness to specific agents, as well as drug administration [37]. Active reproduction of cells in G1, S, G2, and M can be sensitive to most of the available antitumor agents, and in theory, cells can be killed by continuous or scheduled exposure to an equivalent of one complete cell cycle.

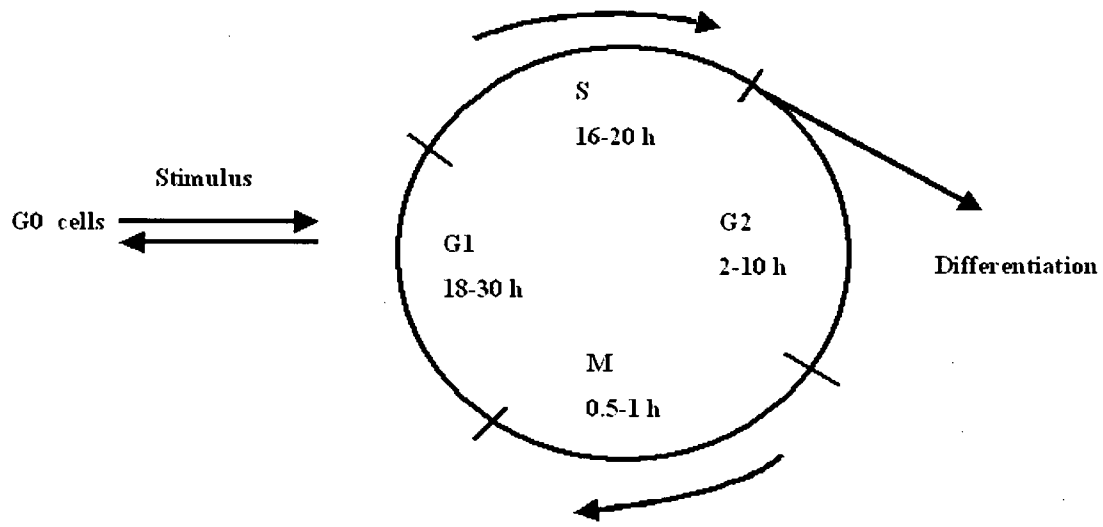


Fig. 1-2. Cell cycle model

Many anticancer drugs are cell cycle specific and act on cycling cells. For example, methotrexate targets DNA synthesis and cisplatin acts on DNA cross/linking mainly on G1 and S phase. Tubulin-I aggregation blockers including vincristine, vinblastine, taxol and topoisomerases II inhibitor doxorubicin, as well as ionizing radiation, act on M phase, however, the cells resting in G0 or prolonged G1 phase show resistance to anticancer drugs. Also, the majority of anticancer drugs do not cause cell death during the G0 phase [15]. Therefore, some of these resting tumor cells remain by escaping the attack of chemotherapy resulting in cancer relapse. In addition to all of this, a particular problem in cancer therapy is the plateau growth in many human tumors. Because of the small growth fraction, the tumor in plateau growth renders many of the cells insensitive to the antimetabolites and makes them relatively unresponsive to many of the other chemotherapeutic agents. Under the appropriate conditions, cells in G0 are capable of entering cell division where growth fraction in plateau growth can be increased and where kinetic resistance is usually considered reversible.

1.4.2 Genetic resistance

Genetic resistance results from naturally selected mutant clones [38, 39]. Tumor cells have increased mutation rates compared to normal cells [40-42]. The mutation affecting the apoptotic machinery could constitute another whole level of drug resistance in tumor cells. Genetic resistance, unlike kinetic resistance, is usually considered irreversible. Subsequent generations of cells remain resistant to drug therapy and can lead to the same biochemical mechanisms of drug resistance. The

process of cancer cells becoming resistant to anticancer drugs is mediated by at least six differentiated mechanisms, as described below [34, 38, 43].

Decreased drug intracellular accumulation

P-glycoprotein (P-gp), the identified mammalian multidrug transporter, pumps various cytotoxic drugs out of the cells. Over expression of P-gp causes cancer cells to become resistant to a great variety of structurally and functionally dissimilar anticancer drugs, such as vinblastine, vincristine, doxorubicin, paclitaxel and many others. P-gp mediated drug resistance is termed classical MDR. Other ABC family transporter members, such as multiple drug resistant associated protein (MRP1), have also been found to be associated with drug resistance in breast cancer, neuroblastomas, and lung cancers [44]. Five human MRP subfamily members MRP2, MRP3, MRP4, MRP5, MRP6 have also been identified. Another protein MXR is coded by Mitoxantrone resistant – associated gene mxr [45]. MXR, also known as breast cancer resistant protein (BCRP) or ABC transporter in placenta (ABCP), is an ABC half-transporter. Overexpression of MXR is associated with resistant to mitoxantrone in cell lines [45, 46]. The features of drug resistance from P-gp, MRPs and MXR overexpression appear to be similar at decreased intracellular levels of drug accumulation even though they are encoded by different genes and differ in molecular structure and mechanisms used in pumping out the drugs [46].

Inactivation or detoxification of drug

The glutathione (GSH) system, which includes at least two enzymes: GSH S-transferase and GSH peroxidase in cells, is one of the most important detoxification processes [47]. GSH S-transferase binds to GSH at reactive alkylating groups in drugs such as nitrogen mustard and cyclophosphamide in order to prevent them from reacting with or cross-linking DNA [47]. Increased activity of the GSH system suggests it constitutes yet another mechanism of MDR [48, 49].

Inability to convert to an active form

The majority of purine and pyrimidine antimetabolites require activation by phosphorylation before they exert cytotoxic effects in cancer cells. A deficiency in active processes is often the cause of clinical resistance [39]. For example, Methotrexate (MTX) is intracellularly polyglutamated by the enzyme FPGS to add glutamate residues. Polyglutamated MTX inhibits tumor cells by tightly binding to dihydrofolate reductase (DHFR) and interrupting pyrimidine and purine biosynthesis. Defective FPGS activity causes low polyglutamated MTX accumulation in cancer cells and therefore results in methotrexate resistance in human tumor cell lines [50].

Altered target protein expression

Many cytotoxic drugs inhibit the essential enzymes involved in the synthesis and maintenance of structure and function of DNA. Cellular resistance may arise from alterations in these proteins, resulting in the protection of tumor cells from the lethal

effects of these drugs. Topoisomerases are essential in DNA transcription and replication. Topoisomerase II alters DNA topology by causing transient double strand breaks in the process of DNA replication. Some effective anticancer agents called topoisomerase II inhibitors, such as DOX and etoposide, induce cytotoxicity in tumor cells interrupting DNA replication of the cells by inhibiting its target protein topoisomerase II. The tumor cells become resistant to topoisomerase II inhibitors either by topoisomerase II underexpression or through the occurrence of gene mutations in the cells [51].

Increased DNA repair capacity

Many anticancer drugs cause cell death by inducing DNA damage. Tumor cells resistant to DNA-damaging agents can be induced by modification of certain pathways and then display an enhanced capacity for drug-induced damage repair. For example, enhanced direct repair mediated by O⁶-alkylguanine DNA alkyltransferase in tumor cells leads to resistance of chloroethylnitrosoureas [52]. Cells have evolved complex and highly effective mechanisms for repairing damaged DNA segments. The repair mechanisms can generally be classified as (1) Non – homologous end joining; (2) base excision repair; (3) nucleotide excision repair; (4) mismatch repair; (5) homologous recombination repair; and (6) single-strand annealing [52-55].

Alerted apoptosis regulation

Most anticancer drugs exert their antitumor effect against cancer cells by inducing apoptosis. Following DNA damage caused by anticancer drugs, p53 induces apoptosis by regulating the expression of downstream proteins, Bcl-2 and BAX [56, 57]. By activating BAX, p53 has the ability induce apoptosis, which is inhibited when Bcl-2 forms homodimers [58] or Bax-Bcl-2 heterodimers. The loss of p53 function, required for cell death, alerts the apoptosis pathway and results in cellular resistance to anticancer therapy in cancer cells [19].

The reasons that cancer cells become MDR are very complex and diverse [48]. It is well known that cancer cells always employ more than one mechanism to develop their drug resistance. The combinations of several drug-resistance mechanisms, including drug transport, detoxification, and apoptotic pathways, have been identified as contributors to cancer cells achieving MDR. For example, Chen et al. and Sharmal et al. demonstrated that MDR results from the combination of P-gp overexpression and topoisomerase II underexpression in breast cancer cells [59, 60]. Even though the development of molecularly targeted anticancer drugs is rapidly changing cancer therapeutics, drug resistance from this new classification of the drugs remains a new clinical concern. Many of these molecular targeted agents, including hormone therapies, trastuzumab, imatinib, and gefitinib exhibit via common resistance mechanisms. These include 1) inadequate target blockade due to sub-optimal drug delivery; 2) altered target expression at the DNA (gene amplification), mRNA or

protein level; 3) an altered target, such as a mutated kinase domain; 4) modified target regulating proteins (e.g. altered expression of co-activators and/or co-repressors for nuclear steroid hormone receptors); 5) signaling by alternative proteins (functional redundancy) or different signaling pathways [61].

1.5 Current management of drug resistance and limitation

Multiple strategies have been developed to help overcome the MDR in cancer. Surgery or radiotherapy is applied to overcome the plateau growth of tumors by reducing tumor bulk and thereby improving the response to systemic chemotherapy or immunotherapy. For example, MDR modulators, such as verapamil, cyclosporin A and PSC-833, can be co-administered with anticancer agents to increase drug accumulation in the tumor cells, by inhibiting the P-gp activity and other drug transporters in the ABC family [62]. It has also been demonstrated that drug resistance developed through most of the drug resistant mechanisms, can be partially overcome by escalating the drug dose in vitro and in vivo. High-dose chemotherapy showed an ability to overcome non P-gp mediated MDR in clinical practice. For example, patients with ovarian carcinoma without overexpression P-gp, failing in conventional treatment regimens, can achieve high rates of positive response with high-dose chemotherapy, combining autologous bone marrow support. In the treatment for lymphoma, the therapeutic efficacy of Hodgkin's disease emphasizes the importance of delivering intensive chemotherapy [13, 63, 64]. Theoretically, if the concentration of the anticancer drugs is maintained long enough, then all of the cells

in the tumor may pass through the vulnerable points G1, S, M and G2 in the cell cycle and become susceptible to the drug's effect. Likewise, cells that are in a resting state, but which can be stimulated into division will become sensitive to the drugs. Combinations of chemotherapy, including drugs that affect resting populations (with many G0 cells), and scheduling the drugs according to the cell cycle length were applied to prevent phase escape and to synchronize cell populations and increase cell kill [65, 66].

Of all the therapeutic strategies mentioned above, chemotherapy is the major modality used for the management of drug resistance; however, chemotherapy often fails to be continued for the time and dosage necessary to eradicate the cancer. The major problem is the toxicities of chemotherapy, including acute hematotoxicity, cardiac toxicity, and neurological toxicity, as well as increased longer-term risk of secondary malignancies and infertility. These toxicities are so prevalent that patients often cannot receive a full dosage or the full length of therapy necessary to cure the cancer. Even for high dose chemotherapy, the dosage of anticancer agents can be maximally increased to 2-fold, but it remains far away from eradicating the cancer cells [63]. Furthermore, the toxic effects of chemotherapy become more life threatening than curative in the late stage of cancer, thus palliation becomes the major treatment for patients with cancer in terminal stages.

The hope for the eventual cure of malignancy rests with the development of safer anticancer agents with enhanced antitumor spectrums. Considering the severe deficiency of current cancer chemotherapeutic agents, it would be desirable to have novel anticancer drugs that are easily administered, well tolerated, and which do not exacerbate clinical symptomatology, but have a wide antitumor spectrum. In addition, surgical intervention should remain possible with drugs used as adjuvant therapy, necessary only to maintenance of adequate hematologic counts and without imposing significant medical risk factors. It is important to note that agents formulated naturally which cross the blood-brain barrier might also hold some promise for brain tumors and metastasis therapy [13].

1.6 Ginsenosides and 20(S)-protopanaxadiol (aPPD)

Ginseng has been used as a drug by people in Eastern Asian regions for 2000 years. Recently, ginseng has gained worldwide attention because of its distinguished pharmacological effects [67]. It has been reported that ginseng has a wide range of positive pharmacological effects in the cardiovascular, endocrine, immune, and central nervous systems [67, 68] and have tonic, immunomodulatory adaptogenic, and anti-aging activities [69]. Particularly, *Panax ginseng* C.A. Meyer which demonstrated non-toxic and non-organic specific preventive effects against various cancers both in animal and human experiments [70]. The beneficial effects of ginseng have precipitated tremendous effort toward discovering the pharmacology of its action through biochemical and molecular biology techniques [69, 71]. Ginsenosides, widely

accepted as major effective components of ginseng, are glycosides containing an aglycone with a dammarane skeleton known as steroidal saponins [70]. Based on their structural differences, ginsenosides are divided into two major categories: the 20(S)-protopanaxadiol (PPD) and 20(S)-protopanaxatriol (PPT). The 20(s)-protopanaxadiol classification contains the most abundant ginsenosides in ginseng, such as ginsenosides Rb1, Rb2, Rb3, Rc, Rd, Rg3, Rh2 and the aglycone PD. The 20(s)-protopanaxatriol classification contains ginsenosides Re, Rf, Rg1, Rg2, Rh1 and aglycone PT [67, 68, 72]. Ginsenosides have also been shown to possess various biological capabilities; including the enhancement of cholesterol biosynthesis, stimulation of serum protein synthesis, as well as immunomodulatory effects [70, 73].

Some ginsenosides, such as Rh1, Rh2 and Rg3 have demonstrated the inhibition of tumor angiogenesis, tumor invasion and metastasis, the control of phenotypic expression and differentiation of tumor cells as well as creating an inhibitory effect on the drug efflux pump P-gp [73, 74]. Molecular studies show that Rh2 can induce apoptosis in many tumor cells [75-77]. It has also been shown that Rh2 can result in remarkable inhibition of human ovarian cancer cells *in vitro* and *in vivo* nude mice, [78-81] and that it also decreases the incidence of lung adenoma and hepatoma induced by aflatoxin B1 in ICR mice [82]. The anticancer activity of metabolites formed by intestinal bacterial, after oral administration of ginseng extract in humans and rats has been studied. Through this research 20-O- (β - D-glucopyranosyl)-20(S)-protopanaxadiol (M1) is one of the major metabolites detected in urine and blood [83,

84]. M1 has been identified as non-toxic and has the ability to inhibit tumor invasion [70, 83, 85].

Aglycone 20(S)-protopanaxadiol (aPPD), belonging to the protopanaxadiol family classification (Fig.1-3), is a metabolic product of orally taken ginseng, resulting following deglycosilation in the gastrointestinal track [84]. It can also be obtained through acid hydrolysis of protopanaxadiol ginsenosides in vitro [86]. aPPD has been shown to have a suppressing cell growth effect on various cancer cells. Recent studies have shown that aPPD is the most nonpolar ginsenoside with the strongest cytotoxicity induced in Caco-2 cells in PPD and PPT classifications by inducing apoptosis and necrosis [87]. Interestingly, Rh2 is found to deglycosylate into aPPD in B16 cells, indicating that Rh2 may in fact act through aPPD to execute its anti-cancer effects [88].

aPPD in our lab was found to activate multiple apoptotic pathways, including activation of caspases, generation of free radicals and inhibition of AKT phosphorylation. aPPD may also act as a selective estrogen receptor modulator, (SERM) and has the potential to prevent breast cancer formation and growth. Moreover, aPPD acted to exert the cytotoxicity of the glioblastoma cell line SF188 with p53 mutation [Jia, et al. unpublished].

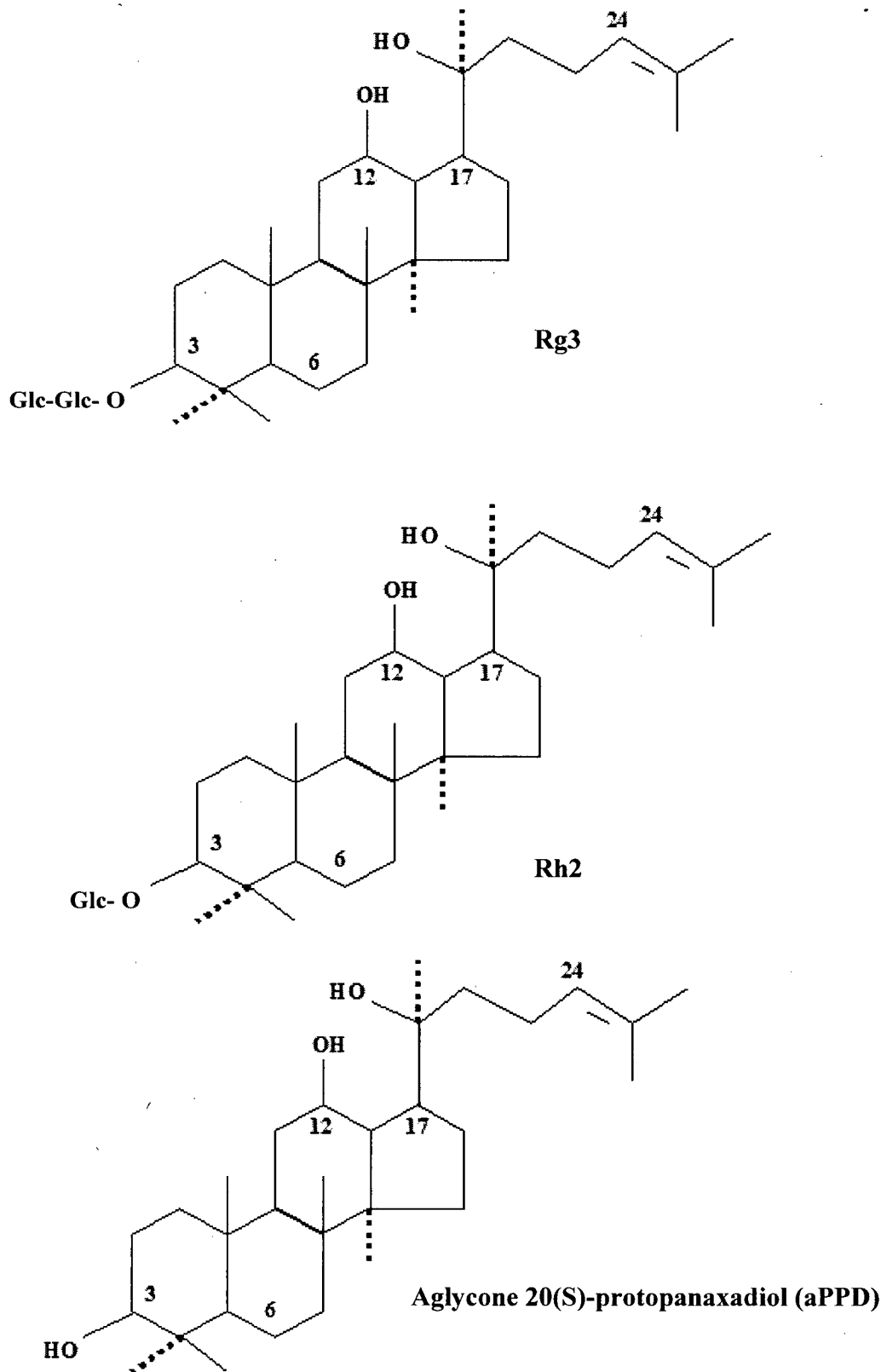


Fig. 1-3. Chemical structure of protopanaxadiol family

Because of the low toxicity of aPPD, it may have great therapeutic potential for tumor treatment, as the toxicity of currently used chemotherapeutics has been hindering the efficacy of chemotherapy. However, the ability of aPPD to inhibit MDR cancer cells has not been investigated. Whether cancer cells can acquire drug resistance to aPPD, as they do from many other anticancer drugs, remains unknown. Furthermore, the mechanism used by aPPD to inhibit cancer cells also remains unclear.

1.7 Objective

The object of this study is to point out the anticancer characteristics of aPPD in P-gp over expression and non-P-gp expression tumor cells, to investigate the ability of tumor cells acquiring drug resistance from aPPD and to explore gene expression profiles of human glioblastoma cells in response to aPPD.

1.8 Hypothesis

Previous studies in our lab have shown that aPPD sensitizes MDR cells to chemotherapeutics, we now hypothesized that aPPD may act through multiple mechanisms including inhibiting P-glycoprotein to block drug efflux and altering expression of certain genes to cause the cell more susceptible to drug induced cytotoxicity.

To test this hypothesis, a series of experiments was conducted and described through my M.Sc. graduate study, which serve to investigate the anticancer activity of aPPD on glioma and other cancer cells. In particular, the effects of aPPD on cancer cells overexpressing P-glycoprotein, and the ability of this compound to reverse P-gp caused MDR will be discussed. Secondly, this study also describes an aPPD-resistant cell line generated through persistent treatment with aPPD. Finally, this study compares the gene expression profiles of the aPPD-resistant and aPPD-sensitive glioma cells with genes responsible for aPPD-induced apoptosis.

REFERENCES

1. Rubin, P., ed. *Clinical oncology : a multidisciplinary approach for physicians and students*. ed. J.P. Williams. 2001, Philadelphia : W.B. Saunders Co: Philadelphia. P106.
2. Sikora, P.P.a.K., ed. *Treatment of cancer*. ed. K.E. Halnan. 1995, Chapman & Hall Medical: London ; New York, N. Y. : Chapman & Hall Medical. P1105-111.
3. Malin Dollinger, E.H.R.a.G.C., ed. *Everyone's guide to cancer therapy*. ed. R. Hasselback. 1995, Somerville House Pub: Toronto. 55.
4. E.E. Vokes, H.M.G., ed. *Oncologic therapies*. 1999, Springer: Berlin ; New York. P206, P38.
5. Schott, M. and W.A. Scherbaum, *Immunotherapy and gene therapy of thyroid cancer*. *Minerva Endocrinol*, 2004. **29**(4): p. 175-87.
6. Oelke, M., C. Krueger, and J.P. Schneck, *Technological advances in adoptive immunotherapy*. *Drugs Today (Barc)*, 2005. **41**(1): p. 13-21.
7. Harrington, K.J., C.M. Nutting, and H.S. Pandha, *Gene therapy for head and neck cancer*. *Cancer Metastasis Rev*, 2005. **24**(1): p. 147-64.
8. Evans, T.R. and W.N. Keith, *Intra-peritoneal administration of genetic therapies: promises and pitfalls*. *Minerva Ginecol*, 2004. **56**(6): p. 529-38.
9. Fenstermaker, R.A. and M.J. Ciesielski, *Immunotherapeutic strategies for malignant glioma*. *Cancer Control*, 2004. **11**(3): p. 181-91.

10. Muggia, F.M., *Relevance of chemotherapy dose and schedule to outcomes in ovarian cancer*. *Semin Oncol*, 2004. **31**(6 Suppl 15): p. 19-24.
11. Perry, M.C., ed. *The chemotherapy source book*. 1996, Williams & Wilkins: Baltimore. p.101-126.
12. Sikora, P.P.a.K., ed. *Treatment of cancer*. 1995: London; New York, N. Y. p.91-108.
13. Chen, B., et al., *Safety and efficacy of high-dose chemotherapy with autologous stem cell transplantation for patients with malignant astrocytomas*. *Cancer*, 2004. **100**(10): p. 2201-7.
14. Bruce C. Baguley, D.J.K., ed. *Anticancer drug development*. 2002, London : Academic: San Diego, Calif. p55-90.
15. Fischer, D.S., ed. *The cancer chemotherapy handbook*. 2003, Mosby: Philadelphia. 1-66.
16. Michael C. Perry, *The chemotherapy source book*, ed. M.C. Perry. 1996, Baltimore: Williams & Wilkins. p.479-555.
17. Herbst, R.S., *Review of epidermal growth factor receptor biology*. *Int J Radiat Oncol Biol Phys*, 2004. **59**(2 Suppl): p. 21-6.
18. Kim, R., et al., *Current status of the molecular mechanisms of anticancer drug-induced apoptosis. The contribution of molecular-level analysis to cancer chemotherapy*. *Cancer Chemother Pharmacol*, 2002. **50**(5): p. 343-52.
19. Gryfe, R., et al., *Molecular biology of colorectal cancer*. *Curr Probl Cancer*, 1997. **21**(5): p. 233-300.

20. Hussein, M.R., A.K. Haemel, and G.S. Wood, *Apoptosis and melanoma: molecular mechanisms*. J Pathol, 2003. **199**(3): p. 275-88.
21. Gross, A., J.M. McDonnell, and S.J. Korsmeyer, *BCL-2 family members and the mitochondria in apoptosis*. Genes Dev, 1999. **13**(15): p. 1899-911.
22. Pinkoski, M.J. and D.R. Green, *Fas ligand, death gene*. Cell Death Differ, 1999. **6**(12): p. 1174-81.
23. Chinnaiyan, A.M., et al., *FADD, a novel death domain-containing protein, interacts with the death domain of Fas and initiates apoptosis*. Cell, 1995. **81**(4): p. 505-12.
24. Scaffidi, C., P.H. Krammer, and M.E. Peter, *Isolation and analysis of components of CD95 (APO-1/Fas) death-inducing signaling complex*. Methods, 1999. **17**(4): p. 287-91.
25. Dive, J.A.H.a.C., ed. *Apoptosis and cancer chemotherapy*. 1999, Humana Press: Totowa, N.J. p.175-187.
26. Bronchud, e.b.M.H., ed. *Principles of molecular oncology*. 2000, Humana Press: Totowa, N.J. p.242.
27. Hawkins, C.J., *TRAIL and malignant glioma*. Vitam Horm, 2004. **67**: p. 427-52.
28. Pollack, I.F., M. Erff, and A. Ashkenazi, *Direct stimulation of apoptotic signaling by soluble Apo2l/tumor necrosis factor-related apoptosis-inducing ligand leads to selective killing of glioma cells*. Clin Cancer Res, 2001. **7**(5): p. 1362-9.

29. Secchiero, P., et al., *TNF-related apoptosis-inducing ligand (TRAIL): a potential candidate for combined treatment of hematological malignancies*. *Curr Pharm Des*, 2004. **10**(29): p. 3673-81.
30. Roth, W. and M. Weller, *Chemotherapy and immunotherapy of malignant glioma: molecular mechanisms and clinical perspectives*. *Cell Mol Life Sci*, 1999. **56**(5-6): p. 481-506.
31. Devarajan, E., et al., *Human breast cancer MCF-7 cell line contains inherently drug-resistant subclones with distinct genotypic and phenotypic features*. *Int J Oncol*, 2002. **20**(5): p. 913-20.
32. Perry, M.C., ed. *The chemotherapy source book*. 2001, Lippincott Williams & Wilkins: Philadelphia. p.63-100.
33. Wilson, A.W., et al., *Surgical management of incompletely excised basal cell carcinomas of the head and neck*. *Br J Oral Maxillofac Surg*, 2004. **42**(4): p. 311-4.
34. Gottesman, M.M., T. Fojo; and S.E. Bates, *Multidrug resistance in cancer: role of ATP-dependent transporters*. *Nat Rev Cancer*, 2002. **2**(1): p. 48-58.
35. *Cancer management : a multidisciplinary approach, medical, surgical & radiation oncology*. 1996, PRR: Huntington, N.Y. p.22.
36. Perry, M.C., ed. *The chemotherapy source book*. 1996: Baltimore. p.6.
37. Fischer, D.S., ed. *The cancer chemotherapy handbook*. 2003, Mosby: Philadelphia. p.14.

38. Perry, M.C., ed. *The chemotherapy source book*. 1996, Williams & Wilkins: Baltimore. 90-108.
39. Perry, M.C., ed. *The chemotherapy source book*. 1996, Williams & Wilkins: Baltimore. 109-119.
40. Elmore, E., T. Kakunaga, and J.C. Barrett, *Comparison of spontaneous mutation rates of normal and chemically transformed human skin fibroblasts*. *Cancer Res*, 1983. **43**(4): p. 1650-5.
41. Seshadri, R., et al., *Mutation rate of normal and malignant human lymphocytes*. *Cancer Res*, 1987. **47**(2): p. 407-9.
42. deFazio, A., E.A. Musgrove, and M.H. Tattersall, *Flow cytometric enumeration of drug-resistant tumor cells*. *Cancer Res*, 1988. **48**(21): p. 6037-43.
43. Krishna, R. and L.D. Mayer, *Multidrug resistance (MDR) in cancer. Mechanisms, reversal using modulators of MDR and the role of MDR modulators in influencing the pharmacokinetics of anticancer drugs*. *Eur J Pharm Sci*, 2000. **11**(4): p. 265-83.
44. Hipfner, D.R., R.G. Deeley, and S.P. Cole, *Structural, mechanistic and clinical aspects of MRP1*. *Biochim Biophys Acta*, 1999. **1461**(2): p. 359-76.
45. Abbott, B.L., et al., *Low levels of ABCG2 expression in adult AML blast samples*. *Blood*, 2002. **100**(13): p. 4594-601.

46. Litman, T., et al., *From MDR to MXR: new understanding of multidrug resistance systems, their properties and clinical significance*. Cell Mol Life Sci, 2001. **58**(7): p. 931-59.
47. Sato, K., S. Tsuchida, and K. Tamai, [*Anti-cancer drug resistance and glutathione S-transferases*]. Gan To Kagaku Ryoho, 1989. **16**(3 Pt 2): p. 592-8.
48. Coldman, J.H.G.a.A.J., ed. *Drug resistance in cancer : models and mechanisms*. 1998, Cambridge University Press: Cambridge, UK ; New York, N.Y. p.59-86.
49. Coldman, J.H.G.a.A.J., ed. *Drug resistance in cancer : models and mechanisms*. 1998, Cambridge University Press: Cambridge, UK ; New York, N.Y. p.66.
50. Banerjee, D., et al., *Novel aspects of resistance to drugs targeted to dihydrofolate reductase and thymidylate synthase*. Biochim Biophys Acta, 2002. **1587**(2-3): p. 164-73.
51. Zijlstra, J.G., et al., *Topoisomerases, new targets in cancer chemotherapy*. Med Oncol Tumor Pharmacother, 1990. **7**(1): p. 11-8.
52. Pegg, A.E., *Repair of O(6)-alkylguanine by alkyltransferases*. Mutat Res, 2000. **462**(2-3): p. 83-100.
53. Buermeier, A.B., et al., *Mammalian DNA mismatch repair*. Annu Rev Genet, 1999. **33**: p. 533-64.
54. Reed, E., *Platinum-DNA adduct, nucleotide excision repair and platinum based anti-cancer chemotherapy*. Cancer Treat Rev, 1998. **24**(5): p. 331-44.

55. Frosina, G., *Overexpression of enzymes that repair endogenous damage to DNA*. Eur J Biochem, 2000. **267**(8): p. 2135-49.
56. Lowe, S.W., et al., *p53-dependent apoptosis modulates the cytotoxicity of anticancer agents*. Cell, 1993. **74**(6): p. 957-67.
57. Miyashita, T., et al., *Identification of a p53-dependent negative response element in the bcl-2 gene*. Cancer Res, 1994. **54**(12): p. 3131-5.
58. Reed, J.C., *Bcl-2: prevention of apoptosis as a mechanism of drug resistance*. Hematol Oncol Clin North Am, 1995. **9**(2): p. 451-73.
59. Chen, Y.N., et al., *Characterization of adriamycin-resistant human breast cancer cells which display overexpression of a novel resistance-related membrane protein*. J Biol Chem, 1990. **265**(17): p. 10073-80.
60. Sharma, R., L. Arnold, and K.S. Gulliya, *Correlation between DNA topoisomerase II activity and cytotoxicity in pMC540 and merodantoin sensitive and resistant human breast cancer cells*. Anticancer Res, 1995. **15**(2): p. 295-304.
61. Vidal, L., et al., *Reversing resistance to targeted therapy*. J Chemother, 2004. **16 Suppl 4**: p. 7-12.
62. Bruce C. Baguley, D.J.K., ed. *Anticancer drug development*. 2002, London : Academic: San Diego, Calif. p.77-79.
63. Odaimi, M. and J. Ajani, *High-dose chemotherapy. Concepts and strategies*. Am J Clin Oncol, 1987. **10**(2): p. 123-32.

64. Tarella, C., et al., *Intensive chemotherapy in patients with lymphoma. Management of the risk of hyperuricemia*. *Contrib Nephrol*, 2005. **147**: p. 93-104.
65. Coffey, J.C., et al., *Excisional surgery for cancer cure: therapy at a cost*. *Lancet Oncol*, 2003. **4**(12): p. 760-8.
66. Perry, M.C., *The chemotherapy source book*. 1996, Baltimore: Williams & Wilkins. p.66.
67. Shibata, S., *Chemistry and cancer preventing activities of ginseng saponins and some related triterpenoid compounds*. *J Korean Med Sci*, 2001. **16 Suppl**: p. S28-37.
68. Popovich, D.G. and D.D. Kitts, *Structure-function relationship exists for ginsenosides in reducing cell proliferation and inducing apoptosis in the human leukemia (THP-1) cell line*. *Arch Biochem Biophys*, 2002. **406**(1): p. 1-8.
69. Lee, Y., et al., *A ginsenoside-Rh1, a component of ginseng saponin, activates estrogen receptor in human breast carcinoma MCF-7 cells*. *J Steroid Biochem Mol Biol*, 2003. **84**(4): p. 463-8.
70. Wakabayashi, C., et al., *An intestinal bacterial metabolite of ginseng protopanaxadiol saponins has the ability to induce apoptosis in tumor cells*. *Biochem Biophys Res Commun*, 1998. **246**(3): p. 725-30.
71. Zhou, S., L.Y. Lim, and B. Chowbay, *Herbal modulation of P-glycoprotein*. *Drug Metab Rev*, 2004. **36**(1): p. 57-104.

72. Radad, K., et al., *Ginsenosides Rb1 and Rg1 effects on mesencephalic dopaminergic cells stressed with glutamate*. Brain Res, 2004. **1021**(1): p. 41-53.
73. Molnar, J., et al., *Membrane associated antitumor effects of crocine-, ginsenoside- and cannabinoid derivates*. Anticancer Res, 2000. **20**(2A): p. 861-7.
74. Kim, S.W., et al., *Reversal of P-glycoprotein-mediated multidrug resistance by ginsenoside Rg(3)*. Biochem Pharmacol, 2003. **65**(1): p. 75-82.
75. Kim, S.E., et al., *Ginsenoside-Rs4, a new type of ginseng saponin concurrently induces apoptosis and selectively elevates protein levels of p53 and p21WAF1 in human hepatoma SK-HEP-1 cells*. Eur J Cancer, 1999. **35**(3): p. 507-11.
76. Kim, H.E., et al., *Ginsenoside RH-2 induces apoptotic cell death in rat C6 glioma via a reactive oxygen- and caspase-dependent but Bcl-X(L)-independent pathway*. Life Sci, 1999. **65**(3): p. PL33-40.
77. Jia, W.W., et al., *Rh2, a compound extracted from ginseng, hypersensitizes multidrug-resistant tumor cells to chemotherapy*. Can J Physiol Pharmacol, 2004. **82**(7): p. 431-7.
78. Kikuchi, Y., et al., *Inhibition of human ovarian cancer cell proliferation in vitro by ginsenoside Rh2 and adjuvant effects to cisplatin in vivo*. Anticancer Drugs, 1991. **2**(1): p. 63-7.

79. Tode, T., et al., [*In vitro and in vivo effects of ginsenoside Rh2 on the proliferation of serous cystadenocarcinoma of the human ovary*]. Nippon Sanka Fujinka Gakkai Zasshi, 1992. **44**(5): p. 589-94.
80. Tode, T., et al., *Inhibitory effects by oral administration of ginsenoside Rh2 on the growth of human ovarian cancer cells in nude mice*. J Cancer Res Clin Oncol, 1993. **120**(1-2): p. 24-6.
81. Tode, T., et al., [*Inhibitory effects of oral administration of ginsenoside Rh2 on tumor growth in nude mice bearing serous cyst adenocarcinoma of the human ovary*]. Nippon Sanka Fujinka Gakkai Zasshi, 1993. **45**(11): p. 1275-82.
82. Yun, T.K., *Experimental and epidemiological evidence on non-organ specific cancer preventive effect of Korean ginseng and identification of active compounds*. Mutat Res, 2003. **523-524**: p. 63-74.
83. Oh, S.H. and B.H. Lee, *A ginseng saponin metabolite-induced apoptosis in HepG2 cells involves a mitochondria-mediated pathway and its downstream caspase-8 activation and Bid cleavage*. Toxicol Appl Pharmacol, 2004. **194**(3): p. 221-9.
84. Tohda, C., et al., *Abeta(25-35)-induced memory impairment, axonal atrophy, and synaptic loss are ameliorated by M1, A metabolite of protopanaxadiol-type saponins*. Neuropsychopharmacology, 2004. **29**(5): p. 860-8.

85. Takei, M., et al., *Dendritic cells maturation promoted by M1 and M4, end products of steroidal ginseng saponins metabolized in digestive tracts, drive a potent Th1 polarization.* *Biochem Pharmacol*, 2004. **68**(3): p. 441-52.
86. Kim, Y.H., et al., *Transglycosylation to ginseng saponins by cyclomaltodextrin glucanotransferases.* *Biosci Biotechnol Biochem*, 2001. **65**(4): p. 875-83.
87. Popovich, D.G. and D.D. Kitts, *Mechanistic studies on protopanaxadiol, Rh2, and ginseng (Panax quinquefolius) extract induced cytotoxicity in intestinal Caco-2 cells.* *J Biochem Mol Toxicol*, 2004. **18**(3): p. 143-9.
88. Ota, T., M. Maeda, and S. Odashima, *Mechanism of action of ginsenoside Rh2: uptake and metabolism of ginsenoside Rh2 by cultured B16 melanoma cells.* *J Pharm Sci*, 1991. **80**(12): p. 1141-6.

CHAPTER 2. EFFECT OF APPD ON P-GLYCOPROTEIN IN MULTIDRUG RESISTANT CELLS

2.1 Introduction

P-gp, an identified mammalian multidrug transporter, pumps various cytotoxic drugs out of the cells and mediates drug resistance termed classical MDR. P-gp is a 170-kDa glycosylated membrane associated transport protein coded by a gene called multiple drug resistance 1 (MDR1), which is located at the long arm of chromosomal location 7q21.1 in humans [1]. Normally, P-gp widely expresses in tissues including adrenal, gravid uterus, kidney, liver, colon, and capillary endothelium in the brain [2]. High expression of P-gp is an important mechanism of the BBB that limits most anticancer drugs from entering into the brain for treatment of intracranial tumors. Concentrations of many anticancer drugs in the brain increased in P-gp knockout mice [3, 4]. Increased expression of P-gp is associated with the intrinsically drug-resistant cancers of the colon, kidney, and adrenal as well as some tumors, which acquire drug resistance after chemotherapy [5]. Over expression of P-gp causes cancer cells to be resistant to a variety of structurally and functionally dissimilar anticancer drugs, such as vinblastine, vincristine, doxorubicin, paclitaxel and many others [2, 4, 6, 7]. Up to 50% of gliomas were found to have P-gp positive cells [8]. P-gp expression levels correlate well with poor response to chemotherapy [9].

P-gp is a protein of 1280 amino acids with 12 transmembrane regions (TM) and two

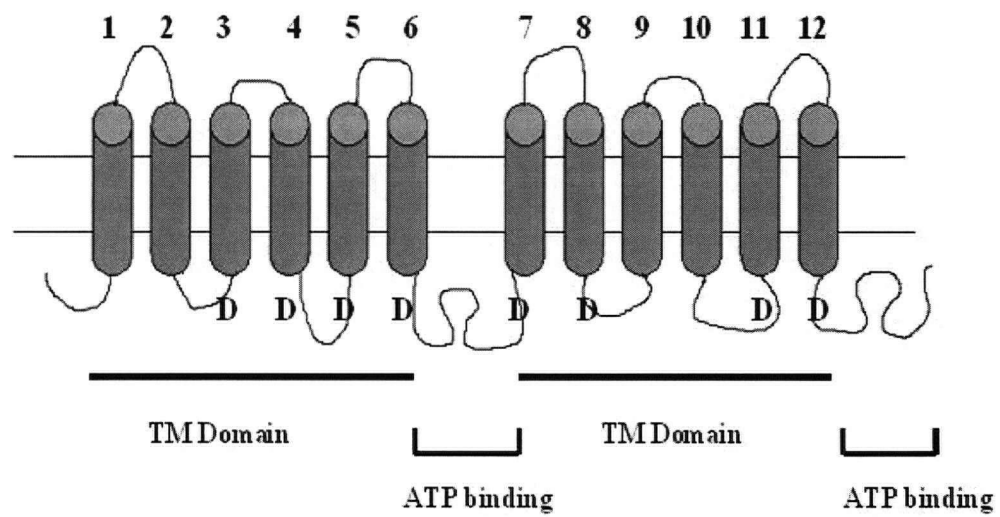


Fig. 2-1. P-gp model

D: drug binding sites

ATP-binding sites (BND), separated by a flexible linker polypeptide region between the Walker A and B motifs (Fig. 2-1) [1, 10, 11]. TM1-6 parallel to TM7-12 is proposed as one of the topology models of P-gp. This model predicts that crosslinking would be possible between TM1/TM7, TM2/TM8, TM3/TM9, TM4/TM10, TM5/TM11 and TM6 /TM12. Loo and colleagues using site-directed mutagenesis studies demonstrated that drug binding sites of P-gp were scattered throughout the molecule and resided in or near the TM 3, 4, 5, 6, 7, 8, 11, 12, the ATP-binding domains and intracellular loops [12]. Particularly, the regions encompassed by TM 5-11 as well as TM 6-12 were involved with drug transport. Protection from inactivation suggested that the residues of TM11-12 were important for the interaction of verapamil, vinblastine and colchicines [6, 10, 12], while TM6 is responsible for nucleotide binding and ATP hydrolysis [13].

P-gp inhibition is an option for improving drug delivery to tumor cells and enhancing the tumor response to chemotherapy. Various compounds, including calcium channel blockers (verapamil), immunosurpressant (cyclosporines), calmodulin inhibitors (chlorpromazine) and many others, have been shown to enhance the cytotoxic activity of various antitumor drugs in MDR cells by antagonizing P-gp and increasing the drug accumulation, whereas these agents show almost no effect on drug-sensitive cells. In general, P-gp can be blocked via three different mechanisms [11]. The first is by blocking binding site competitively, non-competitively or allosterically. For instance, ginsenosides Rg3 was demonstrated to compete with anticancer drugs for

binding to P-gp thereby blocking drug efflux [14]. The second is by interfering with ATP hydrolysis. Quercetin was reported to strongly inhibit Hoechst 33342 transport by inhibiting the ATPase activity of P-gp [15]. The third is by altering the integrity of cell membrane lipids. Reserpine and verapamil were observed to change the physical properties of biomembranes, including altered fluidity and increased permeability by interaction with the lipid bilayer and biomembranes [16]. However, most of the drugs inhibit P-gp functioning by blocking drug-binding sites. Recent studies indicate that there are more than two drug binding sites in P-gp with overlapping drug specificities, but with non-identical drug binding affinities [17, 18]. A P-gp reverse agent can be a P-gp substrate, an inhibitor or both [3, 6, 11, 19, 20]. The property and effect of a compound on P-gp can be further demonstrated by using an ATPase assay with the pure P-gp protein or the cell with intact P-gp expression, and proper probe substrates and inhibitors [10, 21]. A stimulation of the ATPase is the hallmark of P-gp substrate and correlates with increasing P-gp inhibition [6].

Currently, the development of P-gp inhibitors has been disappointing [19]. In clinical trials, the first generation modulators, such as verapamil and cyclosporine A, caused various adverse effects. Because a low potency of P-gp inhibition requires administration of high doses of P-gp inhibitor, adverse pharmacological effects usually occur, including an unacceptable cardiotoxicity caused by verapamil and an immunosuppressive effect induced by cycloporines. Clinical application of the second-generation modulators is also limited because the effects on cytochrome P450

3A4-mediated drug metabolism are unpredictable with these modulators, such as PSC-833, therefore, a safe but also effective dose of a co-administered chemotherapeutic agent is difficult to determine [2, 22]. Considering the limitations of current P-gp modulators, optimal new-generation P-gp inhibitor should have low nonspecific cytotoxicity, high P-gp specificity, and a relatively long duration of action with reversibility as well as good oral bioavailability. These properties along with uncomplicated drug interaction, would be important for the development of new P-gp inhibitors [2].

Ginsenosides Rg3, Rh2 and their aglycone metabolites demonstrated inhibitory effects on cell growth on both MDR and non-MDR cell lines when applied alone [14, 23-27]. A few ginsenosides are also shown to exert the reverse activity of P-gp. These ginsenosides include Rg1, Re in protopanaxatriol (PPT) family [28] as well as Rg3, Rh2 and Rc in protopanaxadiol (PPD) family. All of them significantly sensitize multiple drug resistant cell lines to anticancer drugs both in vitro and in vivo [14, 25, 27]. For the ginsenosides in PPD family, Hasegawa et al indicated that Rh2 enhanced the cytotoxicity of daunomycin and vinblastine in multiple drug resistant P388/ADM cell [27]. Rg3 not only sensitized MDR cell KBV20C to anticancer drugs in vitro, but co-injection of Rg3 and DOX into mice carrying a multiple drug resistant P388 transplantable tumor also significantly increased the survival time of the mice compared to DOX treatment alone [14]. Because aPPD is the metabolic product of ginsenoside Rg3 and Rh2 [29, 30], Rh2 and Rg3 may exert its cytotoxicity and P-gp

inhibitory effect through their deglycosylation product aPPD. Among the ginsenosides in PPD and PPT families, aPPD has demonstrated the strongest anticancer activity to Int-407, Caco-2 and multiple drug resistant cells P388ADM with the lowest IC_{50} s shown in Table 2-1 [27, 31].

Previous studies by our group have also shown that Rh2 and aPPD can significantly enhance the cytotoxicity of various chemotherapy drugs, especially in MDR cancer cells. Since these compounds induce cytotoxicity themselves, one possible mechanism for the chemosensitization effect is that the apoptotic nature of these compounds may synergistically work with chemotherapeutics [32]. Another possible mechanism for the synergy is that aPPD may block P-gp in MDR cells to sensitize the cells to the cytotoxicity induced by chemotherapeutics. An in vivo study in our lab has shown that aPPD inhibited tumor growth and extended the animal's life span in an intracranial glioma model, suggesting that the compound may cross the BBB and part of the mechanism may rest on the inhibitory effect of aPPD on P-gp to overcome BBB and it's the most nonpolar chemical structure in ginsenosides. Therefore, aPPD is the most promising agent for treatment of brain tumors among many other protopanaxadiol ginsenosides. However, there has been lack of direct evidence demonstrating the P-gp inhibitory effect on P-gp by aPPD.

In the present chapter, the effects of aPPD on P-gp in MDR cells of both humans and mice were tested using a P-gp substrate, calcein AM as efflux indicator and verapamil

Table 2-1 IC₅₀ of ginsenosides with P-gp inhibitory effect on multiple drug resistant P388 cells

Ginsenosides [27]	IC ₅₀ (μM)	IC ₅₀ (μg/ml)
aPPD	37.2	17.1
Rh2	62.8	39.6
Rg3	75.3	74.1
Rc	497	535.8
Rg1	250	200
Re	519	491

as a positive control of P-gp blocker. Furthermore, as a preliminary attempt to distinguish the mechanism of aPPD from other P-gp blockers, ATPase activity of P-gp in the presence of aPPD was also measured.

2.2 Materials and methods

2.2.1 Drugs and chemicals

Pure (99.6%) aglycone 20(s)-Protopanaxadiol (aPPD) and crude aPPD were provided by Pegasus Pharmaceuticals Inc. Careseeng (crude aPPD) contains aPPD 57%, 20(s)-protopanaxatriol (aPPT) 23%, Rh2 6%, was used in preliminary study to investigate the anticancer effect of aPPD. Both crude aPPD and aPPD were diluted to 50 mg/ml in 100% ethanol and the stock was kept in 4°C and the aPPD was stable in its purity and component in the experiment demonstrated by HPLC (data not shown). Verapamil, MTT [3-(4,5-dimethylthiazol-2-yl)-2,5- diphenyltetrazolium bromide] was purchased from Sigma- Aldrich (Oakville, Ontario, Canada). Calcein AM was purchased from Molecular Probe Inc (San Diego, CA, USA). Dimethyl sulfoxide (DMSO), SDS was purchased from Bio-RAD Laboratories (Mississauga, Ontario, Canada). Trypsin with 0.03% EDTA was purchased from Invitrogen (Vancouver, B.C. Canada).

2.2.2 Cell lines

P388 is a mouse leukemia cell line [33]. P388adr, the multiple drug resistant cells with P-gp overexpression, and the parental cell line P388 (P388wt) cells were purchased from the ATCC (Manassas, VA, USA). Human breast cancer cells MCF-7adr with P-gp overexpression and the parental cell line MCF-7 (MCF-7 wt) were obtained from the BC Cancer Agency, Vancouver, Canada. All the cells were grown in DMEM (Canadian Life Technologies Inc. Mississauga, Ontario, Canada) containing 10% fetal bovine serum, 100 U/ml penicillin and 100 µg/ml streptomycin. Cells were incubated at 37°C under a humidified atmosphere of 5% CO₂ and media were replaced every 3 days.

2.2.3 In vitro cell viability assay

Cells were maintained in drug free media for three days before the drug treatment. Cell viability assays were conducted by plating attaching cells (3×10^4) or suspension cells (10^5) in each well of a 96-well plate and incubating them for 24 h. The cells were then treated with increasing concentrations of aPPD or chemotherapeutic drugs in the medium supplemented with 2% FBS. Cells were kept in 5% CO₂ at 37°C for the desired time before 50 µl of 1 mg/ml MTT was added to each well. After incubation at 37°C for 4 h, 100 µl of DMSO was added. The color reaction was measured by a spectrometer (µQuant Bio-tech Instrument Inc, Tustin CA) at the wavelength of 570 nm. Cell viability was assessed by the ratio of absorbance of drug-treated cells to untreated controls.

2.2.4 Fluorescent calcein formation assay

Calcein AM is the substrate of P-gp and is able to be pumped out of the cells in P-gp overexpressing cells. Once in the cell, non-fluorescent calcein AM can be converted to fluorescent calcein by the cellular esterases. Since calcein is not a substrate of P-gp, it remains in the cells. The cells with calcein remains inside are fluorescent. In the cells without overexpression of P-gp, calcein AM rapidly penetrates and is converted to free, fluorescent calcein via intracellular esterases, while the free calcein accumulates much more slowly in P-gp overexpression cells. To evaluate the effect of P-gp inhibition by aPPD, P-gp overexpressing MCF-7adr cells were seeded into a 6-well plate and grown for 24 h. The cells were then incubated with a medium containing 40 µg/ml aPPD and 2% FBS in 5% CO₂ at 37° for 15 min. Finally, calcein AM was added to the cells at a final concentration of 0.25 uM. Incubated in 5% CO₂ at 37° for another 15 min, the cells were observed under an inverted fluorescent microscopy (FluoArc, Axiovert -200). Forty micromolar verapamil, a typical P-gp reverse agent, was used as positive control.

2.2.5 Calcein AM efflux inhibition assay

The kinetics of calcein formation can be monitored continuously [34, 35]. When blockers inhibit the pumping activity of P-gp, high levels of fluorescent calcein were produced within the cells and can be assayed by its fluorescence. Calcein accumulation in P388 cells was used for quantitative measurement of the effect of aPPD on P-gp activity. The cells were harvested in logarithmic growth phase and

resuspended in the medium with 2% FBS. P388adr cells 10^6 were plated in each well of a 96-well plate and incubated with crude aPPD 40 $\mu\text{g/ml}$ for 15 min at 37°C. Calcein AM was added to a final concentration of 0.025 μM . Fluorescence accumulation in the cells was measured every 90 s for 2 h, with a microplate fluorescence reader (Spectra MAX Gemini, XS02842) at the wavelength of 494 nm for excitation and 517 nm for emission.

2.2.6 ATPase activity of P-gp assay

Stimulation of ATPase is one of the hallmarks of P-gp substrate [6, 21]. The P-gp associated ATPase activity in the membrane of CH^RB30 cells was determined colorimetrically as the vanadate sensitive release of inorganic phosphate from ATP [36]. A 60 μl reaction mixture containing 40 μg membranes with high levels of P-gp, crude aPPD (0, 2.2, 6.7, 20, and 60 $\mu\text{g/ml}$), 3 mM MgATP, 50 mM Tris-MES, 2 mM EGTA, 50 mM KCl, 2 mM dithiothreitol, and 5 mM sodium azide, was incubated at 37°C for 20 min. Twenty micromolar verapamil served as the positive control in this assay system. An identical reaction mixture containing 100 μM sodium orthovanadate was assayed in parallel. Orthovanadate inhibits P-gp by trapping MgADP in the nucleotide-binding site. Thus, ATPase activity measured in the presence of orthovanadate shows non-Pgp ATPase activity and can be subtracted from the activity generated without orthovanadate, to yield vanadate-sensitive ATPase activity. The reaction was stopped by the addition of 30 μl 10 % SDS + Antifoam A. Two additional reaction mixtures (with or without orthovanadate) but without MgATP,

were also prepared and incubated with the others as controls, and then SDS and MgATP were added, to represent 0 min timepoint of the reaction. The incubations were followed by addition of 200 μ l of 35 mM ammonium molybdate in 15 mM zinc acetate: 10% ascorbic acid (1:4) and incubated for an additional 20 min at 37°C. The liberation of inorganic phosphate was detected using a spectrometer (μ Quant Bio-tech Instrument Inc). Its absorbance was at 800 nm and determined by comparing the absorbance of a phosphate standard curve.

2.2.7 Additive effect of aPPD with verapamil in P-gp inhibition

Human MCF-7adr cells in the logarithmic growth phase were plated in a 96-well plate 3×10^4 in each well and grown for 24 h. The cells were incubated in the medium with 2% FBS containing crude aPPD with increasing concentrations of 0, 2.2, 6.7, 20, 40, 60 μ g/ml in the presence or the absence of 2.5 μ M verapamil. After the cells were incubated with drugs for 15 min at 37°C, calcein AM was added to a final concentration of 0.025 μ M and kept at 37°C for additional 15 min. Using a microplate fluorescence reader (Spectra MAX Gemini, XS02842), fluorescence of calcein in the cells was read at 5 random points in each well with a wavelength of 494 nm for excitation and 517nm for emission. Data were collected as quadruplicates for each concentration in the treatment group.

2.2.8 Endurable effect of P-gp inhibition assay

P388adr cells were suspended in DMEM with 2% FBS and plated in a 96-well plate with cells 10^6 in each well. The cells were incubated with 40 $\mu\text{g/ml}$ crude aPPD for 2h in 5% CO_2 at 37°. At the end of incubation, the cells were washed with PBS followed by centrifugation at $1000 \times g$ for 10 min twice at 4°C, and resuspended in 100 μl medium with 2% FBS. The cells were immediately incubated with 0.025 μM calcein AM in 5% CO_2 at 37° for 15 min. Fluorescence accumulation in the cells was measured with the microplate fluorescence reader described earlier. The cells with drug-free medium were used as the negative control. There were quadruplicate wells for each time point.

2.2.9 Statistical analysis

All data are expressed as mean \pm SD. Student's unpaired t-test (2-tail) was used for comparisons between two means. One-way ANOVA followed by post hoc test was used to compare the difference between the groups of drug treatment and untreated controls, and two-way ANOVA was used to compare two groups of drug treatments using SPSS (SPSS, WI. USA). $P < 0.05$ was considered as significant in the analysis.

2.3 Results

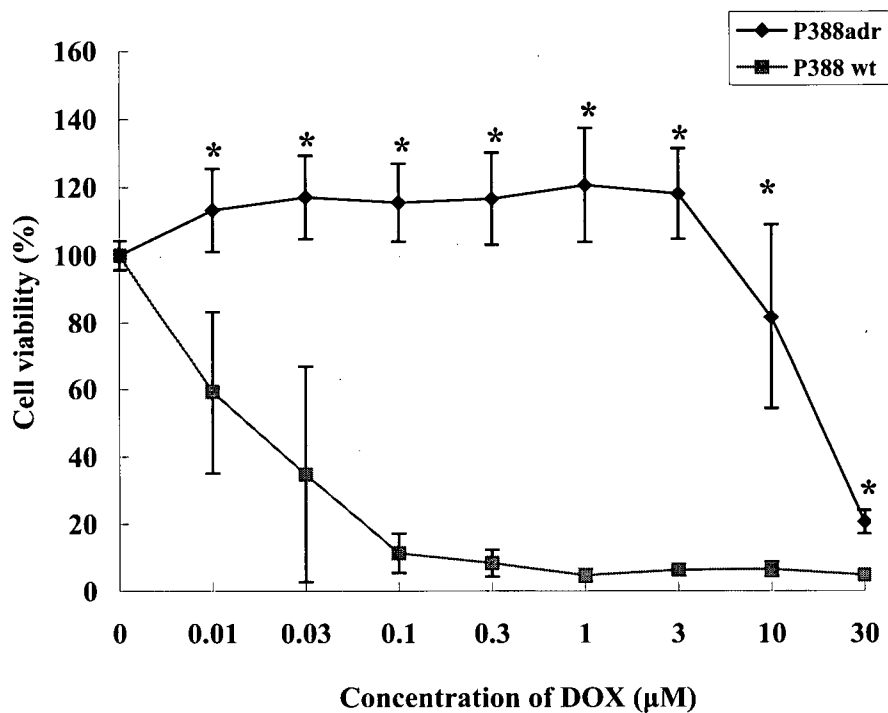
2.3.1 Equal cytotoxicity on P-gp positive and negative cells by aPPD

Sensitivity of both P388wt and its P-gp positive daughter cell line P388adr to DOX and aPPD were measured. Fig.2-2 A showed the viability of P388adr and P388wt cells treated with DOX for 72 h. P388 cells were more than 3-fold more sensitive to DOX than its MDR counterpart P388adr cells. The IC_{50} s of P388adr and P388wt for DOX were $0.177 \pm 0.017 \mu\text{M}$ and $0.626 \pm 0.013 \mu\text{M}$, respectively ($P < 0.01$). It is believed that the resistance to DOX in P388adr cells was caused by overexpression of P-gp [20]. Interestingly, P388adr and P388wt cells had similar IC_{50} s for aPPD induced cytotoxicity (Fig.2-2B). IC_{50} s of aPPD for P388adr and P388wt were $20.16 \pm 3.88 \mu\text{g/ml}$ and $16.89 \pm 1.37 \mu\text{g/ml}$, respectively ($P > 0.05$). Thus, overexpression of P-gp may not influence intracellular concentrations of aPPD, suggesting that aPPD is unlikely to be a substrate of P-gp.

2.3.2 Inhibited P-gp by aPPD

Inhibitory effects of aPPD on P-gp activity were observed in human breast cancer cells MCF-7adr for calcein AM fluorescence accumulation with fluorescent microscopy. Fig. 2-3A showed that in the absence of aPPD and verapamil, the level of fluorescent calcein was low in MCF-7adr cells, suggesting that P-gp was actively pumping its substrate calcein AM out of the cells and resulting in less intracellular fluorescent calcein formation. Fig. 2-3B showed when MCF-7adr cells were

A



B

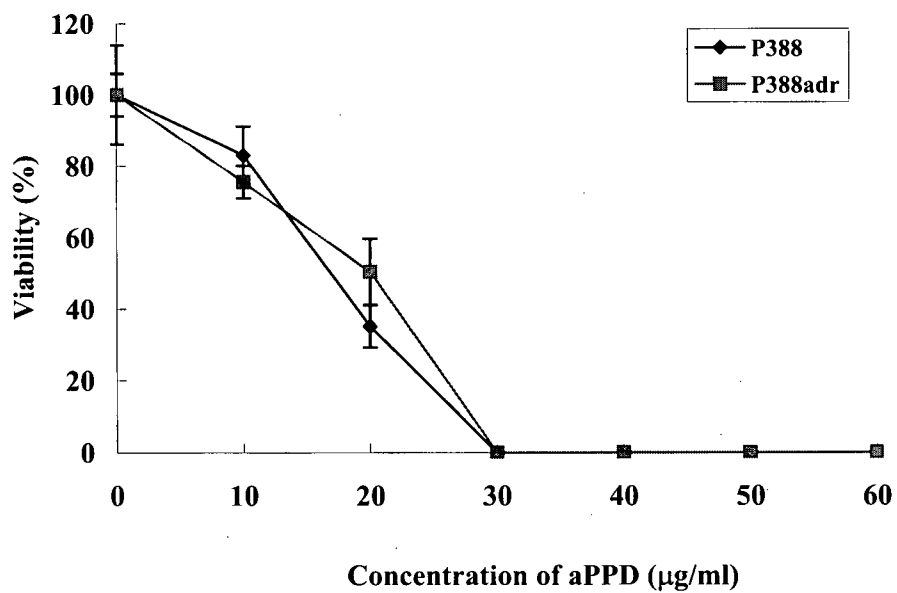


Fig. 2-2. Viability of P388 adr and P388wt cells in the presence of aPPD and

DOX

A) P388adr and P388wt cells were presented in DOX at 37°C for 72 h.

Viability was expressed as percentage of change relative to the control using MTT assay. Each point is the mean \pm SD of three experiments

* $p < 0.01$, p value was calculated from an independent t-test between two cell lines.

$p < 0.01$ in DOX treated groups compared with untreated controls in two cell lines

(Two-way ANOVA followed by Dunnett post hoc test).

B) P388adr and P388wt cells were incubated with indicated concentrations of aPPD at 37°C for 48 h.

Viability was expressed as percentage of change relative to aPPD vehicle control using MTT assay. Each point is the mean \pm SD of three experiments.

$p > 0.05$ vs P388 from an independent t-test between two cell lines.

$p < 0.01$ in aPPD treated groups compared with untreated controls in two cell lines

(Two-way ANOVA followed by Dunnett post hoc test).

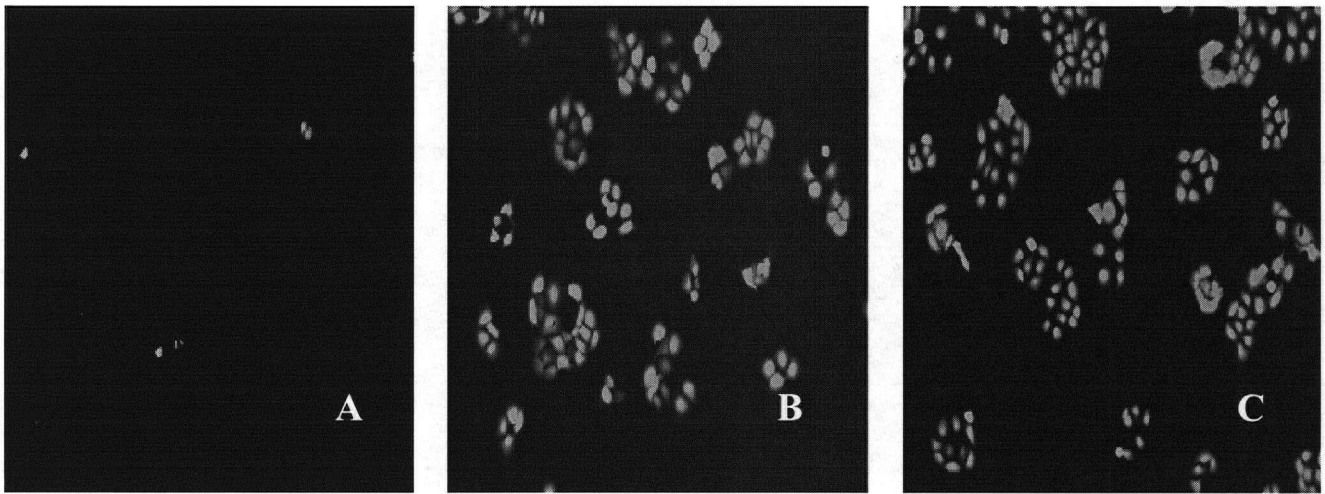


Fig. 2-3. Fluorescent calcein formation in MCF-7adr cells

The cells were incubated with aPPD, with verapamil or without drugs respectively. Fluorescence of calcein in MCF-7adr cells was observed and photographed using an Axiovert -200-inverted fluorescent microscope and a 40 \times phase-contrast objective.

A) MCF-7adr

B) MCF-7adr with aPPD 40 μ g/ml

C) MCF-7adr with verapamil 40 μ M

incubated with aPPD, the levels of fluorescent calcein were dramatically increased in all the cells. Fig. 2-3C shows the effects of verapamil, a substrate and competitive inhibitor of P-gp [10, 21] in the same cells. These results indicate that aPPD at the current concentration exerted an inhibitory effect on P-gp activity, at a similar level to verapamil in MCF-7adr.

To quantitatively evaluate the accumulation of P-gp substrate in cells treated with aPPD, calcein AM efflux by P388adr and P388wt cells in the presence of aPPD was examined. Fig. 2-4 shows the time dependence of calcein formation in P388adr and

wt cells with or without aPPD. It was obvious that calcein accumulation in P388adr, shown in Fig. 2-4A was two-fold lower than that in P388wt as shown in Fig. 2-4B. In the presence of 40 µg/ml aPPD, levels of calcein in P388adr cells increased to more than two-fold of that in the absence of aPPD (Fig. 2-4A). Meanwhile, Crude aPPD had no effect on the levels of calcein in P388wt cells, as shown in Fig. 2-4B.

2.3.3 Reversibly blocked P-gp activity by aPPD

To determine whether aPPD inhibits P-gp permanently or temporarily, P388adr cells were exposed to aPPD for designed time and then the drug was removed. Fig.2-5 shows that the level of intracellular calcein AM fluorescence was increased by 1.5-

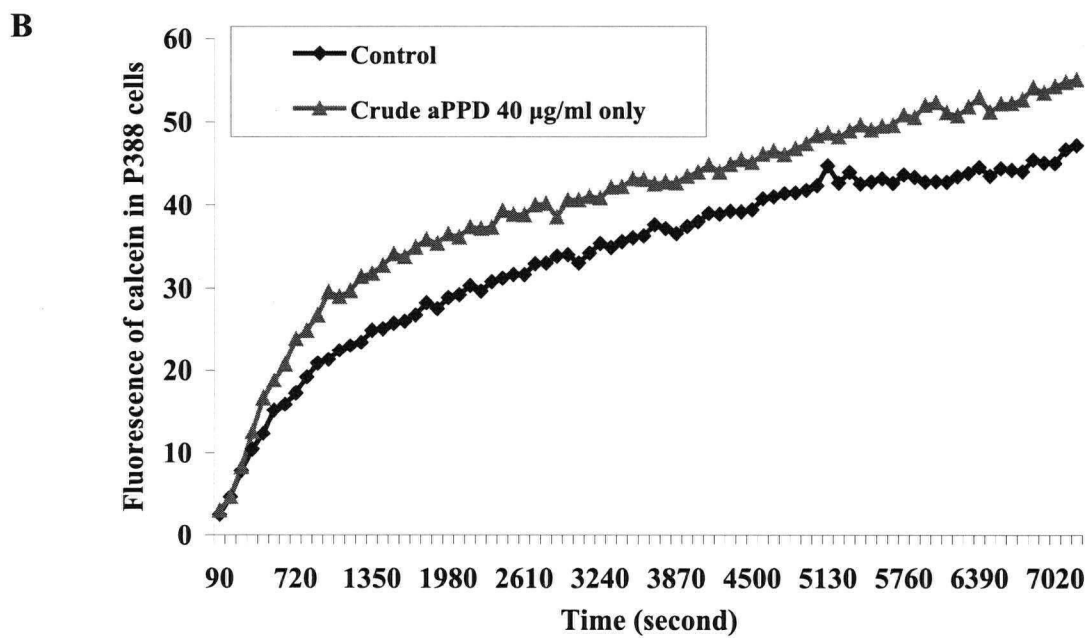
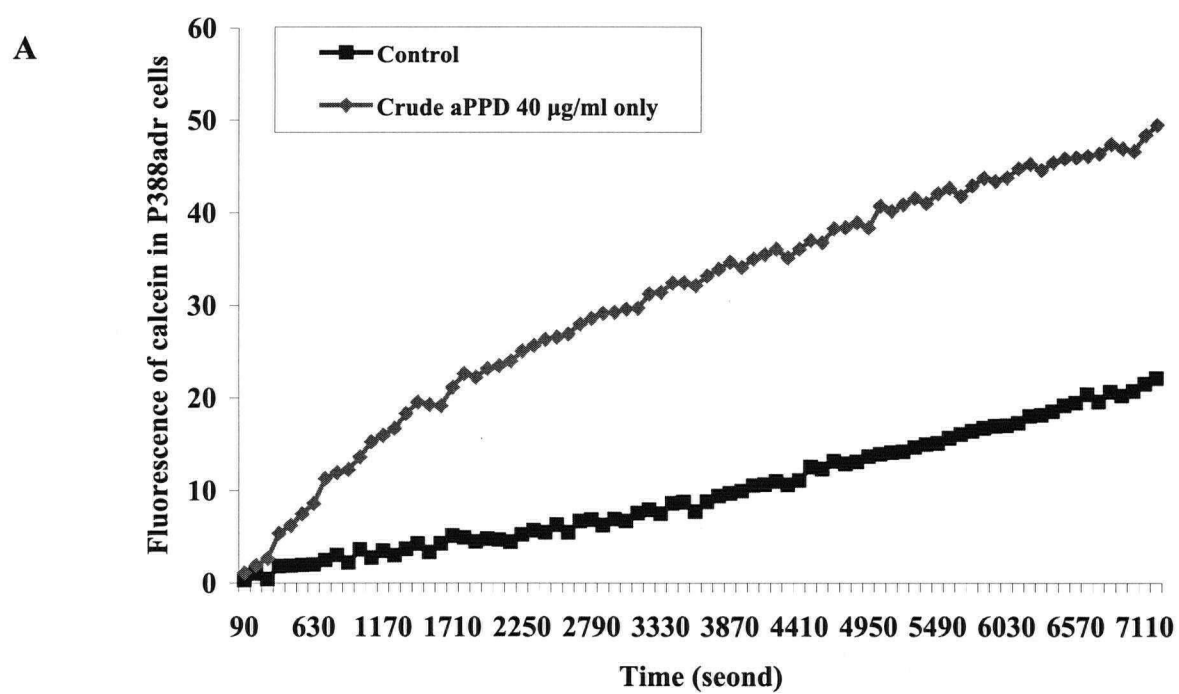


Fig. 2-4. P-gp efflux of P388adr (A) and P388wt (B) in the presence of aPPD

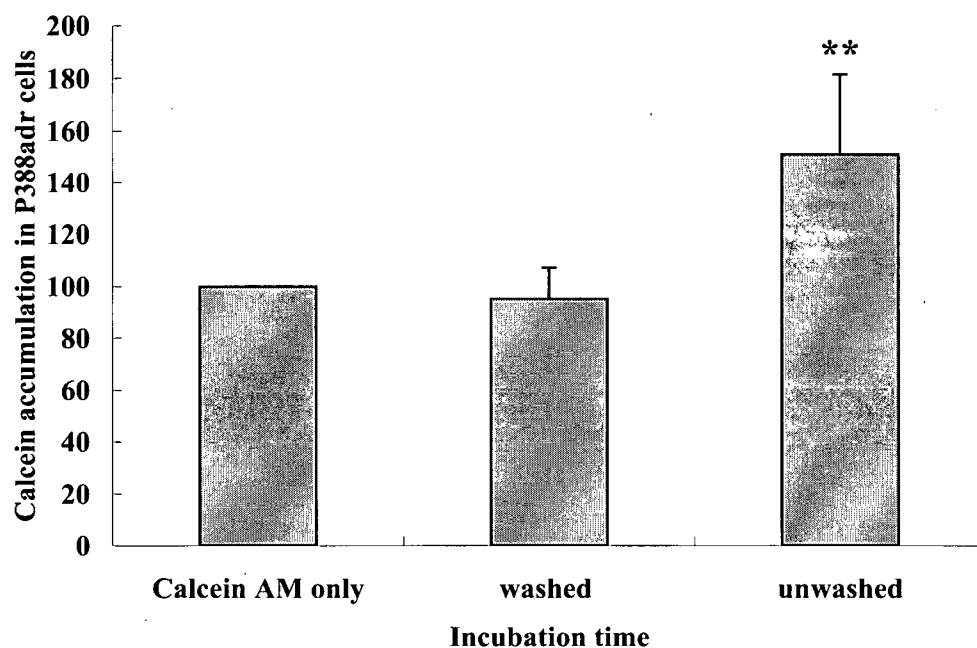


Fig. 2-5. Endurable effect of P-gp inhibition of aPPD

The P388adr cells were incubated in crude aPPD 40 $\mu\text{g/ml}$ at 37°C for 2 h times, then, the cells were washed with PBS or remained in aPPD and calcein accumulation in the cells was represented as the percentage of fluorescence change relative to the aPPD vehicle control. Data are expressed as the mean \pm SD of three experiments.

** , $p < 0.05$, p value was calculated from an independent t-test between the cells with calcein AM and the cells treated with aPPD.

when aPPD was removed from the cells after incubation, the P-gp activity immediately returned to control levels.

2.3.4 Ineffective ATPase activity of P-gp by aPPD

Many P-gp substrates and modulators, such as verapamil, stimulate the P-gp ATPase activity [10]. To further investigate the mechanism of aPPD caused P-gp inhibition, the ATPase activity of P-gp containing membrane was determined. Fig. 2-6 shows that aPPD did not stimulate the ATPase activity of P-gp, while verapamil, on the other hand, stimulated ATPase activity by 2-fold, compared to the control.

2.3.5 An additive effect on P-gp inhibition between verapamil and aPPD

The difference in ATPase activity of P-gp in the presence of verapamil and aPPD suggests that the two agents may inhibit P-gp with different mechanisms. To further explore this possibility, the effect of P-gp activity in cells was tested by treating them with a combination of aPPD and verapamil in human MCF-7adr cells. Fig. 2-7 shows a dose-dependent inhibition on P-gp in MCF-7adr cells with increasing concentrations of aPPD in absence and presence of 2.5 uM verapamil. It was clear that adding 2.5uM verapamil significantly increased intracellular levels of fluorescent calcein at all concentrations of aPPD and the combined effect of the two agents appeared additive in P-gp inhibition.

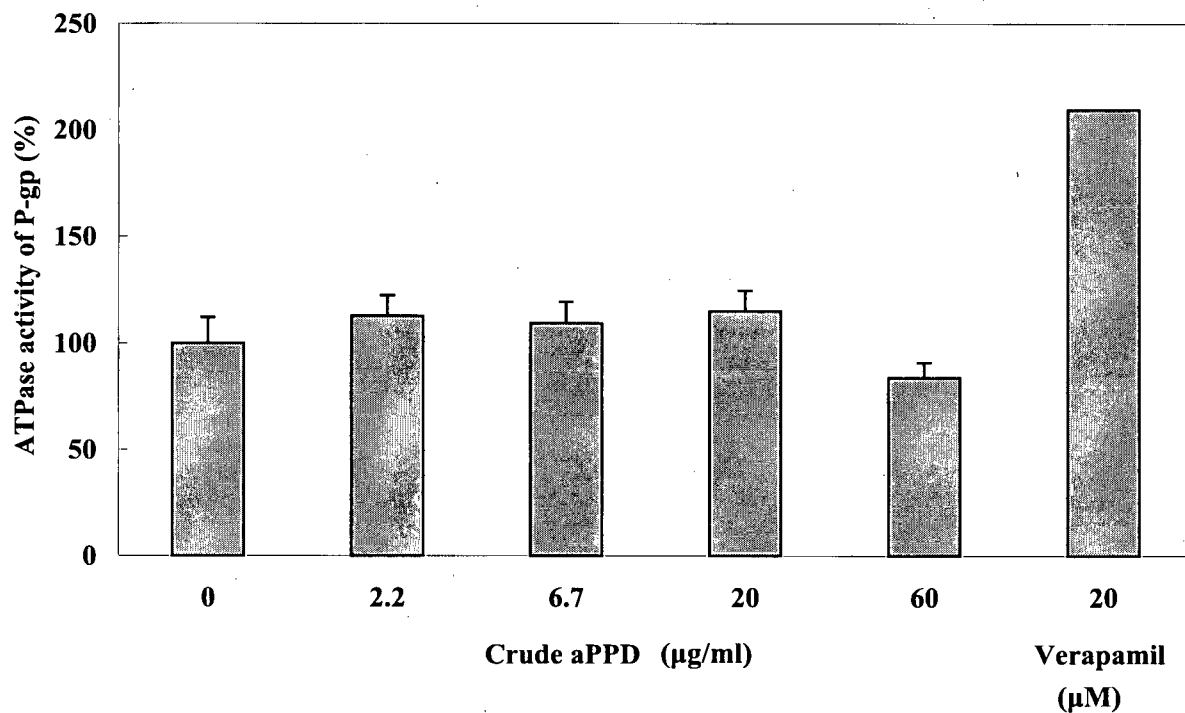


Fig. 2-6. Effect of crude aPPD on ATPase activity of P-gp

ATPase activity of P-gp expressing membranes was measured in the presence of indicated concentrations of crude aPPD or verapamil. Data are expressed as the mean \pm SD of two experiments and represents as percentage of change, compared to the ATPase activity of untreated membrane.

$P > 0.05$ in crude aPPD treated groups compared with untreated control.

(One-way ANOVA)

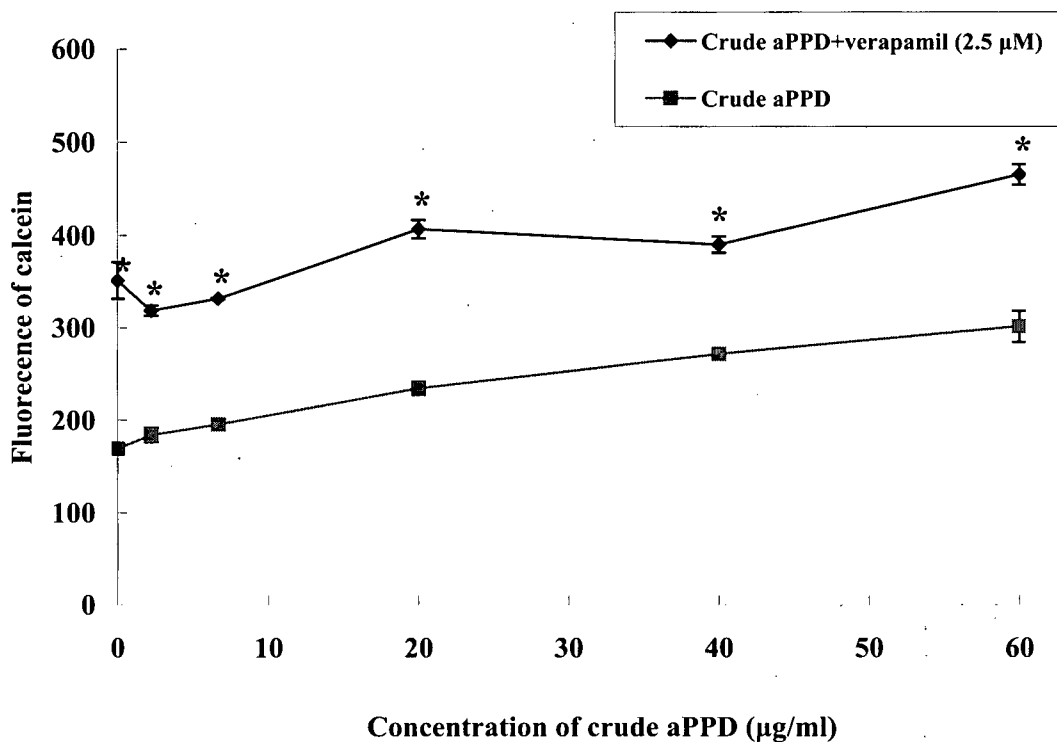


Fig. 2-7. The additive effect of aPPD and verapamil on P-gp efflux ability

Calcein accumulation in MCF-7adr cells, which were incubated with the indicated concentrations of aPPD or aPPD plus verapamil 2.5 μM, was represented as fluorescent intensity. The point of 0 μg/ml crude aPPD represented the effect of verapamil 2.5 μM. Data are expressed as the mean ± SD of four measurements.

*, $p < 0.01$, p value was calculated from an independent t-test between the cell line treated with aPPD and aPPD with verapamil.

$p < 0.01$ in aPPD or aPPD and verapamil 2.5 μM treated groups compared with controls. (Two-way ANOVA)

Table 2-2 P-gp inhibitory effect of verapamil and ginsenosides

P-gp inhibitory effect and mechanism	Verapamil	Ginsenosides (Rg3, Rh2 or aPPD)	Reference
Increased drug accumulation in MDR cells	+	+	[6, 37]
Inhibit P-gp efflux	+	+	[14, 37]
Sensitize MDR cells	+	+	[6, 14]
Uptake by the cells	+	+	[21, 25]
Substrate of P-gp	+	+/-	[21, 25]
Binding to P-gp *	+	+/-	[12, 14]
ATPase stimulation	+	-	[14, 21]
Cytotoxicity to MDR cells	-	+	[14]
Increased P-gp expression	+	-	[14]

Note: +, the compound has the described effect. -, The compound has no described effect. +/- the compound may have the described effect.

*, Verapamil binds to P-gp on TM 6 and 12 and Ginsenosides (Rg3, Rh2 or aPPD) may bind to Azidopine binding site.

2.4 Discussion

This study first indicated that an aglycone ginsenoside aPPD, a metabolic product of the panaxadiol saponins, was a highly effective inhibiting agent for P-gp in MDR cells. The fluorescent calcein formation assay (Fig.2-3) demonstrated that aPPD inhibited the P-gp activity to cause increased drug accumulation in both P388adr and MCF7adr cells that expressed high levels of P-gp. aPPD caused an elevated intracellular concentration of calcein that was specific to P-gp related drug efflux as no increased calcein formation was seen in P-gp negative cells (Fig.2-4).

At the present time, very little information is available on the mechanism of P-gp inhibition by ginsenosides Rg3, Rh2 and aPPD demonstrated in this study. All three compounds are similar in structures with a four trans-ring rigid steroid skeleton. Rg3 and Rh2 but not aPPD have glucopyranoside chain at carbon number 3 [38, 39]. Table 2-2 compares the ginsenosides P-gp inhibitors and verapamil. The three ginsenosides have similar potency as verapamil on P-gp inhibition. Verapamil is known as a substrate of P-gp itself [40]. The ginsenosides, on the other hand, may or may not be the P-gp substrate. Rg3 was shown to compete with the anticancer agent azidopine to bind to P-gp, suggesting the binding site for both P-gp blockers may be the same. However, there is still lack of direct evidence to demonstrate that Rg3 is being transported by P-gp [14]. Rh2 was reported to be a P-gp substrate as verapamil increased the uptake of Rh2 in Caco-2 cells in culture [25]. However, using calcein

AM, the fluorescent substrate of P-gp, Caco-2 did not demonstrate P-gp activity in our lab (data not show). In addition, Xie, et al demonstrated that uptake of aPPD in Caco-2 cells was quite different from that of Rh2 in time course, PH dependence and concentration dependence [25]. Thus, the difference between the chemical structures of the two compounds might have quite a substantial influence in the bioactivity of the two compounds. Our results indicated that the P388wt and P-gp positive P388adr cells demonstrated the same sensitivity to aPPD which further argues against the notion that aPPD are a substrate of P-gp. It would be interesting to further investigate whether the ginsenosides lose their ability of being a substrate of P-gp after the sugar moiety is removed at No.3 carbon. There are two other characteristics that distinguish ginsenoside P-gp blocker (at least aPPD) from verapamil. One is that verapamil causes upregulation of MDR1 mRNA levels and results in increased P-gp expression, but Rg3, Rg1 and Re did not appear to increase P-gp levels [14, 28]. The second is that verapamil stimulated P-gp ATPase activity while aPPD had no effect. Stimulation of ATPase activity is common in P-gp substrates, but not all P-gp substrates or inhibitors enhance ATPase activity. Cyclosporine A, daunorubicin and colchicines are all known P-gp substrates but their interaction with P-gp does not affect ATPase activity [10, 11]. Nevertheless, the difference on ATPase activity differentiates aPPD and verapamil induced P-gp inhibition by their mechanisms. Furthermore, co-administration of aPPD and verapamil (Fig.2-6) showed an additive effect in P-gp inhibition as described earlier. The above results indicated that aPPD binds to P-gp on the binding site different to verapamil, and further confirmed the notion that two

agents act on different sites of P-gp and may inhibit P-gp activity independently [17, 18]. Finally, ginsenosides with P-gp inhibitory effect such as Rg3, Rh2 and aPPD are all with cytotoxicity to cancer cells, but verapamil and many other chemosensitizers are not cytotoxic agents themselves. Interestingly, the inhibitory effect of aPPD on P-gp seems similar to that of cyclosporine A because both compounds did not stimulate ATPase and both of them exerted the cytotoxicity to the tumor cells [41]. However, the exact mechanism binding of aPPD to P-gp needs to be clarified by further studies.

Our results (Fig.2-5) further indicated that aPPD caused P-gp inhibition is reversible as the blockage of P-gp mediated calcein fluorescence efflux completely relied on the presence of aPPD and immediately abolished after removal of aPPD. This is potentially a safeguard for the clinical application of aPPD as a chemosensitizer. As P-gp is also present in normal tissues and plays an important role in preventing accumulation of xenobiotics [2], it would be desirable that the inhibition of P-gp should be reversible.

In conclusion, aPPD as a new “two-in-one” anticancer agent exhibits both cytotoxicity and P-gp inhibitory effects. aPPD reversibly inhibits P-gp by increasing the drug accumulation specifically in MDR cells, but with a different mechanism from that of verapamil.

REFERENCES

1. Dey, S., et al., *Evidence for two nonidentical drug-interaction sites in the human P-glycoprotein*. Proc Natl Acad Sci U S A, 1997. **94**(20): p. 10594-9.
2. Bruce C. Baguley, D.J.K., ed. *Anticancer drug development*. 2002, London : Academic: San Diego, Calif. p.77-79.
3. Kemper, E.M., et al., *Modulation of the blood-brain barrier in oncology: therapeutic opportunities for the treatment of brain tumours?* Cancer Treat Rev, 2004. **30**(5): p. 415-23.
4. Kleihues, P., ed. *Pathology and genetics of tumours of the nervous system*. ed. W.K. Cavenee. 1997, International Agency for Research on Cancer: Lyon. p.14-23.
5. Ambudkar, S.V., et al., *Biochemical, cellular, and pharmacological aspects of the multidrug transporter*. Annu Rev Pharmacol Toxicol, 1999. **39**: p. 361-98.
6. Zhou, S., L.Y. Lim, and B. Chowbay, *Herbal modulation of P-glycoprotein*. Drug Metab Rev, 2004. **36**(1): p. 57-104.
7. Perry, M.C., *The chemotherapy source book*. 1996: p. p.1071.
8. Toth, K., et al., *MDR1 P-glycoprotein is expressed by endothelial cells of newly formed capillaries in human gliomas but is not expressed in the neovasculature of other primary tumors*. Am J Pathol, 1996. **149**(3): p. 853-8.
9. Bradley, G. and V. Ling, *P-glycoprotein, multidrug resistance and tumor progression*. Cancer Metastasis Rev, 1994. **13**(2): p. 223-33.

10. Sharom, F.J., et al., *Insights into the structure and substrate interactions of the P-glycoprotein multidrug transporter from spectroscopic studies*. *Biochim Biophys Acta*, 1999. **1461**(2): p. 327-45.
11. Varma, M.V., et al., *P-glycoprotein inhibitors and their screening: a perspective from bioavailability enhancement*. *Pharmacol Res*, 2003. **48**(4): p. 347-59.
12. Loo, T.W. and D.M. Clarke, *Determining the structure and mechanism of the human multidrug resistance P-glycoprotein using cysteine-scanning mutagenesis and thiol-modification techniques*. *Biochim Biophys Acta*, 1999. **1461**(2): p. 315-25.
13. Beaudet, L., I.L. Urbatsch, and P. Gros, *Mutations in the nucleotide-binding sites of P-glycoprotein that affect substrate specificity modulate substrate-induced adenosine triphosphatase activity*. *Biochemistry*, 1998. **37**(25): p. 9073-82.
14. Kim, S.W., et al., *Reversal of P-glycoprotein-mediated multidrug resistance by ginsenoside Rg(3)*. *Biochem Pharmacol*, 2003. **65**(1): p. 75-82.
15. Shapiro, A.B. and V. Ling, *Effect of quercetin on Hoechst 33342 transport by purified and reconstituted P-glycoprotein*. *Biochem Pharmacol*, 1997. **53**(4): p. 587-96.
16. Drori, S., G.D. Eytan, and Y.G. Assaraf, *Potentiation of anticancer-drug cytotoxicity by multidrug-resistance chemosensitizers involves alterations in*

- membrane fluidity leading to increased membrane permeability. Eur J Biochem, 1995. 228(3): p. 1020-9.*
17. van Veen, H.W., C.F. Higgins, and W.N. Konings, *Molecular basis of multidrug transport by ATP-binding cassette transporters: a proposed two-cylinder engine model. J Mol Microbiol Biotechnol, 2001. 3(2): p. 185-92.*
 18. Shapiro, A.B., et al., *Stimulation of P-glycoprotein-mediated drug transport by prazosin and progesterone. Evidence for a third drug-binding site. Eur J Biochem, 1999. 259(3): p. 841-50.*
 19. Barecki-Roach, M., E.J. Wang, and W.W. Johnson, *Many P-glycoprotein substrates do not inhibit the transport process across cell membranes. Xenobiotica, 2003. 33(2): p. 131-40.*
 20. Leontieva, O.V., M.N. Preobrazhenskaya, and R.J. Bernacki, *Partial circumvention of P-glycoprotein-mediated multidrug resistance by doxorubicin-14-O-hemiadipate. Invest New Drugs, 2002. 20(1): p. 35-48.*
 21. Sharom, F.J., *The P-glycoprotein efflux pump: how does it transport drugs? J Membr Biol, 1997. 160(3): p. 161-75.*
 22. Di Pietro, A., et al., *P-glycoprotein-mediated resistance to chemotherapy in cancer cells: using recombinant cytosolic domains to establish structure-function relationships. Braz J Med Biol Res, 1999. 32(8): p. 925-39.*
 23. Kim, H.S., et al., *Effects of ginsenosides Rg3 and Rh2 on the proliferation of prostate cancer cells. Arch Pharm Res, 2004. 27(4): p. 429-35.*

24. Lee, J.Y., et al., *Antitumor promotional effects of a novel intestinal bacterial metabolite (IH-901) derived from the protopanaxadiol-type ginsenosides in mouse skin*. *Carcinogenesis*, 2005. **26**(2): p. 359-67.
25. Xie, H.T., et al., *Uptake and metabolism of ginsenoside Rh2 and its aglycon protopanaxadiol by Caco-2 cells*. *Biol Pharm Bull*, 2005. **28**(2): p. 383-6.
26. Efferth, T., et al., *Activity of drugs from traditional Chinese medicine toward sensitive and MDR1- or MRP1-overexpressing multidrug-resistant human CCRF-CEM leukemia cells*. *Blood Cells Mol Dis*, 2002. **28**(2): p. 160-8.
27. Hasegawa, H., et al., *Reversal of daunomycin and vinblastine resistance in multidrug-resistant P388 leukemia in vitro through enhanced cytotoxicity by triterpenoids*. *Planta Med*, 1995. **61**(5): p. 409-13.
28. Choi, C.H., G. Kang, and Y.D. Min, *Reversal of P-glycoprotein-mediated multidrug resistance by protopanaxatriol ginsenosides from Korean red ginseng*. *Planta Med*, 2003. **69**(3): p. 235-40.
29. Bae, E.A., et al., *Metabolism of 20(S)- and 20(R)-ginsenoside Rg3 by human intestinal bacteria and its relation to in vitro biological activities*. *Biol Pharm Bull*, 2002. **25**(1): p. 58-63.
30. Fulci, G., N. Ishii, and E.G. Van Meir, *p53 and brain tumors: from gene mutations to gene therapy*. *Brain Pathol*, 1998. **8**(4): p. 599-613.
31. Popovich, D.G. and D.D. Kitts, *Ginsenosides 20(S)-protopanaxadiol and Rh2 reduce cell proliferation and increase sub-G1 cells in two cultured intestinal*

- cell lines, *Int-407 and Caco-2*. *Can J Physiol Pharmacol*, 2004. **82**(3): p. 183-90.
32. Jia, W.W., et al., *Rh2, a compound extracted from ginseng, hypersensitizes multidrug-resistant tumor cells to chemotherapy*. *Can J Physiol Pharmacol*, 2004. **82**(7): p. 431-7.
33. Aboudkhal, S., et al., *Effect of testosterone on growth of P388 leukemia cell line in vivo and in vitro. Distribution of peripheral blood T lymphocytes and cell cycle progression*. *Neoplasma*, 2005. **52**(3): p. 260-6.
34. Essodaigui, M., H.J. Broxterman, and A. Garnier-Suillerot, *Kinetic analysis of calcein and calcein-acetoxymethylester efflux mediated by the multidrug resistance protein and P-glycoprotein*. *Biochemistry*, 1998. **37**(8): p. 2243-50.
35. Essodaigui, M., et al., *Energy-dependent efflux from Leishmania promastigotes of substrates of the mammalian multidrug resistance pumps*. *Mol Biochem Parasitol*, 1999. **100**(1): p. 73-84.
36. Litman, T., et al., *Competitive, non-competitive and cooperative interactions between substrates of P-glycoprotein as measured by its ATPase activity*. *Biochim Biophys Acta*, 1997. **1361**(2): p. 169-76.
37. Krishna, R. and L.D. Mayer, *Multidrug resistance (MDR) in cancer. Mechanisms, reversal using modulators of MDR and the role of MDR modulators in influencing the pharmacokinetics of anticancer drugs*. *Eur J Pharm Sci*, 2000. **11**(4): p. 265-83.

38. Tanaka, O., M. Nagai, and S. Shibata, *Chemical studies on the oriental plant drugs. XVI. The stereochemistry of protopanaxadiol, a genuine sapogenin of ginseng*. Chem Pharm Bull (Tokyo), 1966. **14**(10): p. 1150-6.
39. Radad, K., et al., *Ginsenosides Rb1 and Rg1 effects on mesencephalic dopaminergic cells stressed with glutamate*. Brain Res, 2004. **1021**(1): p. 41-53.
40. Kim, R.B., *Drugs as P-glycoprotein substrates, inhibitors, and inducers*. Drug Metab Rev, 2002. **34**(1-2): p. 47-54.
41. Scala, S., et al., *P-glycoprotein substrates and antagonists cluster into two distinct groups*. Mol Pharmacol, 1997. **51**(6): p. 1024-33.

CHAPTER 3. CHARACTERIZATION OF APPD SELECTED DRUG- RESISTANCE CELL LINE SF188C2R2

3.1 Introduction

Aglycone ginsenoside aPPD has a strong inhibitory effect on glioblastoma cells SF188, which is a human glioma cell line with p53 mutation and elevated O⁶-alkylguanine transferase level [1, 2]. Since many anticancer drugs inhibit cancer cells by inducing apoptosis, p53 mutation results in intrinsic multiple drug resistant in tumor cells [3, 4] due to defective apoptotic pathways. p53 mutation occurs in more than 50% of cancers and particularly high in glioblastomas (> 71%). Currently, no drug or combination of drugs in any dose can be expected to eradicate all of the tumor cells when apoptosis is blocked [5]. Interestingly, it seems that p53 mutation did not cause the cells to be resistant to aPPD. This feature suggest its therapeutic potential of aPPD for the tumor with multiple drug resistance, particular for intracranial tumors, giving it an advantage over currently other anticancer agents.

Cancer cells with multiple drug resistance are naturally selected mutant clones. It has been shown that cancer cells have a poor genetic stability compared with normal cells. For tumor cells, the mutation rate of one gene is about $1/10^5$ cells per generation, which is 10 times higher than that in normal cells ($1/10^6$) [6, 7]. Likewise, tumor cells are more likely to become drug resistant than normal cells. Jaffrezou et al. found that spontaneous mutation clones stably resistant to etoposide could be readily formed in a

human sarcoma cell line by exposure to etoposide. The drug resistant mutation rate ranged from 2.9×10^{-6} to 5.7×10^{-7} [8, 9]. On the other hand, it is arguable that the drug resistance can also be due to the changes in tumor cell activity induced by drug exposure (adaptation) [10-12]. Some studies suggest that the poor prognosis of cancer is due to both the inherited drug resistance of the tumor cells and the emergence of subpopulations of tumor cells that are resistant to drugs [13-17].

The purpose of this part of study was to investigate whether human glioma tumor cells could acquire resistance to aPPD. Further, this study may help to reveal the mechanisms of aPPD-induced cytotoxicity in those cells by comparing the phenotype of aPPD-resistant cell line and its parental aPPD-sensitive cell line.

3.2 Materials and methods

3.2.1 drugs and chemicals

aPPD stocks were kept in 4°C. Verapamil, MTT, Calcein AM, dimethyl sulfoxide (DMSO), SDS and trypsin with 0.03% EDTA were used (See Chapter 2). Paclitaxel, BCNU (Carmustine) (Bristol-Myers Squibb, Quebec, Canada.) doxorubicin, vincristine and cisplatin (Fauding, Ontario, Canada Inc) were purchased from the pharmacy of the British Columbia Cancer Agency. Agarose (Life Technology TM GIBCO BRL) was purchased from University of British Columbia, Vancouver, B.C.

PEI (Polycation Polyethyleneimine, molecular weight: 600) was purchased from Dow Chemical (Midland, MI, USA)

3.2.2 Cell viability assay

See chapter 2

3.2.3 Generation of aPPD-resistant cell lines

Human glioblastoma cell line SF188 obtained from the Brain Tumor Research Center, University of California at San Francisco, was grown as a monolayer in Dulbecco's Modified Eagle's Medium (DMEM) containing 10% fetal bovine serum (FBS). Cells were maintained in a humidified atmosphere of 5% CO₂ in air at 37°C. To induce the aPPD resistant cells, about 10⁶ SF188 cells were exposed to crude aPPD 30 µg/ml in 2% FBS for 24 h before growing in an aPPD- free medium. When the cells reached 60% confluence, the treatment was repeated for another 24 h. The treatments were repeated until no cell death occurred after 24 h in the presence of crude aPPD. These cells were denoted as SF188C2R. They were seeded for one cell per well through a series of dilution into a 24-well plate, and the cells were allowed to grow to single clones. aPPD resistant cell lines from single colonies were established and the cytotoxicity of aPPD to the SF188 parental and selected cells was tested.

3.2.4 Flow cytometry analysis

Cell cycle distribution was monitored following exposure of SF188 or SF188C2R2 cells to aPPD. Briefly, SF188C2R2 and SF188 cells were seeded in 100 mm dishes and cultured overnight. The cells were then incubated in the presence or absence of aPPD, at concentrations of 10 µg/ml, and 15 µg/ml for 36 h. The cells were collected by trypsinization and fixed by 70% ethanol. After washing them with PBS, the cells were diluted to 10^6 /ml and stained with propidium iodide (100 µg/ml) containing DNase - free RNase A 100 µg/ml, in the dark at room temperature for 30 min. DNA content was used to determine the cell cycle distribution according to a standard method on a FACScalibur flow cytometer (Becton-Dickinson). The proportions of cells in the G0/G1, S, and G2/M phases were analyzed using a contour graph mode. Approximately 10,000 cells were counted per sample.

3.2.5 Colony formation assay

One thousand of SF188 C2R2 or SF188 cells were placed in 6-well plates in 0.5% pure agar on a base layer of 1% agar in DMEM medium with 0%, 10%, 15%, 20% FBS respectively in a humidified atmosphere of 5% CO₂ in air at 37°C, 0.5 ml of fresh complete medium was added every 5 days. Colonies with at least 50 cells were counted under a stereomicroscope after 14 days. The plating efficiency was expressed as the number of colonies scored as a percentage of the total number of cells seeded [18].

3.2.6 Growth curve and doubling time

Twenty thousand SF188 cells or SF188C2R2 cells were seeded into each well of a 6-well plate containing 3 ml/well of the culture medium in a humidified atmosphere of 5% CO₂ in air at 37°C. The number of the cells was counted daily for 3 days with a hemocytometer.

3.2.7 Transfection with PHR⁺-CMV-EGFP plasmid DNA

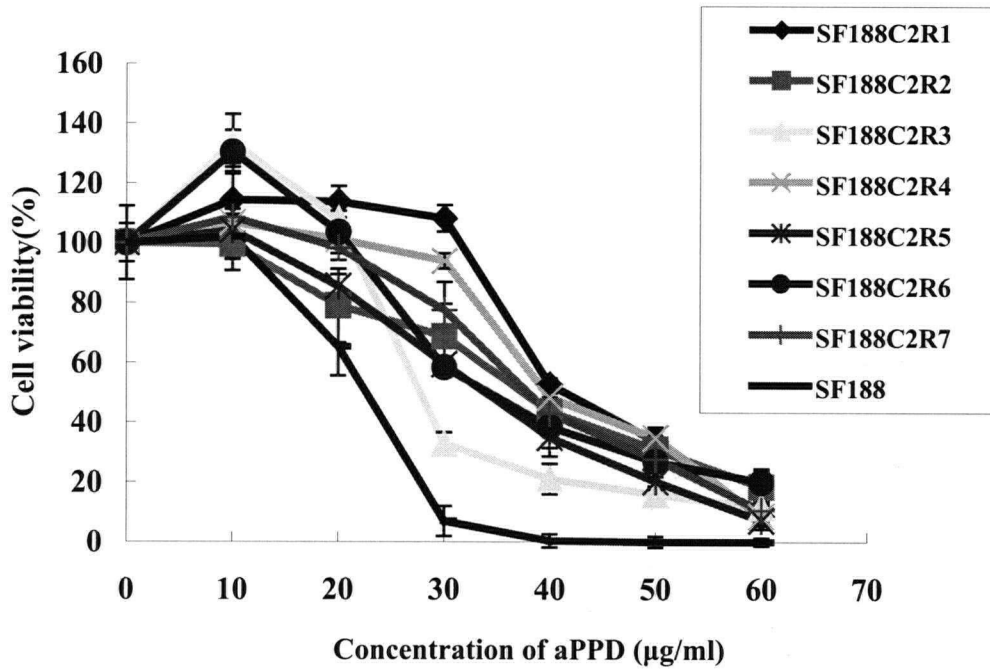
SF188 or SF188C2R2 cells were seeded at a density of 2×10^5 per well in a six-well plate and grown for 24 h. PHR⁺-CMV-EGFP plasmid DNA was transfected with PEI (Polycation Polyethyleneimine) transfection reagent for 6 h. Briefly, 2 µg plasmid DNA and 3 µl of 50% PEI [19] were each dissolved with 200 µl of serum-free medium. Plasmid DNA solution was added to the PEI solution dropwise and the mixtures were kept at room temperature for 20 min. This medium of cells was replaced with the DNA-PEI mixture 400 µl and the cells were incubated in 37°C for 4 h. Then 8 ml of fresh medium was added to the dish and the cells grew for an additional 48 h. GFP fluorescence was visualized and photographed with an invert fluorescent microscope (FluoArc, Axiovert -200). The transfection ratio was counted by the number of fluorescent cells in each view field (40x) divided by the number of the cells in view.

3.3 Results

3.3.1 aPPD- resistant cell line SF188C2R2

Dose-response analysis demonstrated an IC_{50} of crude aPPD for SF188 was 19.67 ± 1.08 $\mu\text{g/ml}$ and IC_{90} was 28.07 ± 0.94 $\mu\text{g/ml}$ (Data not shown). To select aPPD resistant cell lines, the SF188 cells were kept in 30 $\mu\text{g/ml}$ crude aPPD for 24 h followed by growing in crude aPPD-free normal medium until the cells reached 60% confluence. Ten to fifteen colonies of cells were obtained from 10^6 SF188 cells after the first cycle of aPPD treatment. Following 8 selection cycles, 100% cell viability was achieved when treated with 30 $\mu\text{g/ml}$ of crude aPPD for 19 h. Single cells were grown in 96-well dishes and a total of seven cell lines were obtained. These cell lines named SF188C2R1, SF188C2R2, SF188C2R3, SF188C2R4, SF188C2R5, SF188C2R6, and SF188C2R7 and all showed resistance to aPPD (Fig.3-1A), while the vehicle of aPPD (alcohol) was not toxic to SF188 (Fig.3-1B). Among them, SF188C2R2 was used for further study because its proliferation rate was higher than other SF188C2R cell lines. Fig.3-2 showed that SF188C2R2 was 1.6-fold more resistant to aPPD when compared to the parental cells.

A



B

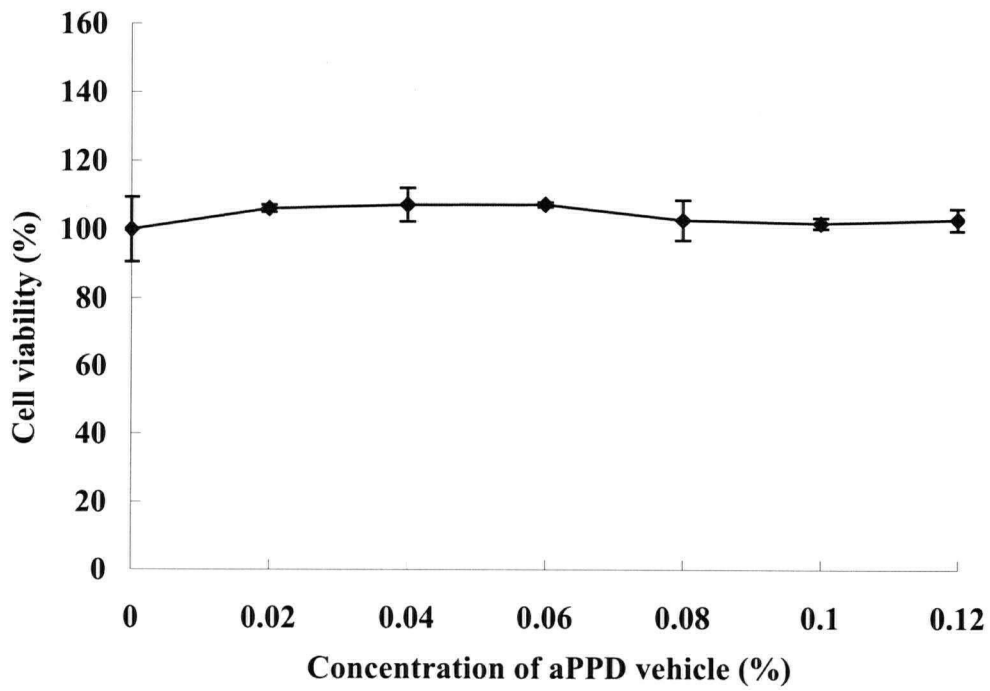


Fig. 3-1. Viability of SF188 and C2R cell lines in the presence of aPPD

A) SF188 and SF188C2R1, C2R2, C2R3, C2R4, C2R5, C2R6 and C2R7 cells were incubated in indicated concentration of aPPD in 2% FBS for 24 h.

Each point is the mean \pm SD of four measurements and represented as percentage of change relative to the aPPD vehicle control.

The viability of all SF188C2R cell lines in aPPD 20 μ g/ml, 30 μ g/ml, 40 μ g/ml, 50 μ g/ml is different from the parental SF188 cells ($p < 0.01$).

*, $p < 0.01$, p value was calculated from an independent t-test between one of SF188C2R cell lines and SF188 cell line.

B) SF 188 cells were treated with aPPD vehicle (alcohol).

Viability is expressed as percentage of change relative to the control using MTT assays. Each point is the mean \pm SD of three experiments.

$P > 0.05$ in vehicle treated group compared with untreated control.

(Two-way ANOVA followed by Dunnett post hoc test)

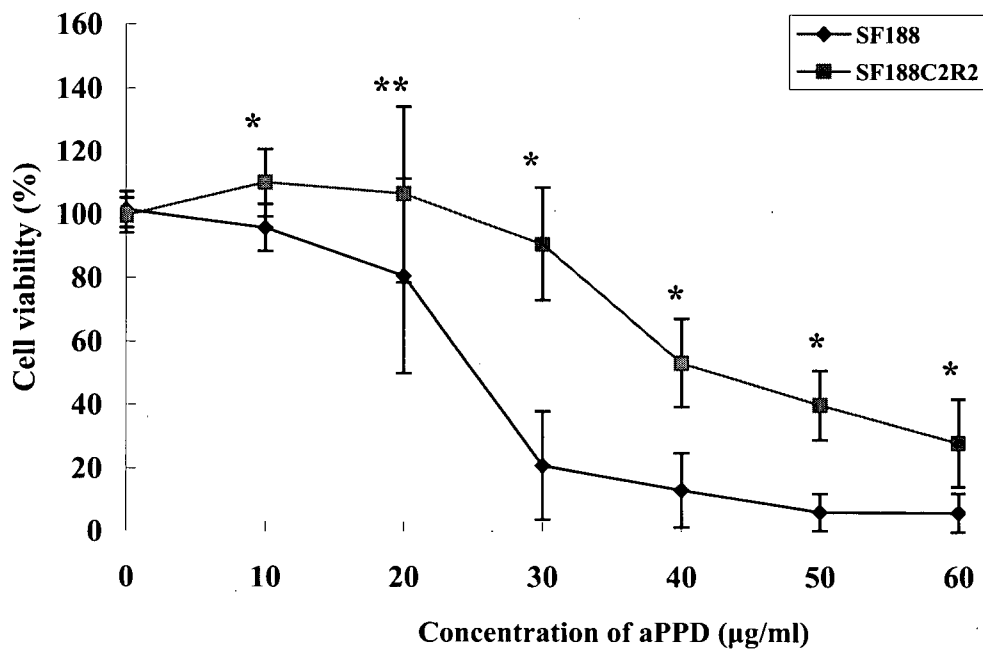


Fig. 3-2. Viability of SF188C2R2 and SF188 in the presence of aPPD

SF188C2R2 and SF188 were growing for 48 h and were incubated with indicated concentrations of aPPD for 24 h. Viability is expressed as a percentage of change relative to the drug vehicle control using MTT assay. Each point is the mean \pm SD of three experiments.

*, $p < 0.01$, p value was calculated from an independent t-test between two cell lines.

$p < 0.05$ in aPPD treated groups compared to untreated controls in two cell lines.

(Two-tail ANOVA followed by Dunnett post hoc)

3.3.2 Growth characteristics of SF188C2R2

To evaluate the growth kinetics of SF188C2R2, colonies assays on soft agar were conducted for both SF188C2R2 and its parental cells SF188. As shown in Table3-1, the plating efficiency for both SF188C2R2 and SF188 was increased with concentrations of FBS. However, the plating efficiency of SF188C2R2 was 2-fold of SF188 (Table3-1). As another index of cell proliferation, the doubling time for both cell lines were measured. SF188C2R2 had a doubling time of 24.2 ± 1.8 h, which was 3-fold shorter than SF188 (68.2 ± 24.5 h), ($P < 0.05$) (Fig. 3-3). Table 3-2 shows the results of colony formation assay for both cell lines. SF188C2R2 had two times more colonies than the parental SF188 cells 14 days ($P < 0.05$).

3.3.3 Cell cycle distribution of SF188C2R2

To examine the effect of aPPD on the cell cycle of the two cell lines, the cell cycles of SF188C2R2 and SF188 were analyzed by flow cytometry before and after treatment with aPPD (SF188 as a control). There was no significant difference in percentages of cells at different phases of the cell cycle for the two cell lines in the absence of aPPD. Incubated with low concentrations of aPPD (10 $\mu\text{g/ml}$, 15 $\mu\text{g/ml}$) for 36 h (Fig.3-4), both SF188 and SF188C2R2 cells showed decreased proportion of cells in S phase (Fig.3-4, Table3-3) indicating a cell cycle arrest. Interestingly, while SF188 cells showed a clear G2-M arrest (Fig.3-4A), SF188C2R2 cells treated with aPPD appeared with increased G1 cells, suggesting a G1 cell cycle arrest (Fig.3-4B, Table 3-3).

Table 3-1 The characteristics of SF188C2R2 and SF188 cell lines

Cell line	Doubling time	Plating efficacy (%)		
	(h)	10% FBS	15% FBS	20% FBS
SF188C2R2	24.2 ± 1.8	15.53 ± 4.06	26.50 ± 3.48	33.27 ± 1.86
SF188wt	68.2 ± 24.5**	6.33 ± 1.53**	13.00 ± 3.21**	15.30 ± 2.26*

The values are means of three identical experiments.

** p<0.05, * p<0.01, p value was calculated from independent t-test between two cell lines.

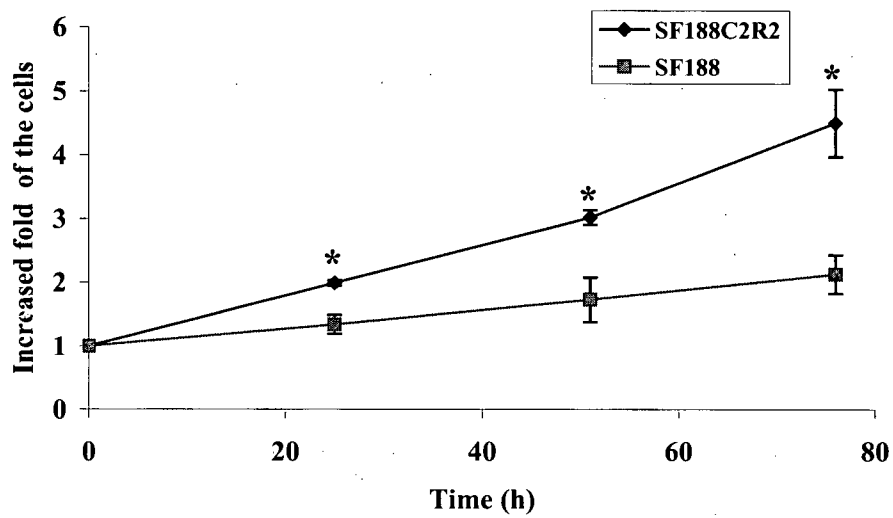


Fig. 3-3. Growth curve of SF188C2R2 and SF188

Each point is the mean \pm SD of three experiments and represented as fold changes relative to the number of seeded cells.

*, $p < 0.01$, p value was calculated from independent t-test between two cell lines.

Table 3-2 Colony formation assay of SF188 and SF188C2R2 cell lines

FBS (%)	SF188	SF188C2R2	P value*
0	0	0	
10	63.3 ± 15.3	155.3 ± 40.6	P<0.05
15	130.0 ± 32.1	265.0 ± 34.8	P<0.01
20	153.0 ± 22.6	332.7 ± 18.6	P<0.01

The values are means of three identical experiments.

* p value was calculated from independent t-test between two cell lines.

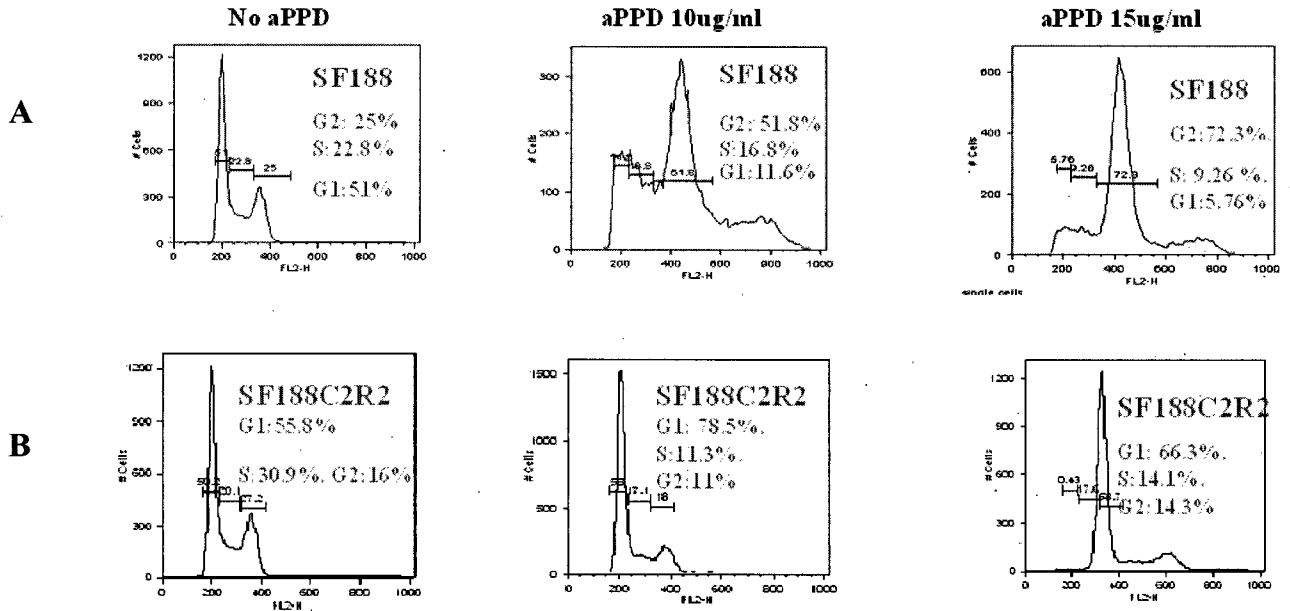


Fig. 3-4. Flow cytometric profiles of SF188C2R2 and SF188 treated with aPPD

A) SF188 and B) SF188C2R2 cells were incubated with aPPD in indicated concentrations of aPPD for 36 h. The percentage of cells in each phase of the cell cycle is shown beside each histogram.

Table 3-3 Effect of aPPD on cell cycle distribution in SF188C2R2 and SF188

aPPD $\mu\text{g/ml}$	Cell line					
	SF188			SF188C2R2*		
	G1	S	G2/M	G1	S	G2/M
0	51	22.8	25	37.57 ± 24.08	19.77 ± 10.04	22.13 ± 14.6
10	11.6	16.8	51.8	73.5 ± 4.33	8.92 ± 4.73	19.5 ± 7.67
15	5.76	9.26	72.3	65.7 ± 16.5	10.13 ± 3.57	19.74 ± 14.34

* Data represent the mean \pm SD of three experiments

3.3.4 Drug resistance profile of SF188C2R2

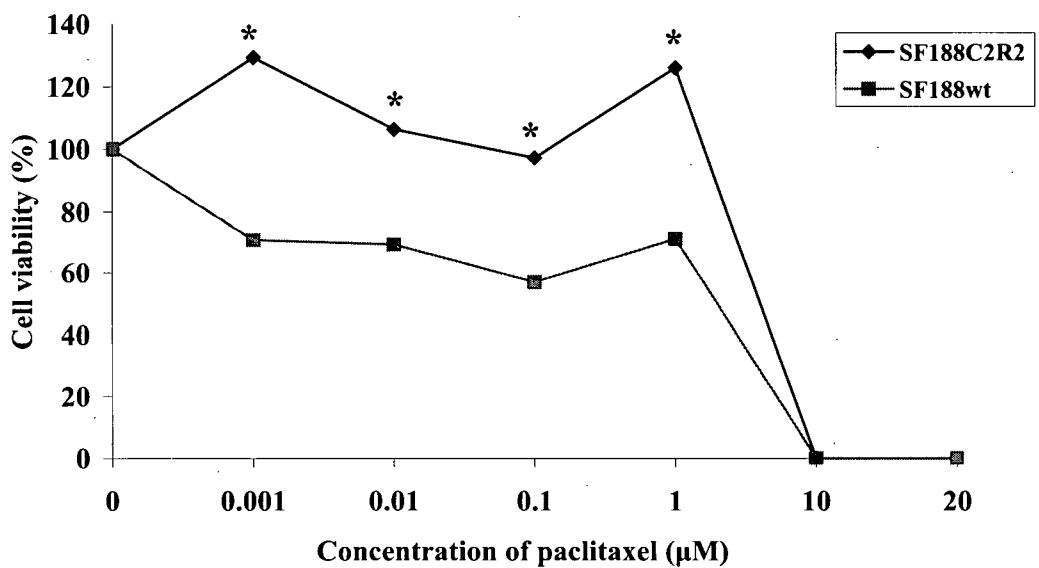
To ask whether selected aPPD-resistant cells would also be resistant to other anticancer agents, viability of the cells treated with various chemotherapeutics was analyzed. Fig.3-5 shows that SF188C2R2 was resistant to paclitaxel, vincristine and cisplatin. On the other hand, SF188C2R2 was significantly more sensitive to doxorubicin (Fig.3-6A1, Fig.3.6A2). There was no significant difference in sensitivity of the two cell lines for BCNU. (Fig.3-6B1 and Fig.3-6 B2). Table 3-4 lists the IC₅₀s of the two cell lines on various anticancer drugs tested.

To determine if the drug resistance of SF188C2R2 was mediated by P-gp, calcein formation assay was performed. Fig.3-7 showed that calcein AM, the substrate of P-gp, accumulated in both SF188C2R2 (Fig.3-7A) and SF188 (Fig.3-7B) cells to form intracellular fluorescent calcein without difference. Thus, the drug resistance of SF188C2R2 across other chemotherapy agents cannot be attributed to overexpression of P-gp.

3.3.5 Resistance to DNA transfection of SF188C2R2

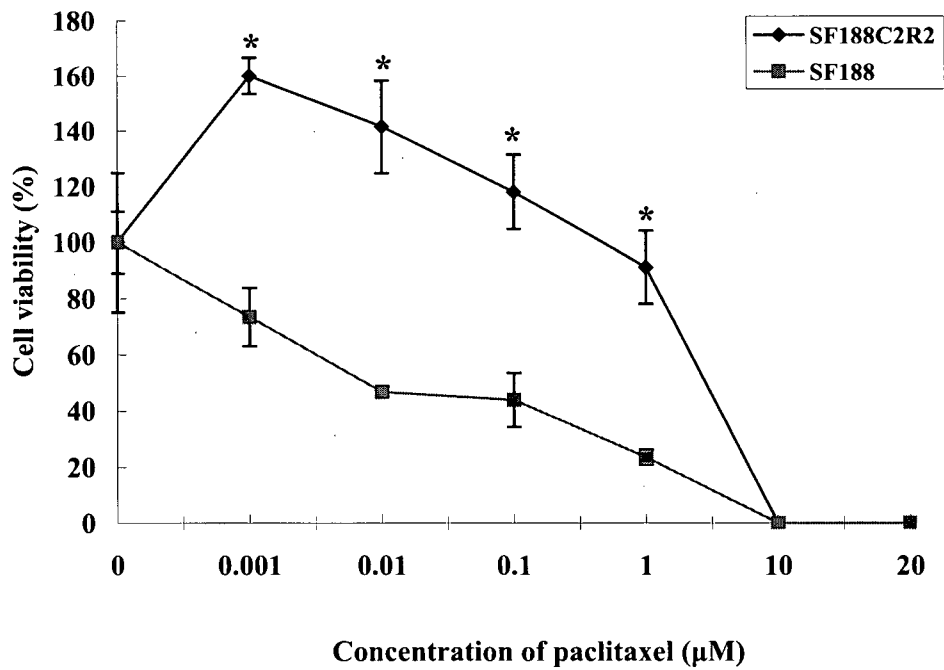
It was unexpectedly found that transfection efficiency of SF188C2R2 was much lower than its parental cell line tested with PHR'-CMV-EGFP. The transfection rates (Fig.3-8) were: SF188C2R2: 2.54% ± 0.14. SF188: 12.86% ± 1.98. The resistant index (the ratio of SF188C2R2 transfection rate vs SF188 transfection rate) was Rf: 5.06, P < 0.05 (Fig. 3-9). The data shows one of three experiments.

A1



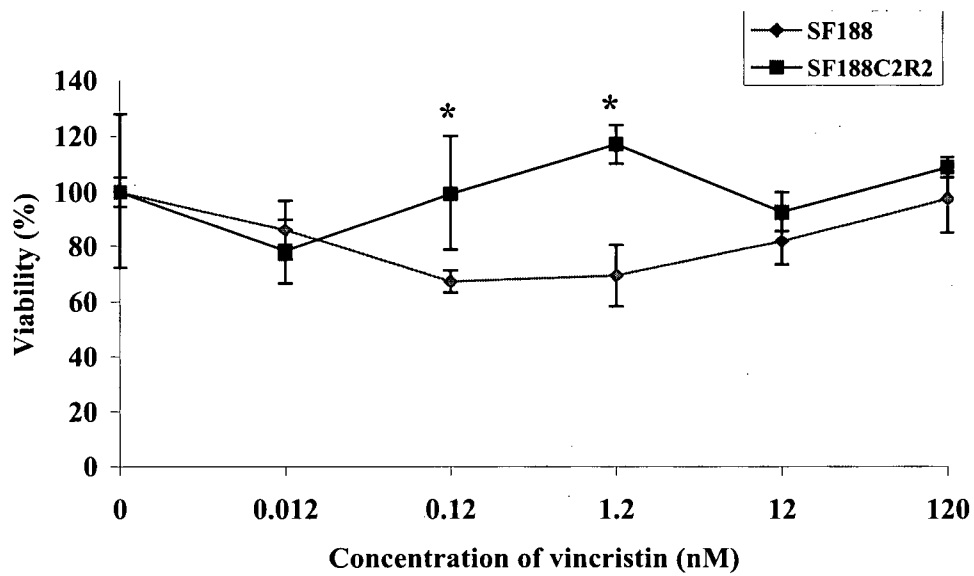
Paclitaxel (29 h)

A2



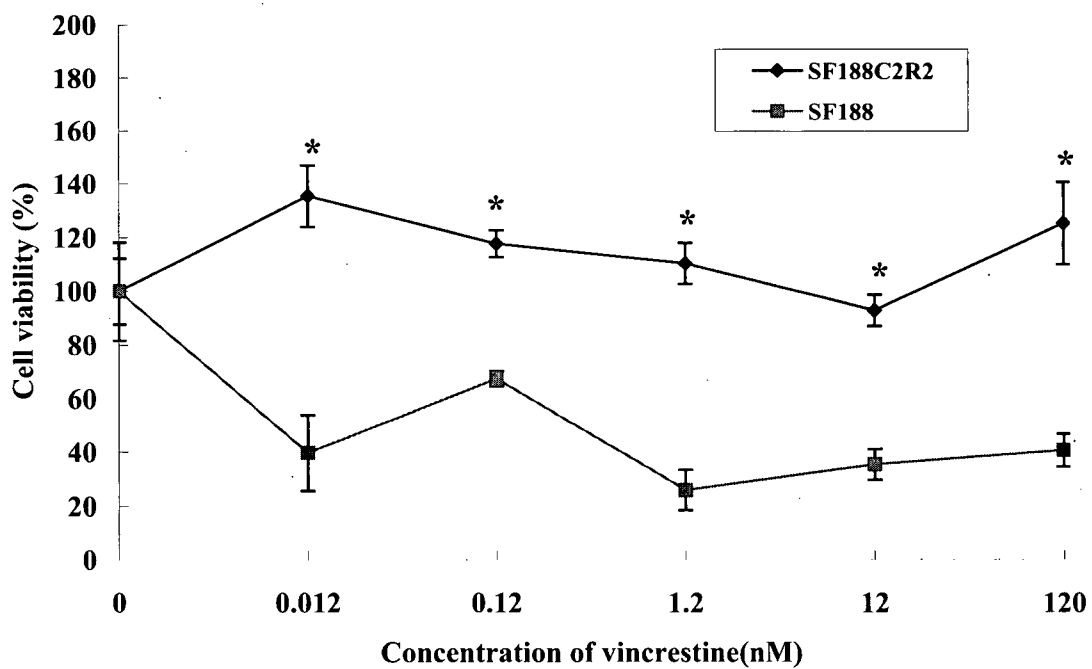
Paclitaxel (58 h)

B1



Vincristine (24 h)

B2



Vincristine (58 h)

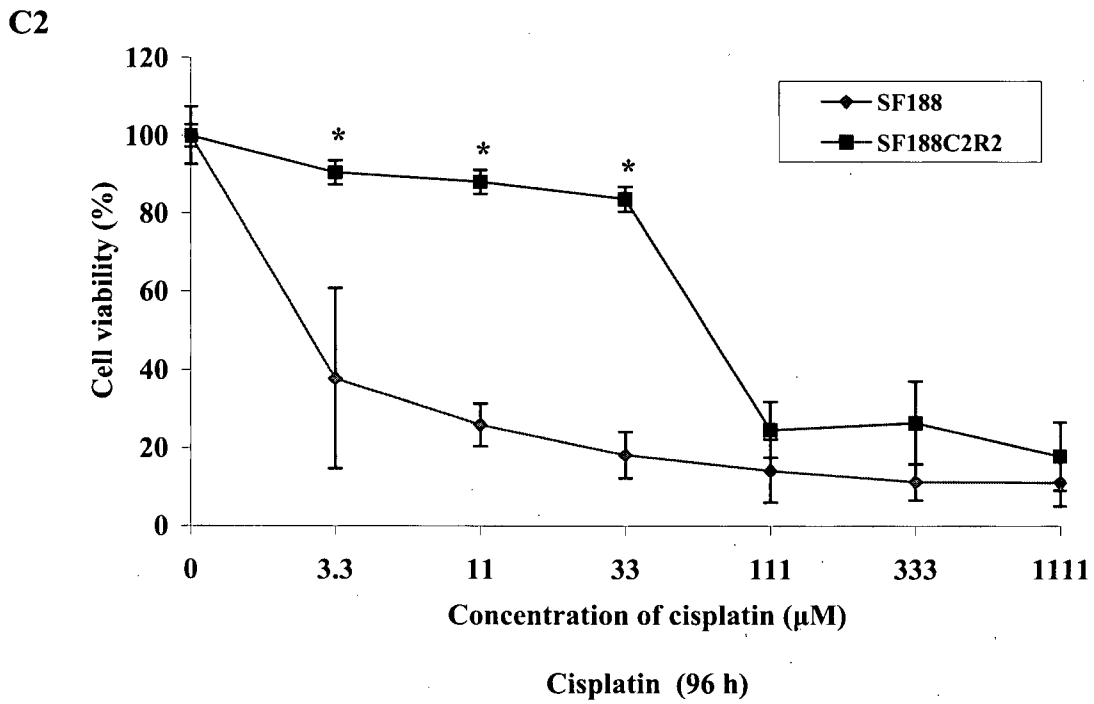
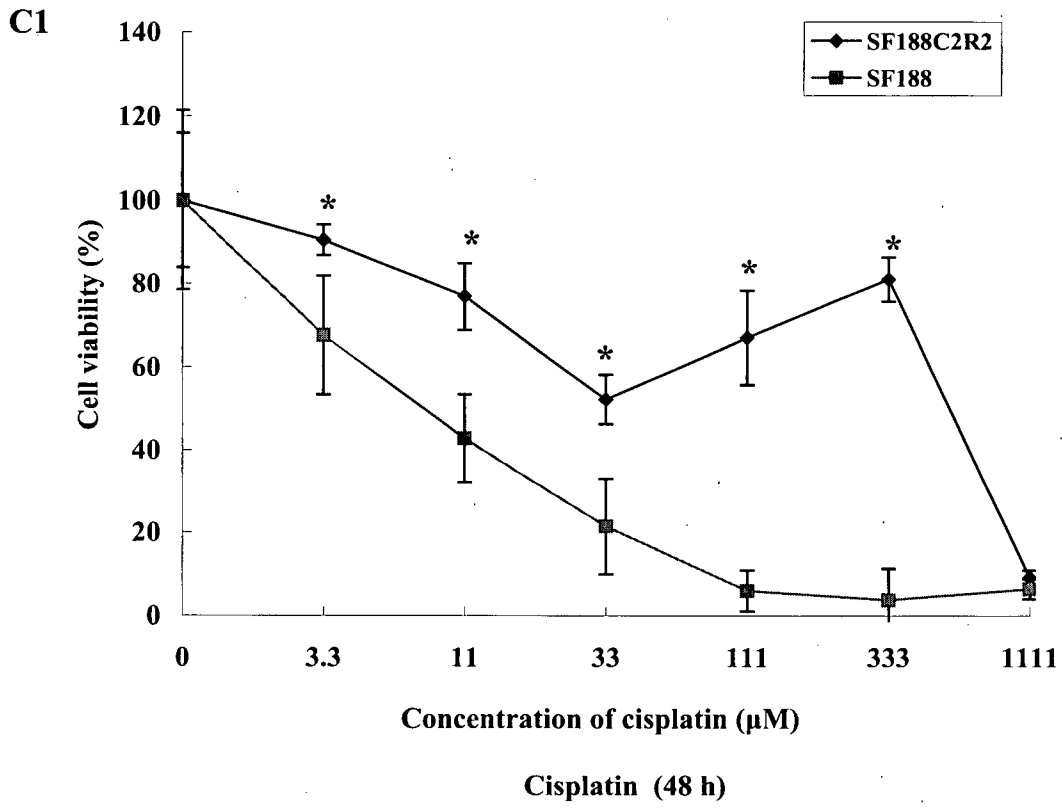


Fig. 3-5. Cross-resistance of SF188C2R2 to various chemotherapeutics

Viability is expressed as a percentage of the solvent control using MTT assay. Each point is the mean \pm SD of four measurements.

A1) and A2) Paclitaxel

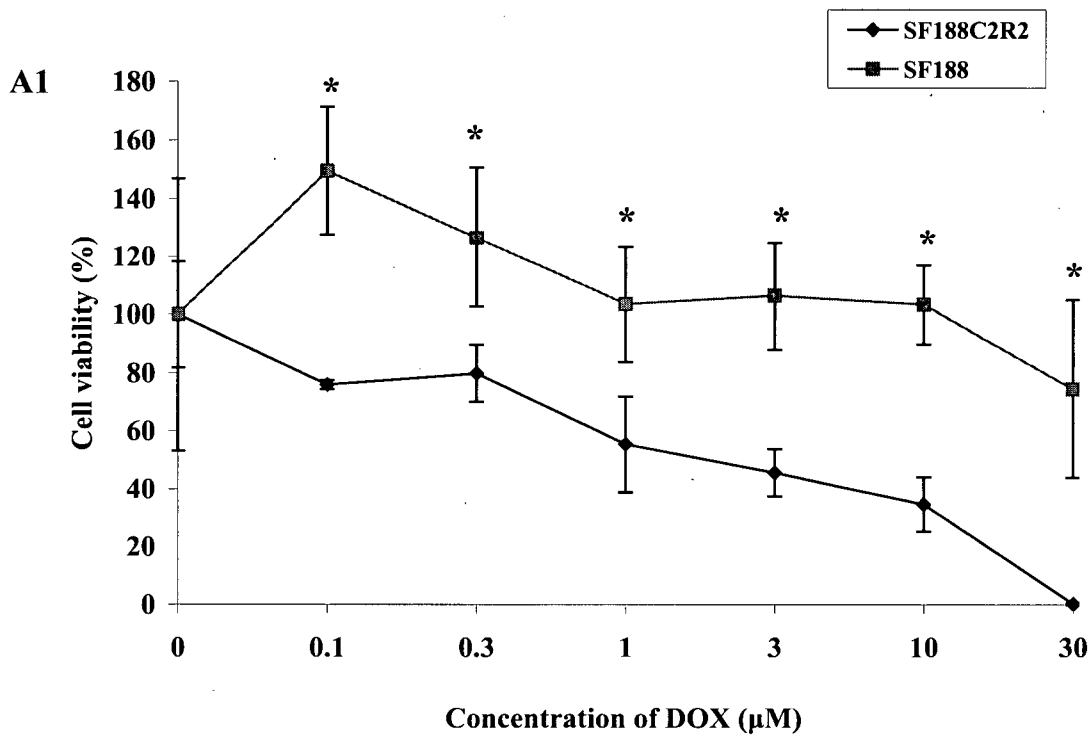
* $p < 0.01$, p value was calculated from an independent t-test between two cell lines.
 $p < 0.05$ in paclitaxel treated groups compared to untreated controls in two cell lines.
(Two-tail ANOVA followed by Dunnett post hoc)

B1) and B2) Vincristin

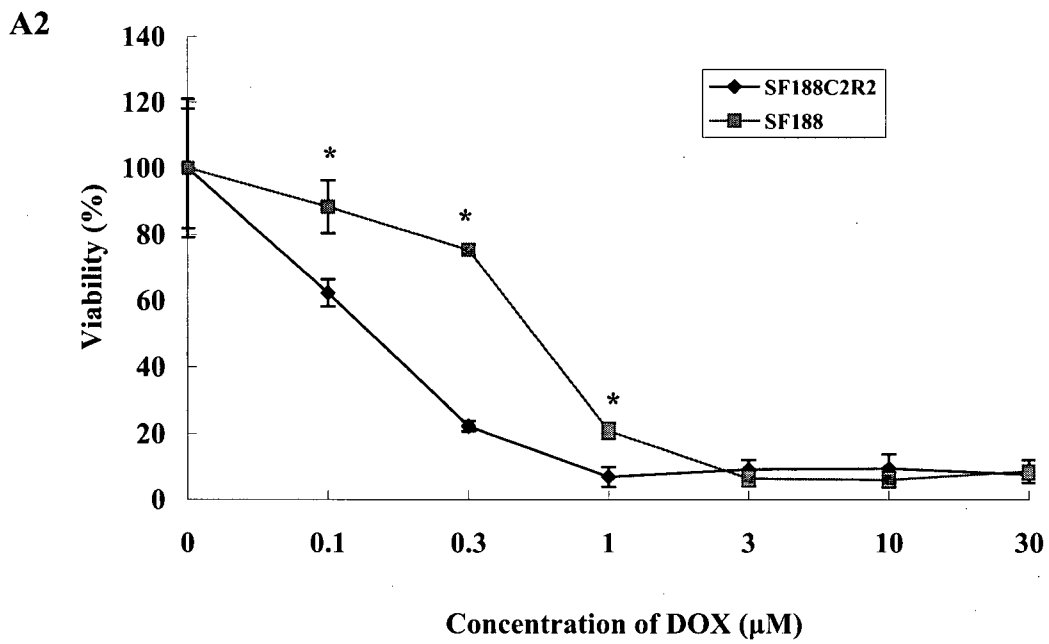
* $p < 0.01$, p value was calculated from an independent t-test between two cell lines.
 $p < 0.05$ in vincristin treated groups compared to untreated controls in two cell lines.
(Two-tail ANOVA followed by Dunnett post hoc)

C1) and C2) Cisplatin

* $p < 0.01$, p value was calculated from an independent t-test between two cell lines.
 $p < 0.05$ in cisplatin treated groups compared to untreated controls in two cell lines.
(Two-tail ANOVA followed by Dunnett post hoc)

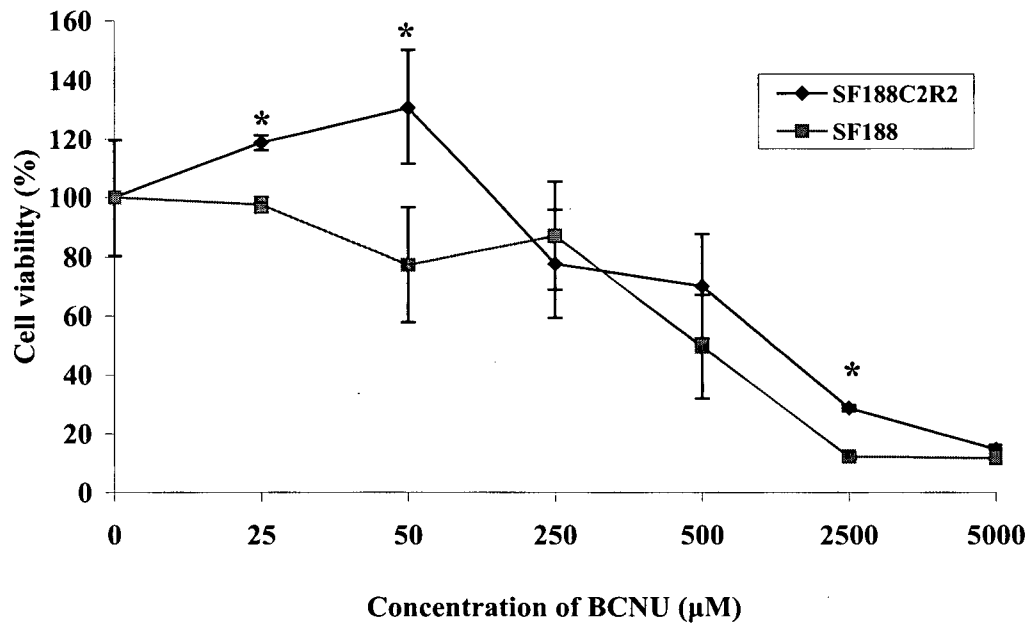


DOX 24 h



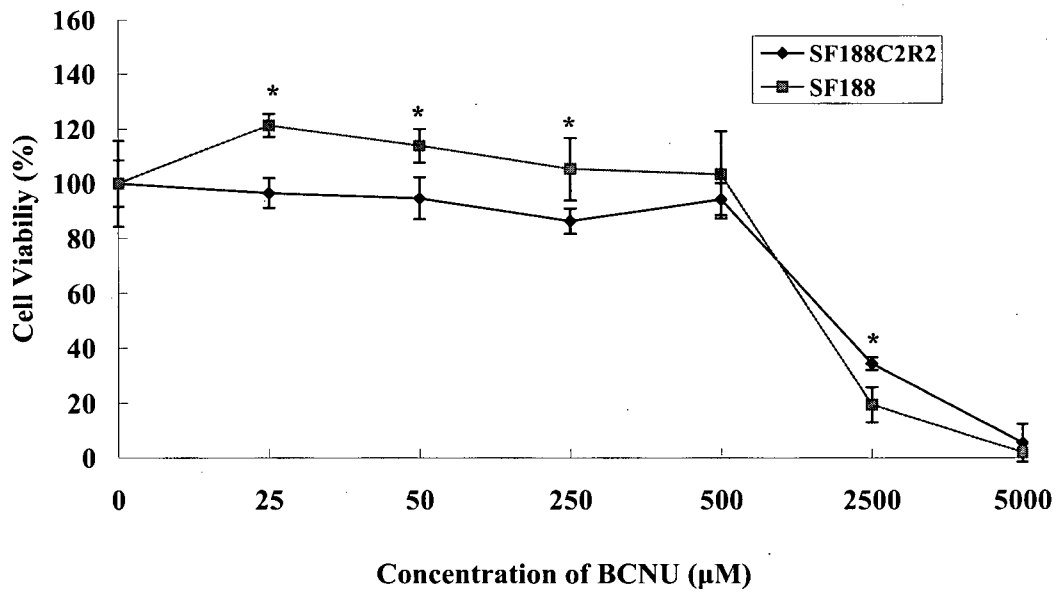
DOX 72 h

B1



BCNU (24 h)

B2



BCNU (72 h)

Fig. 3-6. SF188C2R2 and parental SF188 incubated with DOX and BCNU

Viability is expressed as a percentage of the solvent control using MTT assay. Each point is the mean \pm SD of four measurements.

A1) and A2) DOX

*, $p < 0.01$, p value was calculated from an independent t-test between two cell lines.

$p < 0.05$ in DOX treated groups compared to untreated controls in two cell lines.

(Two-tail ANOVA followed by Dunnett post hoc)

B1) and B2) BCNU

*, $p < 0.01$, p value was calculated from an independent t-test between two cell lines.

$p < 0.05$ in BCNU treated groups compared to untreated controls in two cell lines.

(Two-tail ANOVA followed by Dunnett post hoc)

Table 3-4 Cytotoxicity of aPPD and other anticancer drugs in SF188C2R2 and SF188

Drugs	IC ₅₀ ^a		R _f ^b	P values ^c
	SF188C2R2	SF188		
aPPD (µg/ml) (24 h)	40.92 ± 10.51	24.49 ± 4.21	1.7	<0.05
Taxol (µM) (58 h)	4.52 ± 1.86	0.0089 ± 0.0018	544.9	<0.01
Vincristine (nM) (58 h)	No	0.573 ± 0.13	∞	<0.01
Cisplatin (µM) (48 h)	669.87 ± 21.80	8.78 ± 3.71	76.3	<0.01
DOX (µM) (72 h)	0.177 ± 0.017	0.626 ± 0.013	0.3	<0.01
BCNU (µM) (72 h)	1981.27 ± 305.29	1767.86 ± 85.43	1.1	>0.05

a IC₅₀ values were statistically different (P<0.05) between SF188 and SF188C2R2 cells for all drugs. Data are presented as the means ± SD.

b R_f (resistant factor) was determined by dividing the IC₅₀ of the drug for SF188C2R2 by that of the parental cell line SF188.

c P value was calculated from independent t-test between cell lines

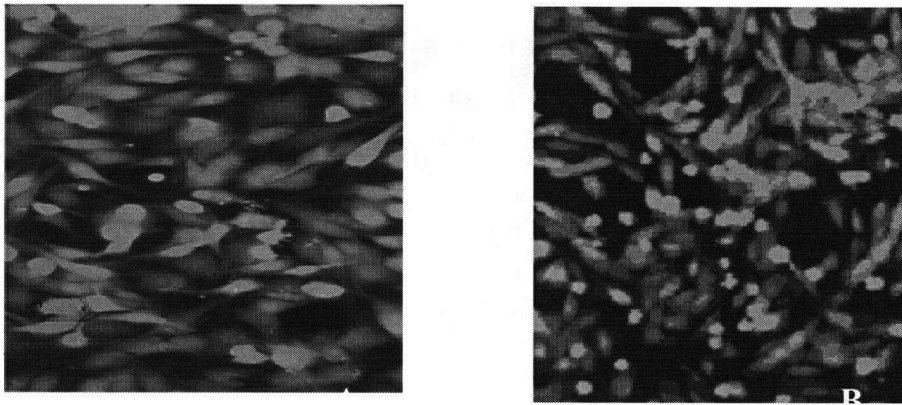


Fig. 3-7. Fluorescent Calcein formation assay in SF188 C2R2 and SF188

A) Fluorescent Calcein formation in SF188C2R2.

B) Fluorescent Calcein formation in SF188.

Cells were photographed using an Axiovert -200 inverted fluorescent microscope and a 40 \times phase-contrast objective

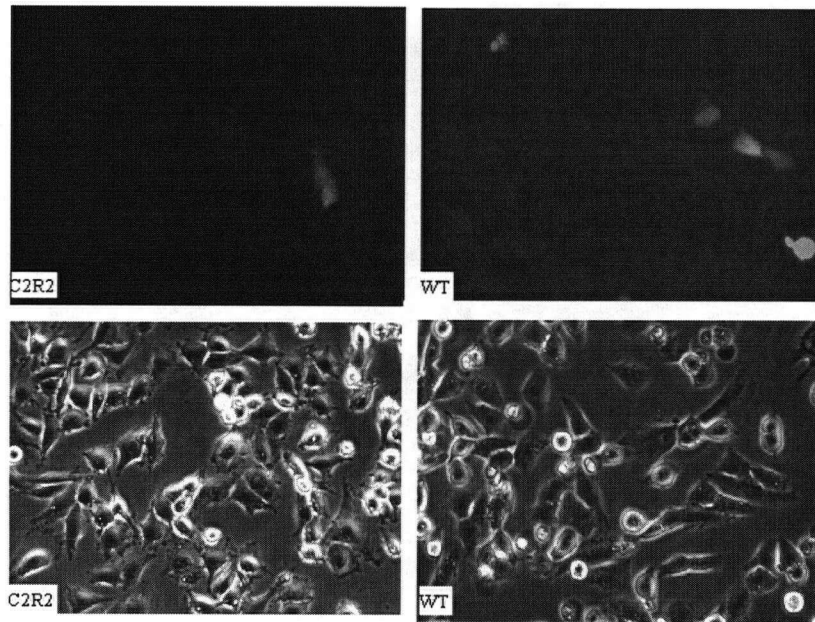
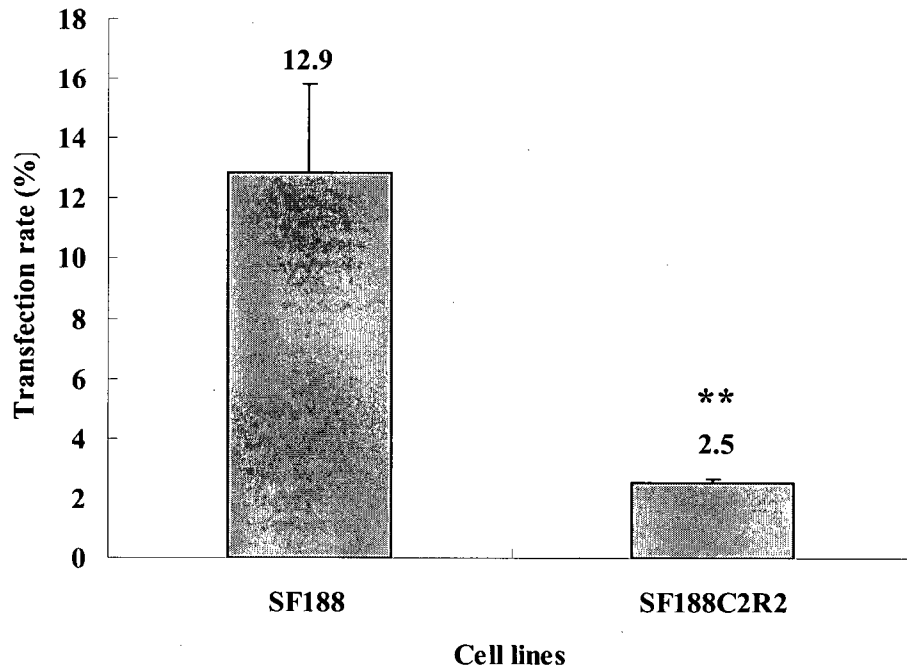


Fig. 3-8. SF188C2R2 transfection with PHR'-CMV-EGFP

SF188 C2R2 or SF188 cells 2×10^5 were transfected with $2 \mu\text{g}$ of PHR'-CMV-EGFP plasmide. 24 h after transfection, the cells were photographed using a FluoArc, Axiovert -200 inverted fluorescent microscope and a $40 \times$ phase-contrast objective.

Rf: 5.09, $p < 0.05$. *Rf* (resistant factor) was determined by the transfection ratio of SF188C2R2 by that of the parental cell line SF188.



**Fig. 3-9. Transfection efficiency of SF188 and SF188C2R2 with lentiviral vector
PHR' – CMV – EGFP**

The ratio was determined from three representative viewing fields captured the fluorescent microscope. Data are expressed as the means \pm SD of the transfected cells in three representative viewing fields.

** , $p < 0.05$, p value was calculated from independent t-test between two cell lines.

3.4 Discussion

Drug resistance is a principal problem in the treatment of cancer and occurs in most anticancer drugs. The establishment of aPPD-resistant cell line demonstrated that cancer cells could acquire drug resistance to aPPD as they do to many other anticancer agents. aPPD-resistant cell line, SF188C2R2, grown from a single cell by aPPD selection, was 2-fold resistant to aPPD compared to its parental cell line SF188. Unlike some other drug-resistant cell lines generated by “stepwise” induction, which usually takes 6 months to establish the drug-resistant cell lines [20-22]. SF188C2R2 was induced by one step with aPPD 30 µg/ml (IC₉₀) in 3 months. Frequency of acquired aPPD-resistant cells, about 1/10⁵ in SF188 cells, was higher than that of other drug resistance developed by gene mutation in tumor cells, which was 1/10⁶ – 1/10⁷ cells per generation [23, 24].

The aPPD-resistant cell line, SF188C2R2 is different from the parental SF188 cells with several distinctly biological features (Table 3-5). SF188C2R2 showed higher rates of proliferation compared to SF188. Secondly, SF188C2R2 exhibited cross-resistance to anticancer drugs with different mechanisms of action (Fig.3-5). Interestingly, SF188C2R2 appeared lower efficiency in plasmid DNA transfection (Fig.3-9). Most strikingly, SF188C2R2 lost the response of G2-M arrest to treatment of low concentrations of aPPD (Fig.3-4).

Recently, Ma and colleagues reported another drug resistant cell line, SF188TR

Table 3-5 Biological features of SF188C2R2 versus SF188

Biological features	SF188C2R2	SF188
Cell growth doubling time	24.2 ± 1.8	68.2 ± 24.5
Colony formation	155.3 ± 40.6	63.3 ± 15.3
Cell cycle	G1 arrest	G2 arrest
aPPD	Resistant	Sensitive
Cross drug resistant	+	-
DOX	Sensitive	Resistant
plasmid DNA transfection	Resistant	Sensitive
P-glycoprotein expression	-	-

derived from SF188 induced by temozolomide [20]. Comparing SF188TR to SF188C2R2 (Table 3-6), both cell lines showed low P-gp activity. Both TMZ- and aPPD-resistant cells demonstrated the profiles of cross-drug resistance and cell cycle distribution with drug treatment different from their parental cells SF188. However, different to SF188C2R2, SF188TR showed no difference in proliferation rate compared to SF188. In addition, the drug resistant profile of SF188TR was different from that of SF188C2R2 (Table 3-7). Even though both SF188TR and SF188C2R2 exhibited resistance to paclitaxel and cisplatin, SF188C2R2 was sensitive to DOX but SF188TR was resistant to DOX. Ma et al further demonstrated that the pro-apoptotic proteins, Bad, Bax and Bcl-X_L, were reduced 2-4-fold in the SF188/TR resistant cells compared to the parental cells but the expression of the anti-apoptotic protein Bcl-2 and Bcl-X_L remained unchanged in both cell lines. Therefore, they inferred that the apoptotic-related mechanism may favor cell survival and provided a common multidrug resistance mechanism for the cross-resistance of SF188/TR cells. However, the above difference indicates that the acquired drug resistance was due to different mechanisms between SF188TR and SF188C2R2. SF188C2R2 is likely a useful tool for further investigation of the mechanism of aPPD inhibiting the cancer cells. SF188C2R2 showed in Fig.3-5 is resistant to alkaloids agent vincristine and paclitaxel, which prevent the formation of chromosome spindles necessary for cell duplication. SF188C2R2 is also resistant to alkylating agent cisplatin, which binds to DNA in cells to prevent DNA replication. The above cross-resistance between aPPD and chemotherapeutics suggests that there might be an unknown mechanism of

Table 3-6 Characteristics of SF188C2R2 and SF188TR

Biological features	SF188C2R2 vs SF188	SF188TR vs SF188 [20]
Doubling time	Shorter	Unchanged
Morphology	Heterogeneous	/
Cell cycle	Unchanged /G2 arrest	Unchanged /G2 arrest
DOX	Sensitive	Resistant
Cisplatin and Taxol	Resistant	Resistant
P-gp	Negative	Negative

resistance developed in the cells that is common for all the above agents, however, calcein formation assay (Fig. 3-7) showed that neither SF188 nor SF188C2R2 overexpress P-gp. Thus, it is not likely that the cross-resistance to the above drugs was due to enhanced drug efflux. Interestingly, SF188C2R2 (Fig. 3-6A1) was 3-fold sensitized to the antitumor antibiotics agent DOX that prevents DNA replication by inhibiting topomerase II activity. This paradoxical phenomenon suggests the existence of multiple pathways interacting with each other in the cells. When a tumor becomes resistant to some anticancer drugs due to alteration of one or more pathways, it is also possible to become sensitive to other agents. Furthermore, SF188C2R2 remained unchanged in response to BCNU, which inhibits DNA replication by forming covalent bonds with DNA and causes single strand DNA breaks (Fig. 3-6B). Previous studies demonstrated that the level of O⁶-alkylguanine transferase, an enzyme capable of repairing the O⁶-alkylguanine lesion, was elevated in SF188 [1, 25, 26], which was one of the mechanisms of SF188 resistant to BCNU. Unchanged resistance to BCNU in SF188C2R2 suggests that some genetic features of parental SF188 remained after selection for aPPD resistance, and the mechanism responsible for BCNU resistance is independent of the mechanisms causing cross-resistance to aPPD and other chemotherapeutics.

SF188 cell line used in the present study was known for its mutation in p53 with a glycine to glutamate substitution at codon 266 (GGA (Gly) → GAA (Glu)) [2]. This mutation occurred in the DNA binding domain of p53 protein, which binds DNA

Table 3-7 Comparison of drug resistant profiles of SF188C2R2 and SF188 TR

	Parent SF188 of SF188C2R2			Parent SF188 of SF188 TR [20]		
	IC ₅₀ (μM)	IC ₅₀ (μM)	Rf*	IC ₅₀ (μM)	IC ₅₀ (μM)	Rf*
Paclitaxel	0.0089±0.0018	4.52±1.86	544.9	0.00172±0.00084	0.00586±0.00223	3.4
Cisplatin	8.78±3.71	669.87±21.80	76.3	0.6837±0.0793	1.11501±0.1823	1.6
Dox	0.626+/-0.013	0.177±0.017	0.3	0.0205±0.00069	0.0598±0.00172	2.9

* Rf (resistant factor) was determined by dividing the IC₅₀ of the drug for SF188C2R2 or SF188TR by that of the parental cell line SF188.

in a sequence-specific manner to activate transcription of a number of genes including p21^{Cip/WAF1}, MDM2 and BAX. p21^{Cip/WAF1} inhibits G1 cyclin dependent kinases, blocking cell cycle progression from G1 into S phase [27-29]. Ma et al. also found that treated with TMZ, the parental cells SF188 were blocked in G2-M phase but the cells distribution in SF188TR remained unchanged after TMZ treatment [20]. They further demonstrated that both SF188 and SF188TR cells contained p53 mutation and failed to transcriptionally induce the p53-response gene p21^{Cip/WAF1}, in response to DNA damage [20]. Our preliminary results also showed a G2/M arrest in SF188 after treatment with low concentrations (10 µg/ml and 15 µg/ml) of aPPD. Interestingly, similar to the SF188TR cells, the G2/M arrest was not seen in aPPD treated SF188C2R2 (Fig.3-4, Table 3-3).

REFERENCES

1. Jean-Claude, B.J., et al., *Tetrazepones are equally cytotoxic to Mer⁺ and Mer⁻ human tumor cell lines*. J Pharmacol Exp Ther, 1999. **288**(2): p. 484-9.
2. Ishii, N., et al., *Frequent co-alterations of TP53, p16/CDKN2A, p14ARF, PTEN tumor suppressor genes in human glioma cell lines*. Brain Pathol, 1999. **9**(3): p. 469-79.
3. Kemper, E.M., et al., *Modulation of the blood-brain barrier in oncology: therapeutic opportunities for the treatment of brain tumours?* Cancer Treat Rev, 2004. **30**(5): p. 415-23.
4. Fulci, G., N. Ishii, and E.G. Van Meir, *p53 and brain tumors: from gene mutations to gene therapy*. Brain Pathol, 1998. **8**(4): p. 599-613.
5. Dive, J.A.H.a.C., ed. *Apoptosis and cancer chemotherapy*. 1999, Humana Press: Totowa, N.J.
6. Perry, M.C., ed. *The chemotherapy source book*. 1996, Williams & Wilkins: Baltimore. 90-108.
7. Perry, M.C., ed. *The chemotherapy source book*. 1996, Williams & Wilkins: Baltimore. 109-119.
8. Jaffrezou, J.P., et al., *Mutation rates and mechanisms of resistance to etoposide determined from fluctuation analysis*. J Natl Cancer Inst, 1994. **86**(15): p. 1152-8.
9. Chen, G., et al., *Prevalence of multidrug resistance related to activation of the mdrl gene in human sarcoma mutants derived by single-step doxorubicin selection*. Cancer Res, 1994. **54**(18): p. 4980-7.

10. Devarajan, E., et al., *Human breast cancer MCF-7 cell line contains inherently drug-resistant subclones with distinct genotypic and phenotypic features*. *Int J Oncol*, 2002. **20**(5): p. 913-20.
11. Mares, V., et al., *Cisplatin induced gamma-glutamyltransferase up-regulation, hypertrophy and differentiation in astrocytic glioma cells in culture*. *Histol Histopathol*, 2003. **18**(3): p. 687-93.
12. Aslanian, A.M. and M.S. Kilberg, *Multiple adaptive mechanisms affect asparagine synthetase substrate availability in asparaginase-resistant MOLT-4 human leukaemia cells*. *Biochem J*, 2001. **358**(Pt 1): p. 59-67.
13. Grana, C., et al., *Pretargeted adjuvant radioimmunotherapy with yttrium-90-biotin in malignant glioma patients: a pilot study*. *Br J Cancer*, 2002. **86**(2): p. 207-12.
14. Yount, G.L., et al., *Transcriptional activation of TRADD mediates p53-independent radiation-induced apoptosis of glioma cells*. *Oncogene*, 2001. **20**(22): p. 2826-35.
15. Tseng, S.H., et al., *Characterization of paclitaxel (Taxol) sensitivity in human glioma- and medulloblastoma-derived cell lines*. *Neuro-oncol*, 1999. **1**(2): p. 101-8.
16. Bobola, M.S., M.S. Berger, and J.R. Silber, *Contribution of O6-methylguanine-DNA methyltransferase to resistance to 1,3-(2-chloroethyl)-1-nitrosourea in human brain tumor-derived cell lines*. *Mol Carcinog*, 1995. **13**(2): p. 81-8.
17. Scheck, A.C., et al., *BCNU-resistant human glioma cells with over-representation of chromosomes 7 and 22 demonstrate increased copy number*

- and expression of platelet-derived growth factor genes. Genes Chromosomes Cancer, 1993. 8(3): p. 137-48.*
18. Lokker, N.A., et al., *Platelet-derived growth factor (PDGF) autocrine signaling regulates survival and mitogenic pathways in glioblastoma cells: evidence that the novel PDGF-C and PDGF-D ligands may play a role in the development of brain tumors. Cancer Res, 2002. 62(13): p. 3729-35.*
 19. Boussif, O., et al., *A versatile vector for gene and oligonucleotide transfer into cells in culture and in vivo: polyethylenimine. Proc Natl Acad Sci U S A, 1995. 92(16): p. 7297-301.*
 20. Ma, J., et al., *Biochemical changes associated with a multidrug-resistant phenotype of a human glioma cell line with temozolomide-acquired resistance. Biochem Pharmacol, 2002. 63(7): p. 1219-28.*
 21. Boyer, J., et al., *Characterization of p53 wild-type and null isogenic colorectal cancer cell lines resistant to 5-fluorouracil, oxaliplatin, and irinotecan. Clin Cancer Res, 2004. 10(6): p. 2158-67.*
 22. Liu, Z.L., et al., *Induction of multidrug resistance in MOLT-4 cells by anticancer agents is closely related to increased expression of functional P-glycoprotein and MDR1 mRNA. Cancer Chemother Pharmacol, 2002. 49(5): p. 391-7.*
 23. Goldie, J.H. and A.J. Coldman, *A mathematic model for relating the drug sensitivity of tumors to their spontaneous mutation rate. Cancer Treat Rep, 1979. 63(11-12): p. 1727-33.*
 24. Perry, M.C., ed. *The chemotherapy source book. 2001, Lippincott Williams & Wilkins: Philadelphia. p.63-100.*

25. Bodell, W.J., et al., *Increased repair of O6-alkylguanine DNA adducts in glioma-derived human cells resistant to the cytotoxic and cytogenetic effects of 1,3-bis(2-chloroethyl)-1-nitrosourea*. *Carcinogenesis*, 1986. **7**(6): p. 879-83.
26. Aida, T. and W.J. Bodell, *Cellular resistance to chloroethylnitrosoureas, nitrogen mustard, and cis-diamminedichloroplatinum(II) in human glial-derived cell lines*. *Cancer Res*, 1987. **47**(5): p. 1361-6.
27. Tweddle, D.A., et al., *The p53 pathway and its inactivation in neuroblastoma*. *Cancer Lett*, 2003. **197**(1-2): p. 93-8.
28. Paul Kleihues, W.K.C., ed. *Pathology and genetics of tumours of the nervous system*. 1997, International Agency for Research on Cancer: Lyon. 4-6.
29. Kleihues, P., ed. *Pathology and genetics of tumours of the nervous system*. ed. W.K. Cavenee. 1997, International Agency for Research on Cancer: Lyon. 16-24.

CHAPTER 4. PRELIMINARY RESULTS OF GENE EXPRESSION PROFILES OF SF188 AND SF188C2R2 CELLS TREATED WITH OR WITHOUT APPD

4.1 Introduction

Many studies have attempted to uncover the molecular mechanism of ginsenosides, including Rh2, Rg3, aPPD and aPPT for the effects of tumor inhibition shown by reducing cell proliferation, blocking cell cycle and inducing apoptosis [1, 2]. A number of complicated signal transduction pathways (e.g., NF- κ B, c-myc, p21^{Cip/WAF1}, and Bcl-X_L) pertinent to cellular growth, differentiation and apoptosis were reported to be involved and responsible for the anticancer activities by the above ginsenosides [3, 4]. Ginsenoside Rg3, one of the panaxadiol (PD) family members, was found to exert potent inhibitory effects on NF- κ B and on the activation of a transcription factor, activator protein-1 (AP-1), which links to c-jun and c-fos oncogenic transactivation in human pro-myelocytic leukemia (HL-60) cells [3]. Rg3 was also demonstrated to cause LNCaP cell death by down-regulating the Bcl-2 gene and concomitantly activating caspase-3 gene and modulated MAP kinases [5]. To induce the cell cycle G1 arrest in LNCaP, Rg3 inhibited PCNA (proliferating cell nuclear antigen) and cyclin kinase 1, which was associated with increased expression of cyclin kinase inhibitor genes p21^{Cip/WAF1} and p27^{Kip} [6]. It was also reported that ginsenosides Rg3 and Rh2, another member of the PD family, caused G1/S arrest in human hepatoma SK-HEP-1 cells by inducing p27^{Kip} and thereby down regulating cyclin E-dependent kinase activity [7]. Rh2 has been shown to suppress the DNA replication in BALB/c3T3 cells via indirect Cdk2 (cyclin-dependent kinase 2) inhibition [8]. In addition, Rh2 induced the expression of p21^{Cip/WAF1} and reduced the levels of cyclin D

resulting in the down-regulation of cyclin/Cdk complex kinase activity, the decrease of decreasing phosphorylation of pRb and the inhibition of E2F release in MCF-7 [9]. Furthermore, the metabolite of ginseng saponin 20 - O - (-D-Glucopyranosyl) - 20(S) - protopanaxadiol (IH901) was reported to inhibit cancer cells via the mitochondrial-mediated pathway in HepG2 cells by activation of caspase-9, -3, and casepase-8 and to cleave Bid and tBid in the amplified mitochondrial pathway [10]. IH-901 was demonstrated to inhibit a tumor promoter 12-O-tetradecanoyphorbol (TPA), which induced COX-2 expression by blocking the ERK and NF-kB signaling cascades [11].

However, all investigations into the mechanisms of anticancer activity of ginsenosides were established on individual genes or single pathway studies. Because genes collaborate in overlapping pathways, single pathway or several key genes studies of the human repertoire of over 30, 000 genes make it hard to provide an entire picture of the complex pathways, which addresses how cancer cells respond to ginsenosides [12, 13]. The limitations of experimental tools used in these studies forced gene expression pattern investigation to be designed around specific hypotheses and is thus framed on the basis of the very limited knowledge we presently possess. These experiments were particularly limited for mammalian study, as the networks are far more complex and poorly elucidated. For instance, new therapeutics for cancer designed to specifically target proteins involved in signalling pathways are not always effective [14]. One of the reasons is that the bias from individual gene or single pathway studies masks the interaction of the signalling pathways in cancer cells. Particularly, Rh2 and aPPD were recently demonstrated to have cytotoxic effects on cancer cells with both apoptotic and necrotic cell characteristics [2]; this suggested that multiple cell death

pathways were activated simultaneously [2, 3]. However, which cell death pathways induced by aPPD in cancer cells remains unclear.

DNA microarray, also known as "DNA chips", are extensions of hybridization-based methods for simultaneous analysis of the patterns of expressions of tens of thousands of genes. It is a rapid, high throughput, novel platform genetic method available for the analyses of many sample at the same time [13]. Moreover, DNA microarrays have been applied to the study of complex changes in patterns of gene expression during the development and progression of cancer. This provides a more comprehensive and less biased view of the pathway networks of given cells or tissues.

Comprehensive molecular profiling from DNA microarrays can be used for the mechanism investigation for the drug inhibiting cancer to identify molecular determinants of a drug response. Consequently, the action of the drug on genes can be revealed. In addition, DNA microarray provides a further basis for benchmarking the generation of analogues and provides important information about pathways potentially modulated by the drug in achieving cytotoxicity. This approach is accomplished by examining microarray profiles of tumor samples before and after drug exposure [15]. Two main implementations of DNA arrays, cDNA and oligonucleotides, have been applied. Each array consists of a solid support on which cDNA or oligonucleotides are arrayed. cDNA array is cDNA clones robotically spotted on a solid surface in the form of PCR products. This approach is flexible to make arrays with different gene sets. However, cDNA clones and PCR products require accurate annotation, collection, and storage of cDNA clones. A cross-contamination of PCR products must be avoided. Oligonucleotides are either directly

synthesized in situ on a support or robotically spotted. The targets are designed with known gene sequences in which the oligonucleotides length varying from 20 to 80 base pairs allow for alternative transcripts to be detected accurately. The main drawback remains the elevated cost. In the following steps, cDNAs or cRNAs (probe) derived from cell lysate mRNAs are labeled with fluorescent, chemiluminescent, or radioactive and hybridized to the target on the array. A DNA array – based assay is the conversion of the image acquired with the scanner into a numeric table that associates multiple values to every gene (or oligonucleotide set) in the array [16]. The array utilized in the present study was CodeLink UniSet Human 20K Bioarray. It is an oligonucleotides array with 20,289 genes. Codelink Expression Bioarray signals are derived from the hybridization of biotin-labelled complementary RNA (cRNA) [17].

The miroarray data analysis, interpretation, and meaningful display are particularly challenging. Currently, dedicated software provides unsupervised and supervised analysis. Unsupervised methods using cluster analysis, self-organizing maps, and principal component analysis define classes without any prior intervention on data, which are organized by clustering genes and/or samples simply according to similarities in their expression profiles. Cluster analysis, probably the most popular method of DNA array data analysis in research, is divided as hierarchical and nonhierarchical clustering. Hierarchical clustering allows for the detection of higher-order relationships between clusters of profiles, whereas, the majority of nonhierarchical classification techniques work by allocating gene expression profiles to a predefined number of clusters. The possibility of exploring different levels of the hierarchy has led many authors to prefer hierarchical clustering to the nonhierarchical alternatives. Supervised techniques are used in defining relevant classes before anal-

ysis. The analyses incorporate external information related to samples studied to identify the optimal set of genes that best discriminate between experimental samples [16].

Because DNA microarrays enable the acquisition of gene expression data on a scale at one time and relate how the gene expression pattern of one gene correlates to the expression of other genes between the samples [18], the objective of this part of study was focused on using DNA microarray to investigate the alteration of gene expression in human glioblastoma cells SF188 and its drug resistant daughter line SF188C2R2 treated with aPPD, in the hope of gaining insight into the molecular mechanisms of cell death mediated by aPPD, and the identification of potential genes that may be further evaluated for possible therapeutic application and new drug development.

4.2 Methods and materials

4.2.1 Drugs and chemicals

aPPD stock 50mg/ml was kept in 4°C (See chapter 2). TRIzol was purchased from Invitrogen. Isopropanol was purchased from Sigma. Agarose was the product of Life Science GIBICO. TaqMan® Reverse Transcription Reagent Kit and SYBR Green (Applied Biosystems, Foster City, CA, USA).

4.2.2 Cell lines

The human glioblastoma cell line SF188 and aPPD-resistant cell line SF188C2R2 generated by our lab (See chapter 3) were grown in DMEM (Canadian Life

Technologies Inc., Burlingto, Ont.) containing 10% fetal bovine serum, 100U/ml penicillin and 100 µg/ml streptomycin. Cells were incubated at 37°C under a humidified atmosphere of 5% CO₂. The medium was replaced every 3 days.

4.2.3 Cell culture and RNA isolation

2.2×10^6 SF188 cells and 1.98×10^6 SF188C2R2 cells were seeded in 100 mm dishes and grew for 48 h. Cells were incubated with or without aPPD 40 µg/ml for 5.5 h. At this point, SF188 had 50% cell death while SF188C2R2 had no cell death. The medium was removed and the cells were washed with 0.1M PBS. RNA samples were isolated using TRIZOL. Briefly, the cells were exposed to TRIZOL reagent 1ml/dish for 3 min at room temperature. Then 0.2 ml chloroform was added to each dish and mixed gently. After 10 min at room temperature, the samples were collected into the tubes and centrifuged at 14,000 RPM for 15 min at 4°C. The supernatant was transferred into new tubes and 0.5 ml isopropanol was added to each tube and mixed. The samples stood at room temperature for 10 minutes, then were centrifuged at 14,000 RPM for 10 minutes at 4°C. The pellets were washed with 1ml 75% ethanol, then dried in the air for 10 min, followed by dissolving in DEPC treated H₂O to the final concentration of 1mg/ml. Protein contamination in each sample was determined by a spectrometer at the wavelengths of 260 nm and 280 nm. The ratio of O.D. 260/280 for each sample was larger than 1.8. The RNA samples were kept in -80°C.

4.2.4 Reverse transcription analysis

TaqMan® Reverse Transcription Reagent Kit (Applied Biosystems, Foster City, CA, USA) was utilized for reverse transcription. The first strand of cDNA was synthesized

in a reaction (10 μ l) containing 1 μ g of total RNA, 1 μ l 10X Master Mix, 0.45 μ l of Reverse transcriptase, RNAase Inhibitor Mix, and 0.4 μ l of RNAse-free water. The reaction was carried out at 25°C for 10 min, then 48°C for 45 s followed by an incubation at 95°C for 5 min. cDNA samples obtained were diluted 10-times for Real-time PCR. The amplified products were resolved on 1% agarose gels and visualized under ultraviolet light after ethidium bromide staining.

4.2.5 Gene expression using bioarrays

Duplicate mRNA samples extracted from SF188 and SF188C2R2 cells in the presence or absence of aPPD, were labeled with Biotin using the CodeLink Bioarray Labeling System in Dr. Prasad's Lab, and processed for hybridization with CodeLink UniSet Human 20 K Bioarray (Amersham Biosciences, Vancouver Canada) through Medbiogene Inc., Vancouver, Canada. The bioarray utilized in the present study contained a collection of approximately 20,289 gene probes and has involved 12 classes of biological processes (Table 4-1)[17, 19]. The CodeLink UniSet Human Bioarray content was based on the public UniGene and RefSeq databases, and sequences for design were derived from Incyte LifeSeq™ Gold and Foundation databases [www.amershambiosciences.com] [17].

4.2.6 Array data analysis

Each sample was normalized to medium signal intensity. The normalized intensities were compared between groups defined by ratios of the averages of the duplicates in each group. Gene expression analysis was based on comparison of 4 pairs of samples including SF188C2R2 vs SF188 (C2R2/wt), SF188C2R2 plus aPPD vs SF188C2R2 (C2R2+a/C2R2), SF188 plus aPPD vs SF188 (Wt+a/Wt), and SF188C2R2 plus aPPD

Table 4-1 CodeLink UniSet Human 20K I gene classification

Major biological process [19]	Number of genes present [17, 19]
Oncogenesis	~ 1000
Cell cycle	~ 1300
Cell-cell signaling	~ 700
Signal transduction	~ 1600
Metabolism	~ 900
Developmental processes	~ 1400
Transcription and translation	~ 1000
Immune and inflammation response	~ 800
Protein phosphorylation	~ 400
Apoptosis	~ 400
RNA processing	~ 300
Ion transport	~ 200

[www.amershambiosciences.com]

vs SF188 plus aPPD (C2R2+a/wt+a). For each gene, only the ratios in the range of 0.8 to 1.2 were considered valid. Hierarchical cluster analysis was performed to group genes with similar patterns of expression using Tige MEV DNA microarray analysis software version 2.2 (DataNaut Incorporated (Washington DC))[19]. Genes with changed expression after aPPD treatment were selected for clustering analysis. The criteria for aPPD regulated gene expression were that the ratio of aPPD-/aPPD+ must be greater than 1.5 for up-regulated genes or less than 0.68 for down-regulated genes [20].

4.2.7 Quantitative real-time PCR

Quantitative comparison of SKIP3 and ATF4 mRNA levels was carried out using real time PCR technology with beta-actin as the endogenous control. Primers for SKIP3 (forward primer 5'-TCTCAGGTCCCACGTAGGCT-3'; reverse primer 5'-ATGATTCCCTGTGGGACAAGC-3'), ATF4 (forward primer 5'-TTGCCTTGCGGACCTCTTC-3'; reverse primer 5'-CCAAGGAGATCCAGTACCTGAAA-3'); beta-actin (forward primer 5'-ACGAGGCCAGAGCAAGAG-3'; reverse primer 5'-TCTCCATGTCGTCCAGTTG-3') and DAP3 (forward primer 5'-GATGCCCTGGATCCCTTTATTC-3'; reverse primer 5'-CCTTTGGGTTATAGTTGGAAACCA-3') were designed using Primer Express software (Applied Biosystems). cDNA was amplified using Taqman thermal cycler (7000 Sequence Detection System, ABI PRISM Applied Biosystems). SYBR green master mix was used under the following conditions: 2 min at 50°C and 10 min at 95°C, followed by 40 cycles of 15 s at 95°C and 1 min at 60°C. Fluorescence data was processed and analyzed with ABI PRISM Sequence Detection Software (Applied Biosystems).

4.2.8 Polymerase chain reaction (PCR) analysis

The PCR reaction was carried out in a DNA thermal cycler (Applied Biosystems, CA, U.S.A) under the following conditions: one cycle of 95°C for 3 min, followed by 40 cycles of 95°C, 30 s, 58°C 30 s, and 72°C 1min, with a final 10 min extension at 72°C. The primers used were 5'-TCTCAGGTCCCACGTAGGCT-3'/5'-ATGATTCCCTGTGGGACAAGC-3', 5'-TTGCCTTGCGGACCTCTTC-3'/5'-CCAAGGAGATCCAGTACCTGAAA-3', and 5'-ACGAGGCCAGAGCAAGAG-3'/5'-TCTCCATGTCGTCCCAGTTG-3' for SKIP3, ATF4, and actin.

4.3 Results

4.3.1 SF188C2R2 gene expression profile differed to that of SF188

To gain insights into the molecular basis of aPPD induced cell death in SF188, a gene expression profile assay was performed with CodeLink UniSet Human 20 K Bioarray. This study was designed to elucidate changes in gene expression at the early stage of cell death in SF188 upon aPPD stimulation and to compare the gene expression profiles of aPPD-sensitive SF188 with aPPD-resistant SF188C2R2 cells. Two independent experiments on each cell lines were performed as duplicates. The correlation of data from the duplicates was in the range of 0.9-0.97. Overall, the signal derived from 6293 genes out of 19, 982 in the microarray was above the threshold of detection with “true” and “good” quality. According to the manufacturer’s guidance, “true” is defined as the signal intensity of the spot that is above 80% trim mean for

the negative control and “good” is defined as the spot that is free of any defects. While, some genes consistently showed data quality as “false” and “empty” in some samples. “False” is defined as the signal intensity of the spot that is lower than 80% trim mean for the negative control and “empty” is defined as the spots that near a background level where the mean background plus one standard deviation is greater than the signal mean. The genes with the data quality showing “false” and “empty” indicated the expressions of these genes were extremely low. To elucidate the changes of gene expression induced by aPPD, four sample pairs were analyzed as indicated in “Methods”. Accordingly, genes with a ratio larger than 2 in each pair were defined as up-regulated, between 0.5 and 1.5 were defined as no change and less than 0.5 were defined as down-regulated [21]. Hierarchical clusters were built up with the 3703 genes using Tige MEV version 2.2 DNA microarray analysis software. Fig. 4-1 illustrates color coded gene expression changes. It is apparent that many genes express differently in SF188C2R2 from that of SF188 both in rest status and in their response to aPPD treatment. Table 4-2 shows that the aPPD-resistant cells SF188C2R2 had 41.6% genes with their expression levels similar to SF188, while 58.4% of the genes were differently expressed. Among the differently expressed genes, 43.2% were down-regulated and 15.2% were over-expressed in SF188C2R2 cells compared to that of SF188. Consistent with increased proliferation of SF188C2R2 (see Chapter 3), a number of proliferation related genes were up-regulated in SF188C2R2 cells as listed in Table 4-3. These genes include BRUNOL4, FRAG1, FGFR1, EMR2 in FGF family and BDNF (Brain derived neurotrophic factor). Interestingly, aPPD treatment did not significantly change the expression levels of those genes.

Table 4-2 Gene expression in SF188C2R2 and SF188 in the presence or absence of aPPD

Gene expression	C2R2/wt		C2R2+a/C2R2		Wt+a/Wt		C2R2+a/wt+a	
	Number of gene	%						
Up-regulated genes	956	15.2	139	2.2	323	5.1	1399	22.2
Unchanged gene	2618	41.6	6116	97.2	4472	71.1	2714	43.1
Down-regulated genes	2719	43.2	38	0.6	1498	23.8	2180	34.6
Total changed genes	3675	58.4	177	2.8	1821	28.9	3579	56.9
Total genes	6293							

Table 4-3 Gene expression relating to cell proliferation

	C2R2/Wt	Description
BRUNOL4	2.17	Human FGFR signalling adaptor SNT-1
FRAG1	1.65	FGF receptor activating protein 1
FGFR1	1.50	Fibroblast growth factor receptor 1 (FMS-related tyrosine kinase 2, Peiffer syndrome), transcript variant 9
EMR2	1.53	EGF-like module containing, mucin-like, hormone receptor-like sequence 2.
BDNF	8.02	Brain-derived neurotrophic factor

4.3.2 Gene expression changes in both SF188C2R2 and SF188 treated by aPPD

To evaluate changes in gene expression induced by aPPD in SF188 and SF188C2R2 cells, DNA array data were filtered based on the ratios of C2R2+aPPD/C2R2 and Wt+aPPD/Wt. There were a large number of genes with expression in SF188 different to that in SF188C2R2 treated with aPPD. While it was apparent that in the presence of aPPD, most genes remained unchanged in both cell lines, SF188 had 10-fold more genes changed in their expression than SF188C2R2 after aPPD treatment. Table 4-2 showed that 177 genes (2.81%) in SF188C2R2 were significantly changed after treatment with aPPD while 1821 (28.9%) genes in SF188 altered their expression levels. Most interestingly, aPPD caused gene expression change (Fig. 4-2) was mainly up-regulation in SF188C2R2 (139/177, 78.5% of total changed genes), but was mainly down-regulation in SF188 (1498/1821, 82.3% of changed genes).

4.3.2.1 Apoptotic gene expression in SF188 and SF188C2R2 treated by aPPD

A total of 372 genes out of 19,982 genes examined were apoptosis related. 260 and 203 apoptotic genes expressed in SF188 and SF188C2R2 treated by aPPD, respectively. Apoptotic gene cluster analysis shown in Fig. 4-3 demonstrated that the expression of many apoptotic genes in SF188 were different from that in SF188C2R2 in response to aPPD treatment. Most interestingly, aPPD induced up-regulation of apoptotic genes in both SF188 and SF188C2R2, but more genes were down-regulated in SF188 than in SF188C2R2 (Fig 4-4). Therefore, the profile of significantly changed apoptotic genes in SF188 (Table 4-4) was quite different to that of SF188C2R2 (Table 4-5) following treatment with aPPD.

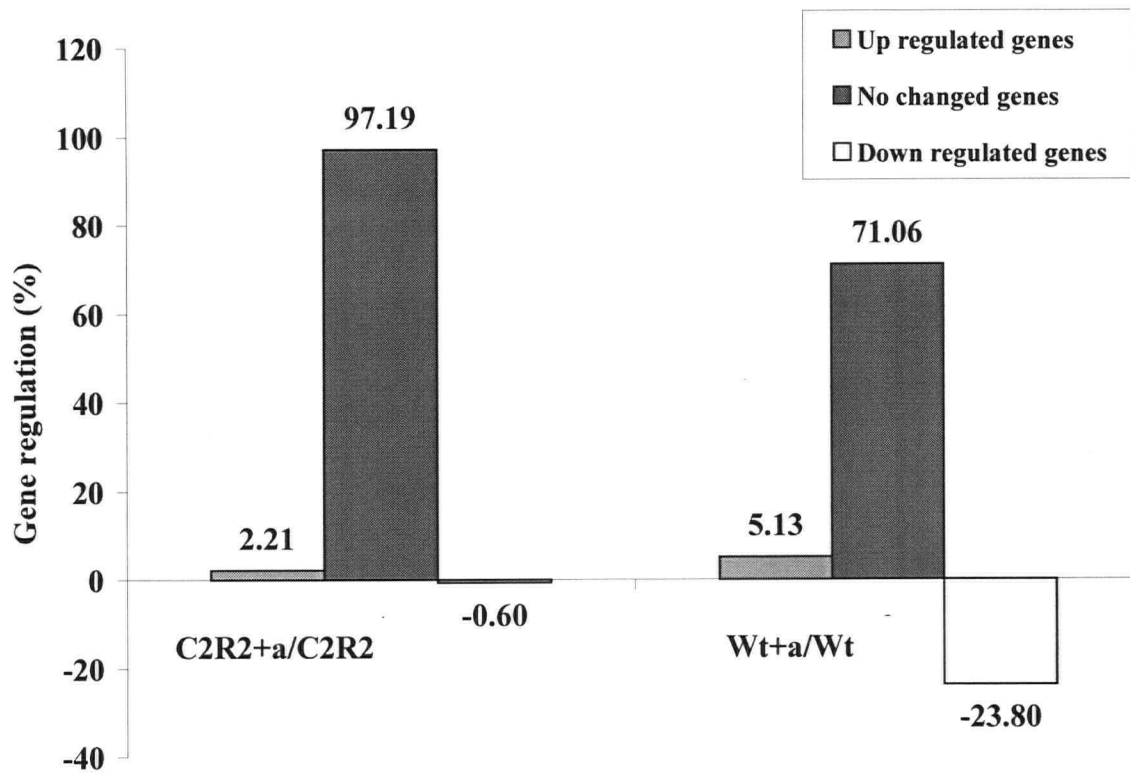


Fig. 4-2. Gene expression pattern in SF188C2R2 (C2R2) and SF188 (Wt) in the presence or absence of aPPD

Data were expressed as percentage of total qualified genes for analysis in the cells.

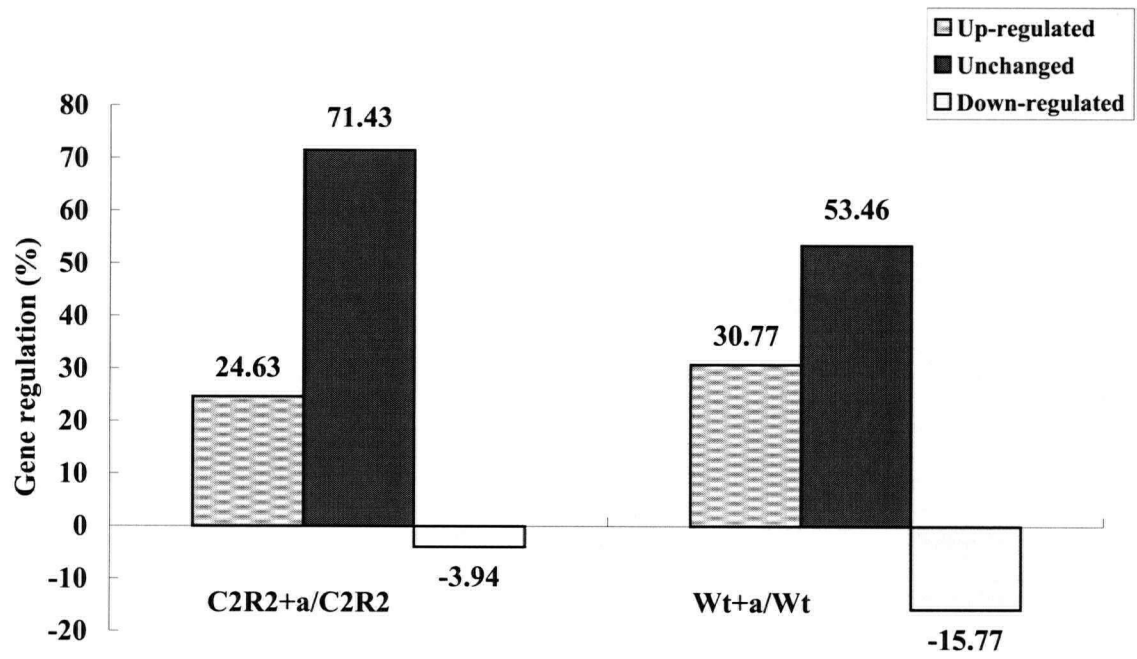


Fig. 4-4. Apoptotic gene expression pattern

It is worth pointing out that those genes in MAPK, mitochondrial and death-receptor dependent pathways, which were the main cell death pathways, changed expression levels after aPPD treatment in both cell lines (Fig. 4-5). SKIP3, DAP3, ATF4 and TNF- α were up-regulated in SF188 in the presence of aPPD (Fig. 4-6) shown by the array data and verified by quantitative real-time RT-PCR. It confirmed that gene expression levels of SKIP3 and ATF4 were up-regulated in SF188 and SF188C2R2 by aPPD treatment (Fig. 4-7). However, SKIP3 in SF188 was 10-fold higher than that of SF188C2R2. ATF4 is the partner gene of SKIP3. Fig. 4-8 showed that, paralleled to SKIP, ATF4 was also up-regulated in SF188 and SF188C2R2 cells treated with aPPD. DAP3 in cDNA array analysis was shown as up-regulated by aPPD, however, qRT-PCR of DAP3 using primers for DAP3 variant 2 did not confirm the DNA microarray data. Therefore, further study may be necessary by using other variant specific primers to verify the results.

4.3.2.2 Anti-apoptotic gene expression in SF188 and SF188C2R2 treated by aPPD

A total of 23 genes out of 6293 genes are associated with anti-apoptosis effect (Table 4-6). Fig 4-9 showed that there were more anti-apoptosis genes down-regulated in SF188 than in SF188C2R2 by aPPD. Moreover, Table 4-6 showed that SF188 had 5 (21.7%) genes down-regulated (Fig 4-9) including IGF1R, TNFSF5, CBX4, BAG1 and BNIP3, but no gene up-regulated. Contrarily, SF188C2R2 had 2 genes, IER3 and MCL1 up-regulated but no gene down-regulation in the presence of aPPD.

Table 4-4 Significantly changed apoptotic genes in aPPD treated SF188 cells

OGS	Wt+a/Wt	Description
TRIB3	6.78	Chromosome 20 open reading frame 97
BCAP31	4.95	Accessory protein BAP31
DAP3	4.25	Death associated protein 3, transcript variant 2, nuclear gene encoding mitochondrial protein
ATF4	3.33	Activating transcription factor 4 (TAX-responsive enhancer element B67)
NCKAP1	3.11	Nck-associated protein 1
DNAJA3	3.07	Tumorous imaginal discs (drosophila) homolog
EP300	3.06	E1a binding protein p300
SFRP1	3.01	Secreted frizzled-related protein 1
PIG7	2.91	LPS-induced TNF-alpha factor
GADD45 α	2.80	Growth arrest and dna-damage-inducible, alpha
CTNNAL1	2.74	Catenin (cadherin-associated protein), alpha-like 1
CUL1	2.62	Cullin 1
CASP4	2.58	Caspase 4, apoptosis-related cysteine protease, transcript variant alpha
ESPL1	2.38	Extra spindle poles like 1 (s Cerevisiae)
INHBA	2.23	Inhibin, beta a (activin a, activin ab alpha polypeptide)
BIRC6	2.07	Baculoviral IAP repeat-containing 6 (apollon)
DAPK1	2.02	Death-associated protein kinase 1
TNFRSF21	0.49	Tumor necrosis factor receptor sturn on ER family, member 21
CASP5	0.48	Caspase 5, apoptosis-related cysteine protease
FAIM	0.48	Hypothetical protein flj10582
SFRP5	0.47	Secreted frizzled-related protein 5
BOK	0.46	Bcl-2-related ovarian killer protein-like

BCLAF1	0.46	KIAA0164 gene product
FASTK	0.44	Fast kinase, transcript variant 2
PDCD8	0.44	Programmed cell death 8 (apoptosis-inducing factor), nuclear gene encoding mitochondrial protein, transcript variant 2
FKSG2	0.43	Apoptosis inhibitor
MX1	0.43	Human p78 protein , complete cds
TIAL1	0.42	TIA1 cytotoxic granule-associated rna binding protein-like 1, transcript variant 2
TRAF1	0.42	TNF receptor-associated factor 1
BCL2L12	0.42	Bcl2-like 12 (proline rich), transcript variant 1
PCBP4	0.41	Poly(RC) binding protein 4, transcript variant 4
CBX4	0.40	Chromobox homolog 4 (pc class homolog, drosophila)
PAK1	0.40	P21/CDC42/RAC1-activated kinase 1 (STE20 homolog, yeast)
BNIP3	0.39	Bcl2/adenovirus e1b 19kd interacting protein 3, nuclear gene encoding mitochondrial protein
PLAGL1	0.38	Pleiomorphic adenoma gene-like 1, transcript variant 1
SMAC	0.38	Second mitochondria-derived activator of caspase
IGF1R	0.36	Insulin-like growth factor 1 receptor
DNM2	0.36	Dynamin 2
TNFRSF25	0.35	Tumor necrosis factor receptor sturn on ER family, member 12 (translocating chain-association membrane protein)
TXNL1	0.35	Thioredoxin-like, 32kd
ZNF443	0.34	Krturn on pel-type zinc finger (C2H2)
TNFRSF9	0.33	Tumor necrosis factor receptor sturn on ER family, member 9

TRAF5	0.32	TNF receptor-associated factor 5
TNFSF5	0.32	Tumor necrosis factor (ligand) sturn on ER family, member 5 (Hyper-igm syndrome)
GLRX2	0.32	Glutaredoxin 2
BAG1	0.30	Bcl2-associated athanogene
NOX5	0.29	Nadph oxidase, EF hand calcium-binding domain 5
BCAP29	0.28	B-cell receptor-associated protein bap29
LGALS7	0.27	Lectin, galactoside-binding, soluble, 7 (GALECTIN 7)
EDAR	0.27	Ectodysplasin 1, anhidrotic receptor
TESK2	0.26	Testis-specific kinase 2
PDCD5	0.25	Programmed cell death 5
BAD	0.21	Bcl2-antagonist of cell death, transcript variant 2
NGFR	0.20	Nerve growth factor receptor (TNFR sturn on ER family, member 16)

Table 4-5 Significantly changed apoptotic genes in aPPD treated SF188C2R2 cells

OGS	C2R2+a/C2R2	Description
GADD45 α	10.11	Growth arrest and DNA-damage-inducible, alpha
GADD45 β	7.04	Growth arrest and DNA-damage-inducible, beta
AXUD1	5.20	AXIN1 up-regulated
TRIB3	4.94	Chromosome 20 open reading frame 97
MCL1	3.10	Myeloid cell leukemia sequence 1 (Bcl2-related)
BIRC6	2.96	Baculoviral iap repeat-containing 6 (APOLLON)
TRAF4	2.89	TNF receptor-associated factor 4 (TRAF4), transcript variant 1
TNFRSF12A	2.77	Type I transmembrane protein fn14 (FN14)
NFKBIA	2.62	Nuclear factor of kappa light polypeptide gene enhancer in b-cells inhibitor, alpha
PEA15	2.60	Calsequestrin 1 (fast-twitch, skeletal muscle) (CASQ1), nuclear gene encoding mitochondrial protein
CASP5	2.59	Caspase 5, apoptosis-related cysteine protease
IER3	2.58	Immediate early response 3 (IER3), transcript variant short
SIAH1	2.58	Seven in absentia homolog 1 (drosophila)
PRLR	2.38	Prolactin receptor
CASP9	2.17	Caspase 9, apoptosis-related cysteine protease, transcript variant beta
ERCC3	2.17	Excision repair cross-complementing rodent repair deficiency, complementation group 3 (xeroderma pigmentosum group b complementing)
DATF1	2.11	Human for KIAA0333 gene, partial CDs
BNIP1	2.06	Bcl2/adenovirus e1b 19kd interacting protein 1, transcript variant BNIP1
INHBA	2.06	Inhibin, beta a (activin a, activin ab alpha polypeptide)

PPM1F	0.18	KIAA0015 gene product
CARD4	0.10	Caspase recruitment domain family, member 4
CASPASE 4	0.06	Caspase 4, apoptosis-related cysteine protease, transcript variant alpha

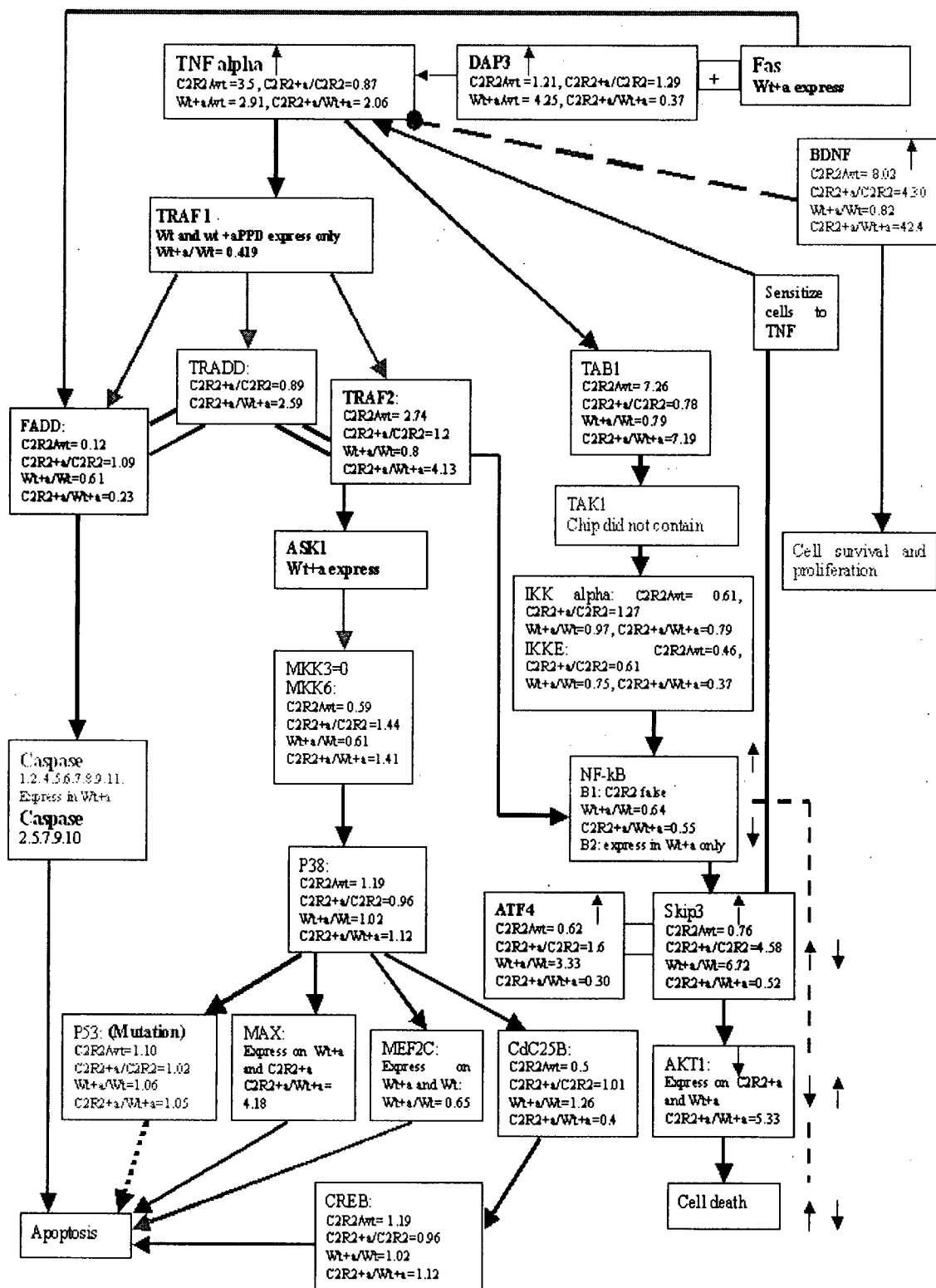


Fig. 4-5. TNF- α and NF- κ B pathway network

Three cell death pathways were activated in SF188.

1. TNF- α recruits FADD, and TRADD through TNF receptor 1 (TRAF1) binding to caspase 8 to form the death-initiating signaling complex (DISC), consequently induce apoptosis.
2. Activated TRAF1 combines to TNF receptor-associated factor (TRAF2) to form a heterodimeric complex, with the involvement of TRAF1-TRAF2 complex, TNF- α mediates activation of MAPK pathway to trigger apoptosis via p53 independent pathways.
3. TNF- α activates NF- κ B with the TRAF1-TRAF2 complex or TAB1 to induce cell death via SKIP3 which negatively feedback regulated NF- κ B and AKT1.

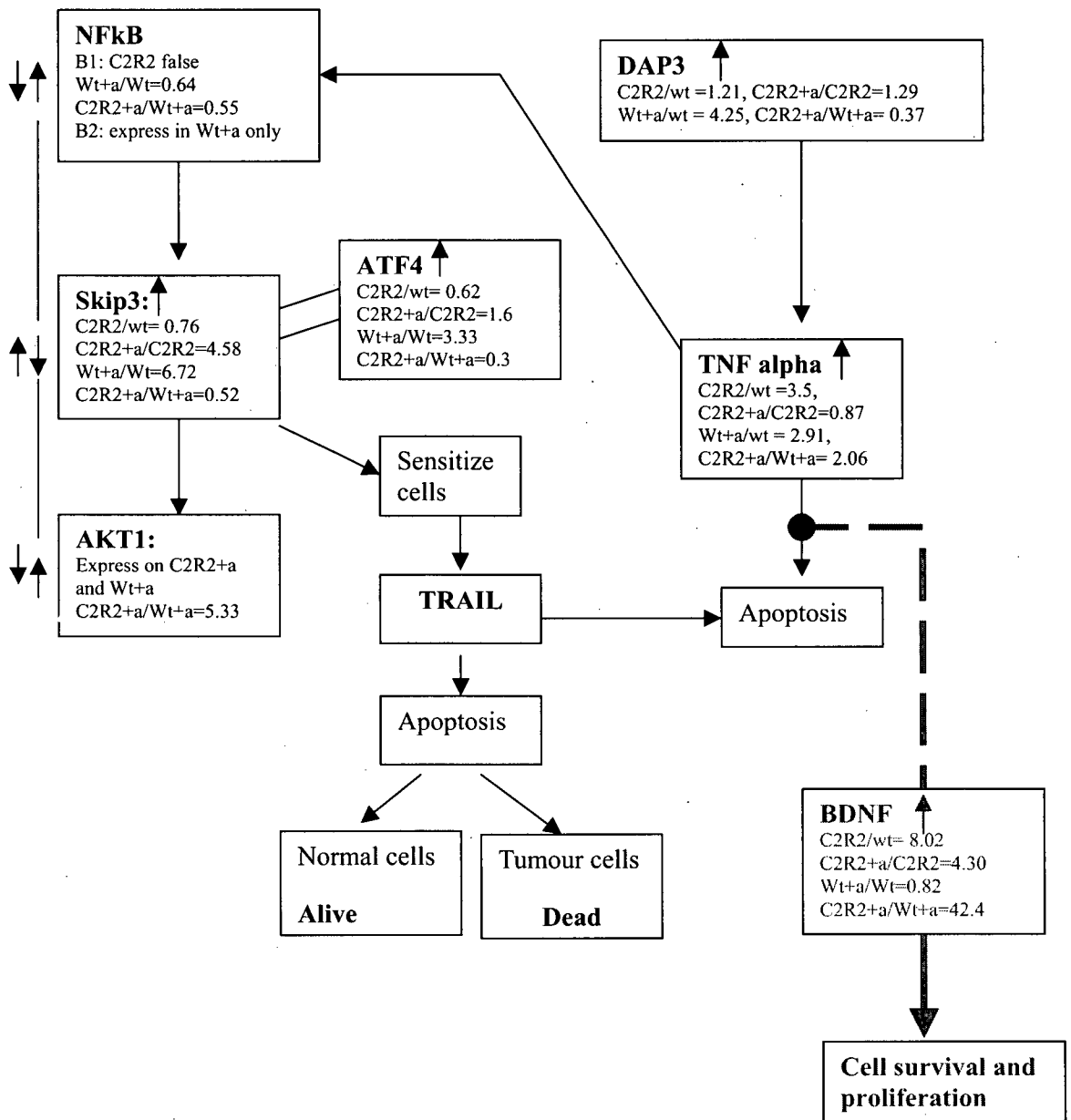


Fig. 4-6. SKIP3 pathway

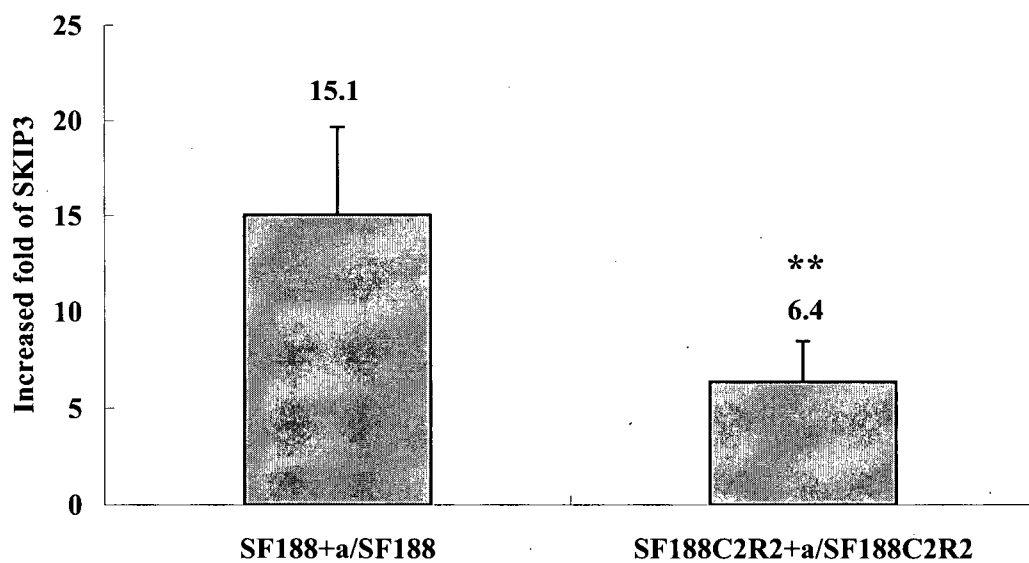
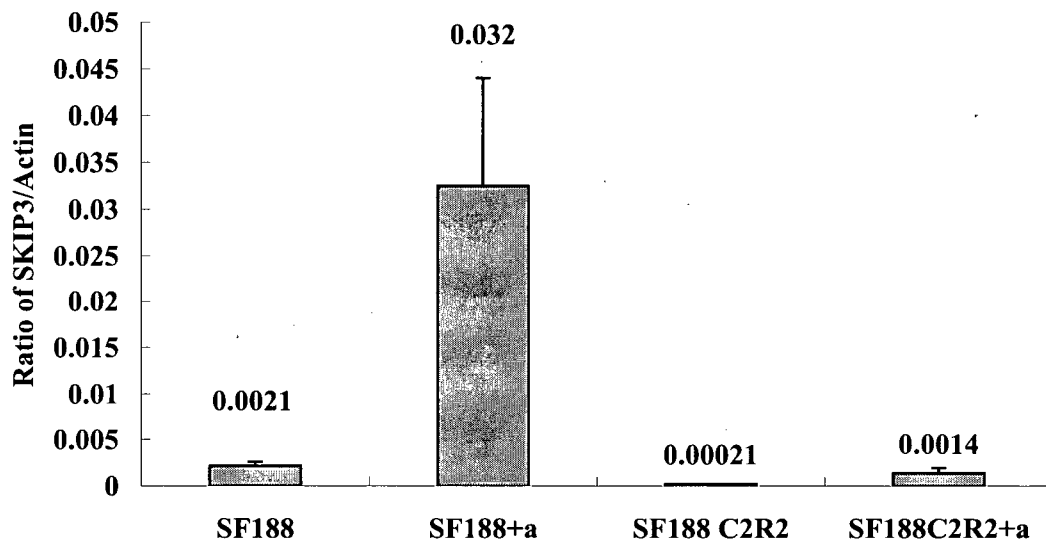


Fig. 4-7. Real-time quantitative RT-PCR for SKIP3

** , $p < 0.05$ vs SF188+a/ SF188

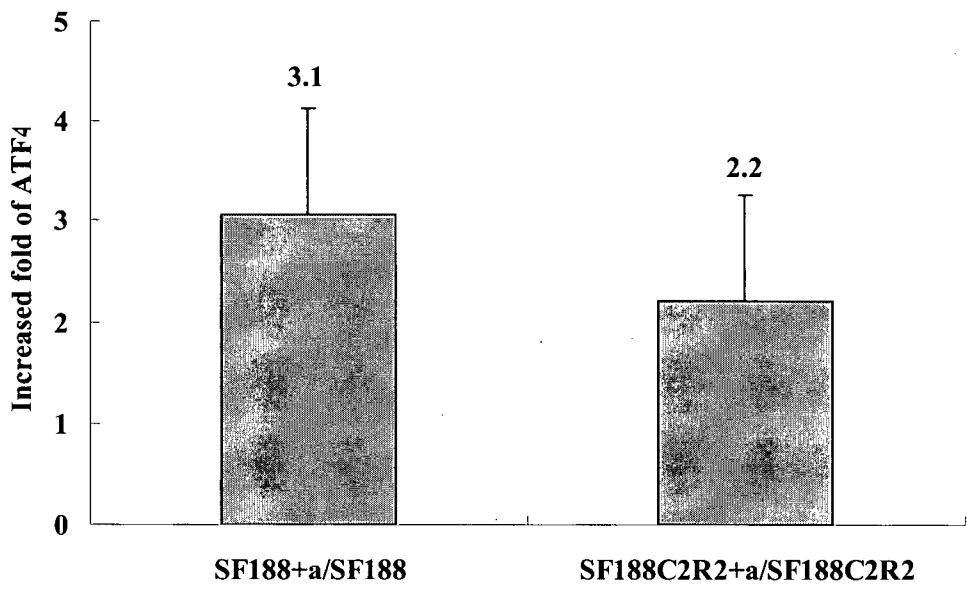
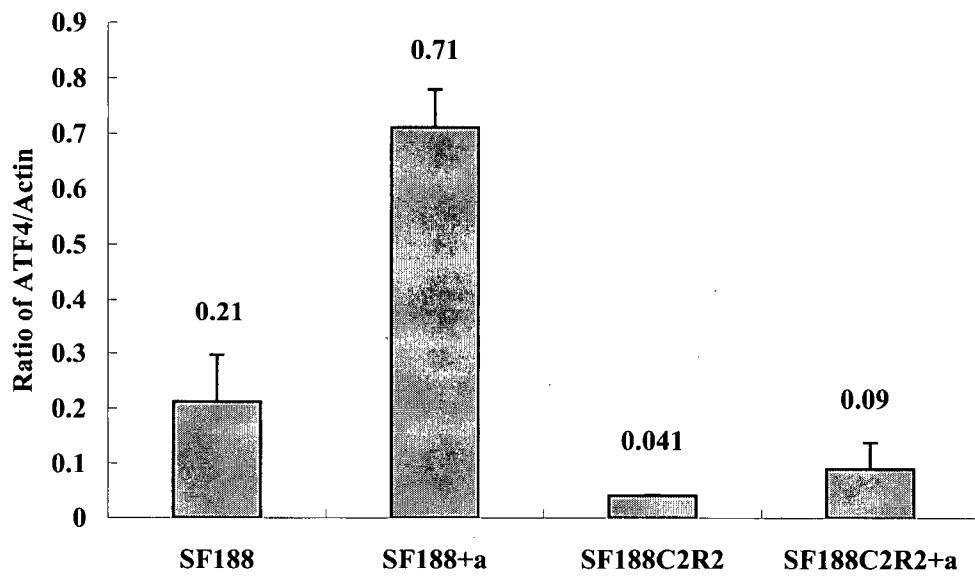


Fig. 4-8. Real-time quantitative RT-PCR for ATF4

Table 4-6 Anti-apoptosis gene expression

OGS	C2R2+a/C2R2	Wt+a/Wt	Description
IER3	2.58	1.64	Immediate early response 3, transcript variant short
MCL1	3.1	1.57	Myeloid cell leukemia sequence 1 (Bcl2-related)
RTN4	1.63	1.81	Reticulon 4
BECN1	1.34	0.95	Beclin 1 (coiled-coil, myosin-like Bcl2 interacting protein)
BFAR	1.23	0.87	Apoptosis regulator
FOXO1A	1.18	0.69	Forkhead box o1a (Rhabdomyosarcoma)
IGF1R	1.16	0.36	Insulin-like growth factor 1 receptor
BAG3	1.11	0.74	Bcl2-associated athanogene 3
CFLAR	1.10	0.61	Casp8 and FADD-like apoptosis regulator
TGFB1	1.07	0.65	Transforming growth factor, beta 1
PEA15	1.05	0.81	Phosphoprotein enriched in astrocytes 15
TNF	1.05	0.85	Tumor necrosis factor (tnf sturn on ER family, member 2)
HDAC3	0.99	0.53	602629572F1 cDNA, 5' end
TNFSF5	0.97	0.32	Tumor necrosis factor (ligand) sturn on erfamily, member 5 (hyper-igm syndrome)
CBX4	0.96	0.40	Chromobox homolog 4 (PC class homolog, drosophila)
NOTCH2	0.93	0.79	Notch homolog 2 (drosophila)
BCL2L1	0.90	0.79	Bcl2-like 1
BAG1	0.86	0.30	Bcl2-associated athanogene

HDAC3	0.86	1.67	Histone deacetylase 3
MAPK8IP2	0.84	0.74	Mitogen-activated protein kinase 8 interacting protein 2
HTATIP2	0.82	1.77	HIV-1 TAT interactive protein 2.30 kd
BNIP3	0.80	0.39	Bcl2/adenovirus e1b 19kd interacting protein 3 (BNIP3), nuclear gene encoding mitochondrial protein
BIRC5	0.79	0.53	Baculoviral IAP repeat-containing 5 (survivin)

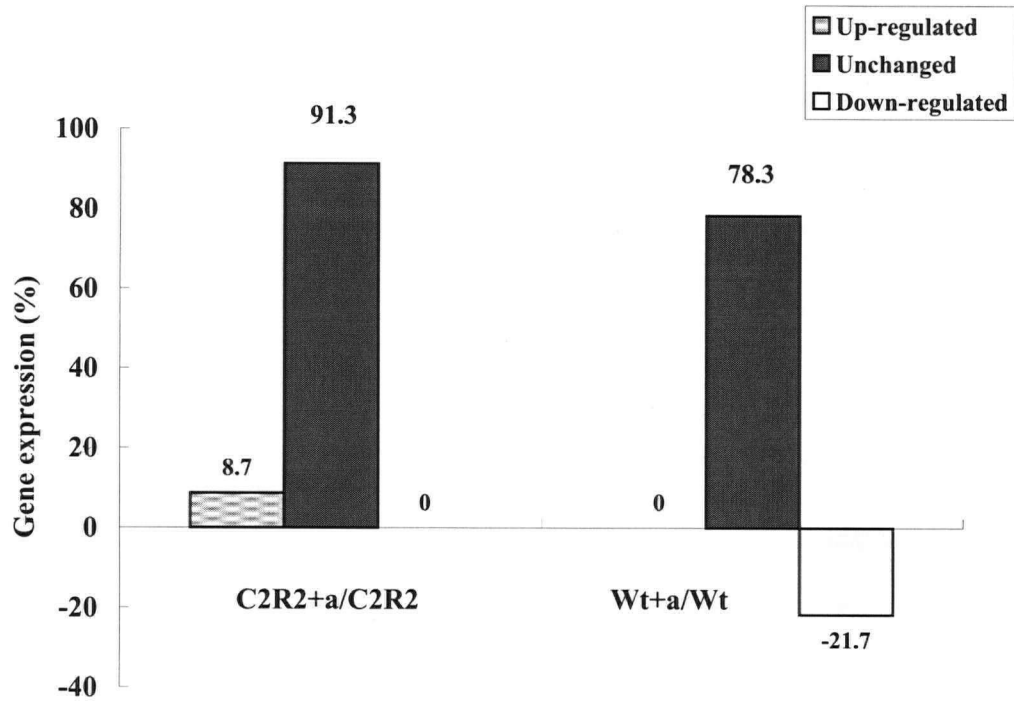


Fig. 4-9. Anti-apoptotic gene expression patterns

4.4 Discussion

This study was based on microarray experiments designed to elucidate the molecular mechanisms of aPPD-induced cell death. In addition, since the mRNA was collected at the same time point after treatment with aPPD at which SF188 showed 50% death, while there still was no cytotoxicity shown in SF188C2R2 cells, the difference in gene expression profiles of the two cell lines may reveal the cause of aPPD-resistance observed in SF188C2R2 cells. Using unsupervised analysis in this study, including clustering analysis, the ratio comparison of samples before and after aPPD treatment, the gene expression pattern in SF188 and SF188C2R2 and the genes involving cell death pathway induced by aPPD were extensively analyzed. The results of DNA array data supported the idea that gene expression profile in SF188C2R2 significantly differed to that of the parental cell line SF188 with astonishing 58.4% genes in SF188C2R2 (Table 4-2). The difference in gene expression profiles between the two cell lines without any drug treatment forms the base of genetic difference between the two cell lines, which was partially reflected by the difference in phenotype, such as morphology, cell growth rate, and drug resistance, etc, described in Chapter III. It is highly likely that the relatively large number of altered genes may be co-regulated [22], for instance, that several members of fibroblast growth factor (FGF) family including BRUNOL4, FRAG1, FGFR1 and EMR2 were all over-expressed together. BDNF is also found highly expressed in SF188C2R2. Activation of FGF pathway induces cellular migration, proliferation and differentiation. High levels of expression in these genes in SF188C2R2 may contribute to the hyper-proliferation of the cells described in Chapter 3.

Treated with aPPD, 3579 (56.9%) genes showed different expression levels in SF188 and C2R2 cells. More genes altered their expression levels in SF188, which underwent apoptosis, than in SF188C2R2, which remained morphologically unchanged (Table 4-2). Interestingly, aPPD induced changes in gene expression in SF188 cells were mainly down-regulated but aPPD had the opposite effect on SF188C2R2 cells that mainly caused gene up-regulation (Fig.4-2).

Since aPPD quickly induces apoptosis in SF188 glioma cells and many other tumor cells, special attention was given to expression profiles of apoptosis related genes with and without aPPD treatment. Despite several attempts of using various analytical strategies, it was not possible identify any commonly known pathways that are up- or down- regulated by aPPD treatment although quite a few apoptosis related genes were significantly activated. Among them, SKIP3 (TRIB3) and GADD45 were up-regulated in both SF188 and SF188C2R2 cells.

GADD45, known as 4F154, CELK08314, Y24D9A.4a, Y24D9A.4b, Y24D9A.4c, is a 165-amino acid nuclear protein whose expression also is p53-dependent. It is known that DADD45 plays important roles in negative growth control, including growth suppression and apoptosis [23]. GADD45 is further demonstrated to interact with PCNA, Cdc2 and the cyclin-dependent kinase inhibitor p21^{WAF1/CIP1}[24]. Both GADD45 α and GADD45 β may induce p38/JNK activation. GADD45 α induces a G2/M arrest but not GADD45 β [25].

SKIP3, known as NIPK, SINK, TRB3, SKIP3, TRIB3 (Tribbles homolog 3 (Drosophila)) and C20orf97, is a new member of the kinase-like Drosophila tribbles

family. SKIP3 gene locates at chromosome 20 open reading frame 97 [32]. Human ATF4, also known as CREB2, TAXREB67 and C/ATF, a member of the ATF/CREB (activating transcription factor/ cyclic AMP response element binding protein) family of basic region-leucine zipper (bZIP) transcription factors, is the partner gene SKIP3 [26]. Wu et al demonstrated that over expression of SKIP3 inhibited NF- κ B-dependent transcription induced by tumor necrosis factor (TNF) stimulation or its downstream signaling proteins, but did not inhibit NF- κ B translocation to the nucleus and binding to DNA. SKIP3 is a putative protein kinase that is induced by the transcription factor NF- κ B and negatively regulating serine-threonine kinase AKT1 and NF- κ B to act on cell survival regulation. SKIP3 can also sensitize the cells to TNF- and TRAIL-induced apoptosis. Taken together, this data suggests that SKIP3 is critically involved in a novel negative feedback control pathway of NF- κ B-induced by gene expression, and which may evoke selective cell death in SF188 when treated with aPPD [27-29]. Moreover, all of these were involved in the TNF- α and NF- κ B pathway network. Therefore, the TNF- α and NF- κ B pathway network (Fig.4-6) is possibly one of the important pathways involved in aPPD-induced cytotoxicity in the glioma cells.

Upon treatment with aPPD, gene AKT1 displayed a significantly different response between the two cell lines. With the treatment with aPPD, AKT1 level in SF188C2R2 was 5.33 fold higher than the wild type. AKT, the serine/threonine protein kinase, is a critical mediator of cell survival and activated AKT protect cells from apoptosis induced by ultraviolet radiation and ionizing radiation. Three closely related isoforms of AKT, AKT1, AKT2 and AKT3 are found expression in different tumor cells [30] [31]. Evidence suggests that increased signaling through AKT would clearly be a

survival advantage to tumor cells in the face of stress challenges, including DNA damage, hypoxia, and exposure to Fas ligand and cytokinase as well [32, 33]. AKT1 is overexpressed in 20% of gastric adenocarcinomas and human breast cancer cell lines [34, 35]. The expression of AKT1 in SF188 was also lower than in SF188C2R2. Therefore, even the SKIP3/AKT1 pathway in SF188C2R2 was activated after treatment with aPPD, it might not be as strong as SF188. Increased AKT1 in SF188C2R2 may attribute to the resistance of SF188C2R2 to aPPD-induced apoptosis. Due to time constraints, only three genes could be verified with real-time RT-PCR. The three genes were DAP3, SKIP3 and ATF4 as they are most related to each other. Results of qRT-PCR for SKIP3 (Fig. 4-6) and ATF4 (Fig. 4-7) confirmed the results of DNA microarray analysis in both SF188 and SF188C2R2.

In conclusion, this DNA microarray experimental approach provided global profiles of gene expression, of which SF188 C2R2 differs from SF188wt both in its resting status as well as in its response to aPPD treatment. High expression of BDNF and some genes of the FGF family in SF188C2R2 may be associated with the proliferation of SF188C2R2. The pathways involved with TNF- α were possible mechanisms for aPPD-induced apoptosis in SF188. Meanwhile, raised levels of some anti-apoptosis genes in SF188C2R2 may attribute to the aPPD-resistance of SF188C2R2. The activity of TNF- α / NF- κ B pathway induced by aPPD explored here remains to be verified and more comprehensive gene collaboration in overlapping pathways in both SF188 and SF188C2R2 cell lines in response to aPPD should be identified.

REFERENCES

1. Popovich, D.G. and D.D. Kitts, *Ginsenosides 20(S)-protopanaxadiol and Rh2 reduce cell proliferation and increase sub-G1 cells in two cultured intestinal cell lines, Int-407 and Caco-2*. *Can J Physiol Pharmacol*, 2004. **82**(3): p. 183-90.
2. Popovich, D.G. and D.D. Kitts, *Mechanistic studies on protopanaxadiol, Rh2, and ginseng (Panax quinquefolius) extract induced cytotoxicity in intestinal Caco-2 cells*. *J Biochem Mol Toxicol*, 2004. **18**(3): p. 143-9.
3. Keum, Y.S., et al., *Inhibitory effects of the ginsenoside Rg3 on phorbol ester-induced cyclooxygenase-2 expression, NF-kappaB activation and tumor promotion*. *Mutat Res*, 2003. **523-524**: p. 75-85.
4. Yun, T.K., *Experimental and epidemiological evidence on non-organ specific cancer preventive effect of Korean ginseng and identification of active compounds*. *Mutat Res*, 2003. **523-524**: p. 63-74.
5. Kim, H.S., et al., *Effects of ginsenosides Rg3 and Rh2 on the proliferation of prostate cancer cells*. *Arch Pharm Res*, 2004. **27**(4): p. 429-35.
6. Liu, W.K., S.X. Xu, and C.T. Che, *Anti-proliferative effect of ginseng saponins on human prostate cancer cell line*. *Life Sci*, 2000. **67**(11): p. 1297-306.
7. Kim, Y.S., et al., *Ginsenoside Rh2 induces apoptosis independently of Bcl-2, Bcl-xL, or Bax in C6Bu-1 cells*. *Arch Pharm Res*, 1999. **22**(5): p. 448-53.
8. Tatsuka, M., M. Maeda, and T. Ota, *Anticarcinogenic effect and enhancement of metastatic potential of BALB/c 3T3 cells by ginsenoside Rh(2)*. *Jpn J Cancer Res*, 2001. **92**(11): p. 1184-9.

9. Oh, M., et al., *Anti-proliferating effects of ginsenoside Rh2 on MCF-7 human breast cancer cells*. *Int J Oncol*, 1999. **14**(5): p. 869-75.
10. Oh, S.H. and B.H. Lee, *A ginseng saponin metabolite-induced apoptosis in HepG2 cells involves a mitochondria-mediated pathway and its downstream caspase-8 activation and Bid cleavage*. *Toxicol Appl Pharmacol*, 2004. **194**(3): p. 221-9.
11. Lee, J.Y., et al., *Antitumor promotional effects of a novel intestinal bacterial metabolite (IH-901) derived from the protopanaxadiol-type ginsenosides in mouse skin*. *Carcinogenesis*, 2005. **26**(2): p. 359-67.
12. Mischel, P.S., T.F. Cloughesy, and S.F. Nelson, *DNA-microarray analysis of brain cancer: molecular classification for therapy*. *Nat Rev Neurosci*, 2004. **5**(10): p. 782-92.
13. Eschrich, S. and T.J. Yeatman, *DNA microarrays and data analysis: an overview*. *Surgery*, 2004. **136**(3): p. 500-3.
14. Ochs, M.F., et al., *Bayesian decomposition: analyzing microarray data within a biological context*. *Ann N Y Acad Sci*, 2004. **1020**: p. 212-26.
15. Olson, J.A., Jr., *Application of microarray profiling to clinical trials in cancer*. *Surgery*, 2004. **136**(3): p. 519-23.
16. Mocellin, S., et al., *DNA array-based gene profiling in tumor immunology*. *Clin Cancer Res*, 2004. **10**(14): p. 4597-606.
17. Fischer, D.S., ed. *The cancer chemotherapy handbook*. 2003, Mosby: Philadelphia.
18. Chang, J.C., S.G. Hilsenbeck, and S.A. Fuqua, *Genomic approaches in the management and treatment of breast cancer*. *Br J Cancer*, 2005. **92**(4): p. 618-24.

19. P. Reizenstein, G.M., ed. *Management of minimal residual malignancy in man*. 1988, Pergamon Press: Oxford ; New York.
20. Prolla, T.A., *Multiple roads to the aging phenotype: insights from the molecular dissection of progerias through DNA microarray analysis*. *Mech Ageing Dev*, 2005. **126**(4): p. 461-5.
21. Ohta, K., et al., *DNA microarray analysis of gene expression in iris and ciliary body of rat eyes with endotoxin-induced uveitis*. *Exp Eye Res*, 2005. **80**(3): p. 401-12.
22. Davidson, L.A., et al., *Chemopreventive n-3 polyunsaturated fatty acids reprogram genetic signatures during colon cancer initiation and progression in the rat*. *Cancer Res*, 2004. **64**(18): p. 6797-804.
23. Vairapandi, M., *Characterization of DNA demethylation in normal and cancerous cell lines and the regulatory role of cell cycle proteins in human DNA demethylase activity*. *J Cell Biochem*, 2004. **91**(3): p. 572-83.
24. Yang, Q., et al., *Identification of a functional domain in a GADD45-mediated G2/M checkpoint*. *J Biol Chem*, 2000. **275**(47): p. 36892-8.
25. Takekawa, M. and H. Saito, *A family of stress-inducible GADD45-like proteins mediate activation of the stress-responsive MTK1/MEKK4 MAPKKK*. *Cell*, 1998. **95**(4): p. 521-30.
26. Ord, D. and T. Ord, *Mouse NIPK interacts with ATF4 and affects its transcriptional activity*. *Exp Cell Res*, 2003. **286**(2): p. 308-20.
27. Wu, M., et al., *SINK is a p65-interacting negative regulator of NF-kappaB-dependent transcription*. *J Biol Chem*, 2003. **278**(29): p. 27072-9.
28. Du, K., et al., *TRB3: a tribbles homolog that inhibits Akt/PKB activation by insulin in liver*. *Science*, 2003. **300**(5625): p. 1574-7.

29. Saltiel, A.R., *Putting the brakes on insulin signaling*. N Engl J Med, 2003. **349**(26): p. 2560-2.
30. Cheng, J.Q., et al., *Amplification of AKT2 in human pancreatic cells and inhibition of AKT2 expression and tumorigenicity by antisense RNA*. Proc Natl Acad Sci U S A, 1996. **93**(8): p. 3636-41.
31. Bruce C. Baguley, D.J.K., ed. *Anticancer drug development*. 2002, London : Academic: San Diego, Calif. p38-40.
32. Chen, R.H., et al., *Suppression of transforming growth factor-beta-induced apoptosis through a phosphatidylinositol 3-kinase/Akt-dependent pathway*. Oncogene, 1998. **17**(15): p. 1959-68.
33. Liu, Q., et al., *SHIP is a negative regulator of growth factor receptor-mediated PKB/Akt activation and myeloid cell survival*. Genes Dev, 1999. **13**(7): p. 786-91.
34. Ahmad, S., N. Singh, and R.I. Glazer, *Role of AKT1 in 17beta-estradiol- and insulin-like growth factor I (IGF-I)-dependent proliferation and prevention of apoptosis in MCF-7 breast carcinoma cells*. Biochem Pharmacol, 1999. **58**(3): p. 425-30.
35. Staal, S.P., *Molecular cloning of the akt oncogene and its human homologues AKT1 and AKT2: amplification of AKT1 in a primary human gastric adenocarcinoma*. Proc Natl Acad Sci U S A, 1987. **84**(14): p. 5034-7.

CHAPTER 5. GENERAL CONCLUSION

Multiple drug resistance and toxicity of anticancer drugs have been a major impact on eradicating cancer with chemotherapy. 20(s)-protopanaxadiol (aPPD), an aglycone derivative of protopanaxadiol ginsenosides family, has been reported to possess anticancer activity in ginsenosides family with low toxicity in normal tissues. However, the mechanisms of aPPD mediated cancer inhibition remain unknown. In the current study, we investigated the cytotoxicity of aPPD on P-gp overexpressing cell lines and effects of aPPD on P-gp efflux activity. We have characterized an aPPD-resistant cell line obtained by repeated treatment with aPPD. We also established gene expression profiles of glioma cells with and without aPPD treatment using a cRNA array analysis.

Our data showed that aPPD increased accumulation of P-gp substrate in the cancer cells with high levels of P-gp expression. Unlike many other P-gp blockers, aPPD did not affect the ATPase activity of P-gp. Moreover, aPPD enhanced the inhibitory effect of verapamil on P-gp mediated drug efflux. Our results showed that the aPPD-resistant cell line SF188C2R2 was more proliferative, unable to demonstrate G1-arrest to aPPD and also cross resistant to other drugs including vincristine, cisplatin, and paclitaxel. The cRNA microarray results indicated that aPPD changed gene expression in SF188 glioma cells mainly by down-regulating the anti-apoptotic genes and the aPPD-resistant SF188 C2R2 cells were less responsive to aPPD induced changes in gene expression.

The above results indicate that aPPD may sensitize MDR tumor cells to chemotherapeutics through multiple mechanisms. It blocks P-gp transporter to inhibit drug efflux allowing drug accumulation inside of cells. In addition, aPPD down-regulates expression of anti-apoptotic genes to render the cells more susceptible to chemotherapeutics induced apoptosis. Actually, the gene expression profile for aPPD-resistant SF188C2R2 cells, which showed that aPPD failed to cause down-regulation of those anti-apoptosis genes, was in consistence with the fact that this cell line cross-resistant to several structurally unrelated chemotherapy drugs. Thus, we concluded that aPPD is a multi-functional compound that sensitizes MDR cells not only by reversing P-gp but also weakening the survival mechanism of tumor cells. These results render the compound as a promising candidate of chemosensitizer for tumor treatment. It therefore deserves further study to understand the interaction between aPPD and P-gp protein as well as the regulatory effect on anti-apoptotic pathways in the drug resistant cancer cells.